

Supplementary material

Synthesis, computational studies, antimycobacterial and antibacterial properties of pyrazinoic acid-isoniazid hybrid conjugates

Siva S. Panda,^{*a} Adel S. Girgis,^{*b} Bibhuti B. Mishra,^c Mohamed Elagawany,^{ad}
Venkatasai Devarapalli,^a William F. Littlefield,^a Ahmed Samir,^e Walid Fayad,^f Nehmedo
G. Fawzy,^b Aladdin M. Srour^g and Riham M. Bokhtia^{ah}

^a*Department of Chemistry & Physics, Augusta University, Augusta, GA 30912, USA.*

^b*Department of Pesticide Chemistry, National Research Centre, Dokki, Giza 12622, Egypt.*

^c*Department of Immunology and Microbial Disease, Albany Medical College, 47 New Scotland Avenue, Albany, NY-12208, USA.*

^d*Department of Pharmaceutical Chemistry, Faculty of Pharmacy, Damanhour University, Damanhour, Egypt.*

^e*Microbiology Department, Faculty of Veterinary Medicine, Cairo University, Cairo, Egypt.*

^f*Drug Bioassay-Cell Culture Laboratory, Pharmacognosy Department, National Research Centre, Dokki, Giza, 12622. Egypt.*

^g*Department of Therapeutic Chemistry, National Research Centre, Dokki, Giza 12622, Egypt.*

^h*Department of Pharmaceutical Organic Chemistry, Faculty of Pharmacy, Zagazig University, Zagazig, 44519, Egypt.*

* Corresponding authors. E-mail: sspanda12@gmail.com, girgisas10@yahoo.com

Table titles

Table S1. Anti-proliferative properties of the synthesized compounds against RPE1 cell line.

Table S2. Descriptor of the BMLR-QSAR model for the tested compounds against *Mycobacterium marinum*.

Table S3. Observed and estimated MIC values for the tested compounds against *Mycobacterium marinum* according to the BMLR-QSAR model.

Table S4. Molecular descriptor values of the BMLR-QSAR model for the tested compounds against *Mycobacterium marinum* according to the BMLR-QSAR model.

Table S5. Descriptor of the BMLR-QSAR model for the tested compounds against *Mycobacterium fortuitum*.

Table S6. Observed and estimated MIC values for the tested compounds against *Mycobacterium fortuitum* according to the BMLR-QSAR model.

Table S7. Molecular descriptor values of the BMLR-QSAR model for the tested compounds against *Mycobacterium fortuitum* according to the BMLR-QSAR model.

Table S8. Descriptor of the BMLR-QSAR model for the tested compounds against *Mycobacterium tuberculosis*.

Table S9. Observed and estimated % growth inhibition at 30 $\mu\text{g/mL}$ values for the tested compounds against *Mycobacterium tuberculosis* according to the BMLR-QSAR model.

Table S10. Molecular descriptor values of the BMLR-QSAR model for the tested compounds against *Mycobacterium tuberculosis* according to the BMLR-QSAR model.

Table S11. Estimated/predicted activity values for the tested compounds against *M. marinum* and *M. fortuitum* mapped with the generated 3D-pharmacophore models.

Table S11. Estimated/predicted activity values for the tested compounds against *M. tuberculosis* mapped with the generated 3D-pharmacophore model.

Figure captions

Fig. S1. (A) Constraint distances “HBA-1 – HBA-2 = 4.800, HBA-1 – HBD = 3.026, HBA-2 – HBD = 4.909 Å” and (B) constraint angles “HBA-1 – HBA-2 – HBD = 36.29°” of the generated 3D-pharmacophore for the synthesized bio-active compounds against

Mycobacterium marinum which contains two hydrogen bonding acceptors (HBA-1, HBA-2; green) and one hydrogen bonding donor (HBD; purple).

Fig. S2. 3D-pharmacophore mapped on the synthesized bio-active compounds against *Mycobacterium marinum*.

Fig. S3. (A) Constraint distances “HBD-1 – HBD-2 = 8.500, HBD-1 – HBA = 4.271, HBD-2 – HBA = 5.844 Å” and (B) constraint angles “HBD-1 – HBD-2 – HBA = 27.45 °” of the generated 3D-pharmacophore for the synthesized bio-active compounds against *Mycobacterium fortuitum* which contains two hydrogen bonding donors (HBD-1, HBD-2; purple) and one hydrogen bonding acceptor (HBA; green).

Fig. S4. 3D-pharmacophore mapped on the synthesized bio-active compounds against *Mycobacterium fortuitum*.

Fig. S5. (A) Constraint distances “HBA – HBD = 3.292, HBA – H = 6.327, HBD – H = 3.343 Å” and (B) constraint angles “HBA – HBD – H = 144.97 °” of the generated 3D-pharmacophore for the synthesized bio-active compounds against *Mycobacterium tuberculosis* which contains hydrogen bonding acceptor (HBA; green), hydrogen bonding donor (HBD; purple) and hydrophobic (H; light blue).

Fig. S6. 3D-pharmacophore mapped on the synthesized bio-active compounds against *Mycobacterium tuberculosis*.

¹H NMR, ¹³C NMR and HRMS spectral charts of the synthesized compounds.

HPLC spectra of compounds **12e** and **12f**

Table S1. Anti-proliferative properties of the synthesized compounds against RPE1 cell line.

Entry	Compound	Percentage of cell proliferation \pm SD
1	10a	84.6 \pm 0.7
2	10b	82.1 \pm 3.0
3	10c	81.8 \pm 5.5
4	10d	82.9 \pm 8.5
5	10e	90.4 \pm 3.3
6	10f	86.5 \pm 4.2
7	10g	80.1 \pm 7.4
8	12a	80.1 \pm 4.2
9	12b	96.4 \pm 2.7
10	12c	84.6 \pm 3.7
11	12e	83.2 \pm 5.7
12	12f	95.5 \pm 8.6
13	12g	92.2 \pm 1.2
14	13	88.2 \pm 5.1
15	16	83.5 \pm 7.4

Table S2. Descriptor of the BMLR-QSAR model for the tested compounds against *Mycobacterium marinum*.

Entry	ID	Coefficient	<i>s</i>	<i>t</i>	Descriptor
1	0	74.8101	12.160	6.152	Intercept
2	<i>D</i> ₁	-0.176724	0.037	-4.762	Max. e-n attraction for bond C-N
3	<i>D</i> ₂	-0.113573	0.017	-6.809	Max. e-e repulsion for bond C-C

$N = 11, n = 2, R^2 = 0.908, R^2_{cvOO} = 0.829, F = 39.543, s^2 = 0.003$

$\text{Log}(\text{MIC}, \mu\text{M}) = 74.8101 - (0.176724 \times D_1) - (0.113573 \times D_2)$

Table S3. Observed and estimated MIC values for the tested compounds against *Mycobacterium marinum* according to the BMLR-QSAR model.

Entry	Compd.	Observed MIC, mM	Estimated MIC, μM	Error ^a
1	PZA	81.2	86.8	-5.6
2	INH	72.9	80.5	-7.6
3	10a	84.3	79.8	4.5
4	12a	56.1	46.7	9.4
5	12b	58.4	57.4	1.0
6	12c	56.1	52.5	3.6
7	12d	26.7	30.8	-4.1
8	12e	51.2	46.3	4.9
9	12g	46.6	44.8	1.8
10	13	41.1	48.0	-6.9
11	16	82.6	82.3	0.3

^a Error is the difference between the observed and estimated biological activity (MIC) values.

Table S4. Molecular descriptor values of the BMLR-QSAR model for the tested compounds against *Mycobacterium marinum* according to the BMLR-QSAR model.

Entry	Compd.	Descriptors ^a	
		D_1	D_2
1	PZA	330.1631	127.8817
2	INH	329.9877	128.4424
3	10a	330.4742	127.7163
4	12a	330.664	129.4675
5	12b	330.6187	128.7496
6	12c	330.4774	129.3105
7	12d	330.7008	131.0057
8	12e	330.426	129.8765
9	12g	330.3036	130.193
10	13	330.8481	129.0796
11	16	329.2578	129.4907

^a D_1 = Max. e-n attraction for bond C-N, D_2 = Max. e-e repulsion for bond C-C.

Table S5. Descriptor of the BMLR-QSAR model for the tested compounds against *Mycobacterium fortuitum*.

Entry	ID	Coefficient	s	t	Descriptor
1	0	-2.6795	0.388	-6.913	Intercept
2	D_1	0.0298467	0.003	11.054	Max. e-e repulsion for atom N
3	D_2	80.0736	3.734	21.444	Avg. electroph. react. index for atom N

$N = 11, n = 2, R^2 = 0.984, R^2_{cvOO} = 0.962, F = 240.314, s^2 = 0.001$

$\text{Log}(\text{MIC}, \mu\text{M}) = -2.6795 + (0.0298467 \times D_1) - (80.0736 \times D_2)$

Table S6. Observed and estimated MIC values for the tested compounds against *Mycobacterium fortuitum* according to the BMLR-QSAR model.

Entry	Compd.	Observed MIC, mM	Estimated MIC, μ M	Error ^a
1	PZA	81.2	78.4	2.8
2	INH	145.8	152.9	-7.1
3	10a	84.3	81.5	2.8
4	12a	56.1	54.3	1.8
5	12b	58.4	55.9	2.5
6	12c	56.1	54.0	2.1
7	12d	53.4	57.9	-4.5
8	12e	51.2	53.6	-2.4
9	12g	46.6	48.2	-1.6
10	13	41.1	42.0	-0.9
11	16	82.6	79.0	3.6

^a Error is the difference between the observed and estimated biological activity (MIC) values.

Table S7. Molecular descriptor values of the BMLR-QSAR model for the tested compounds against *Mycobacterium fortuitum* according to the BMLR-QSAR model.

Entry	Compd.	Descriptors ^a	
		D_1	D_2
1	PZA	147.356	0.00219
2	INH	142.5146	0.00762
3	10a	142.6322	0.00416
4	12a	142.502	0.00201
5	12b	142.4075	0.00221
6	12c	142.064	0.00215
7	12d	142.7317	0.00227
8	12e	142.3404	0.002
9	12g	144.0619	0.00078
10	13	137.0116	0.00266
11	16	137.8948	0.00576

^a D_1 = Max. e-e repulsion for atom N, D_2 = Avg. electroph. react. index for atom N.

Table S8. Descriptor of the BMLR-QSAR model for the tested compounds against *Mycobacterium tuberculosis*.

Entry	ID	Coefficient	<i>s</i>	<i>t</i>	Descriptor
1	0	7.80777	1.172	6.660	Intercept
2	D_1	0.282997	0.030	9.543	Min. e-e repulsion for bond H-N
3	D_2	0.102738	0.014	7.207	Max. e-e repulsion for bond H-C
4	D_3	-1.69416	0.113	-14.963	Max. coulombic interaction for bond C-O

$N = 13, n = 3, R^2 = 0.965, R^2_{cvOO} = 0.892, F = 82.181, s^2 = 0.004$

$\text{Log}(\% \text{ growth inhibition at } 30 \mu\text{g/mL}) = 7.80777 + (0.282997 \times D_1) + (0.102738 \times D_2) - (1.69416 \times D_3)$

Table S9. Observed and estimated % growth inhibition at 30 $\mu\text{g/mL}$ values for the tested compounds against *Mycobacterium tuberculosis* according to the BMLR-QSAR model.

Entry	Compd.	Observed % growth inhibition at 30 $\mu\text{g/mL}$	Estimated % growth inhibition at 30 $\mu\text{g/mL}$	Error ^a
1	10a	88.8	88.8	0.0
2	10b	91	73.8	17.2
3	10c	84.3	91.0	-6.7
4	10d	80.2	87.7	-7.5
5	10e	60.4	65.4	-5.0
6	10g	8.8	9.0	-0.2
7	12a	68.9	77.5	-8.6
8	12b	84.2	86.9	-2.7
9	12c	84.1	76.4	7.7
10	12e	94.8	89.5	5.3
11	12g	96	80.4	15.6
12	13	90.1	83.2	6.9
13	16	78.1	95.6	-17.5

^a Error is the difference between the observed and estimated biological activity (% growth inhibition at 30 $\mu\text{g/mL}$) values.

Table S10. Molecular descriptor values of the BMLR-QSAR model for the tested compounds against *Mycobacterium tuberculosis* according to the BMLR-QSAR model.

Entry	Compd.	Descriptors ^a		
		D_1	D_2	D_3
1	10a	38.6098	34.3797	11.9929
2	10b	38.1408	34.23	11.9529
3	10c	38.6149	34.3592	11.9862
4	10d	38.1846	34.7702	11.9488
5	10e	38.9176	32.7731	12.0254
6	10g	37.3978	32.1811	12.2441
7	12a	36.8163	34.4923	11.735
8	12b	36.5537	34.548	11.6651
9	12c	38.0372	34.6277	11.9508
10	12e	37.7514	32.6895	11.7449
11	12g	37.3659	32.5331	11.6986
12	13	37.439	31.3733	11.6316
13	16	37.6267	31.677	11.6459

^a D_1 = Min. e-e repulsion for bond H-N, D_2 = Max. e-e repulsion for bond H-C, D_3 = Max. coulombic interaction for bond C-O.

Table S11. Estimated/predicted activity values for the tested compounds against *M. marinum* and *M. fortuitum* mapped with the generated 3D-pharmacophore models.

Entry	Compd.	<i>Mycobacterium marinum</i>		<i>Mycobacterium fortuitum</i>	
		Observed	Estimated	Observed	Estimated
		MIC, μM	MIC, μM	MIC, μM	MIC, μM
1	PZA	81.2	138.5	81.2	88.2
2	INH	72.9	77.4	145.8	96.7
3	10a	84.3	83.2	84.3	91.5
4	12a	56.1	46.9	56.1	52.7
5	12b	58.4	43.7	58.4	56.9
6	12c	56.1	45.2	56.1	52.3
7	12d	26.7	33.4	53.4	50.6
8	12e	51.2	39.3	51.2	48.0
9	12g	46.6	38.1	46.6	44.7
10	13	41.1	67.4	41.1	75.7
11	16	82.6	65.2	82.6	75.8

Table S12. Estimated/predicted activity values for the tested compounds against *M. tuberculosis* mapped with the generated 3D-pharmacophore model.

Entry	Compd.	Observed (% growth inhibition at 30 $\mu\text{g/mL}$)	Estimated (% growth inhibition at 30 $\mu\text{g/mL}$)
1	10a	88.8	61.6
2	10b	91.0	59.2
3	10c	84.3	81.2
4	10d	80.2	63.6
5	10e	60.4	50.7
6	10g	8.8	20.2
7	12a	68.9	88.3
8	12b	84.2	92.4
9	12c	84.1	88.7
10	12e	94.8	92.0
11	12g	96.0	95.8
12	13	90.1	89.6
13	16	78.1	89.4

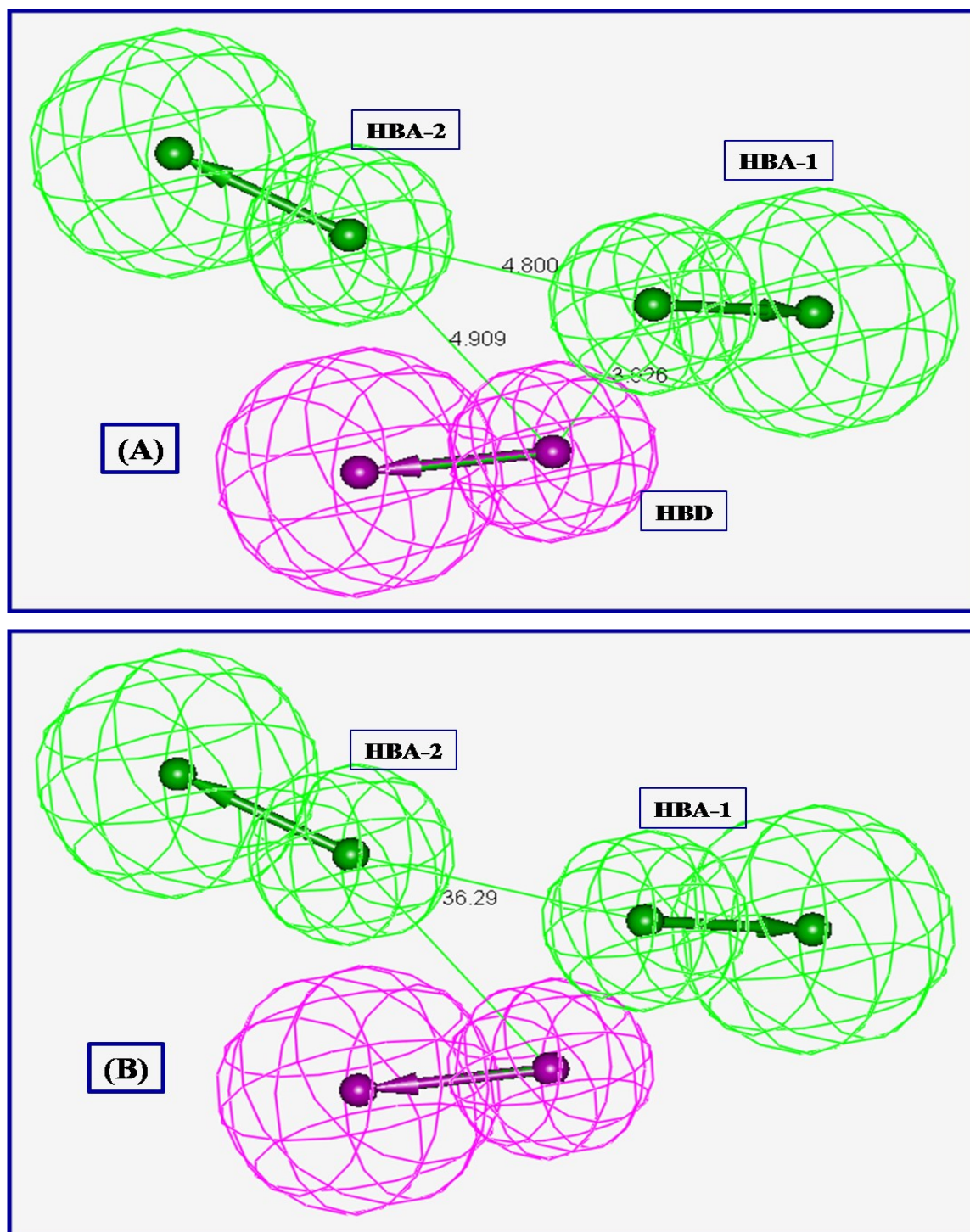
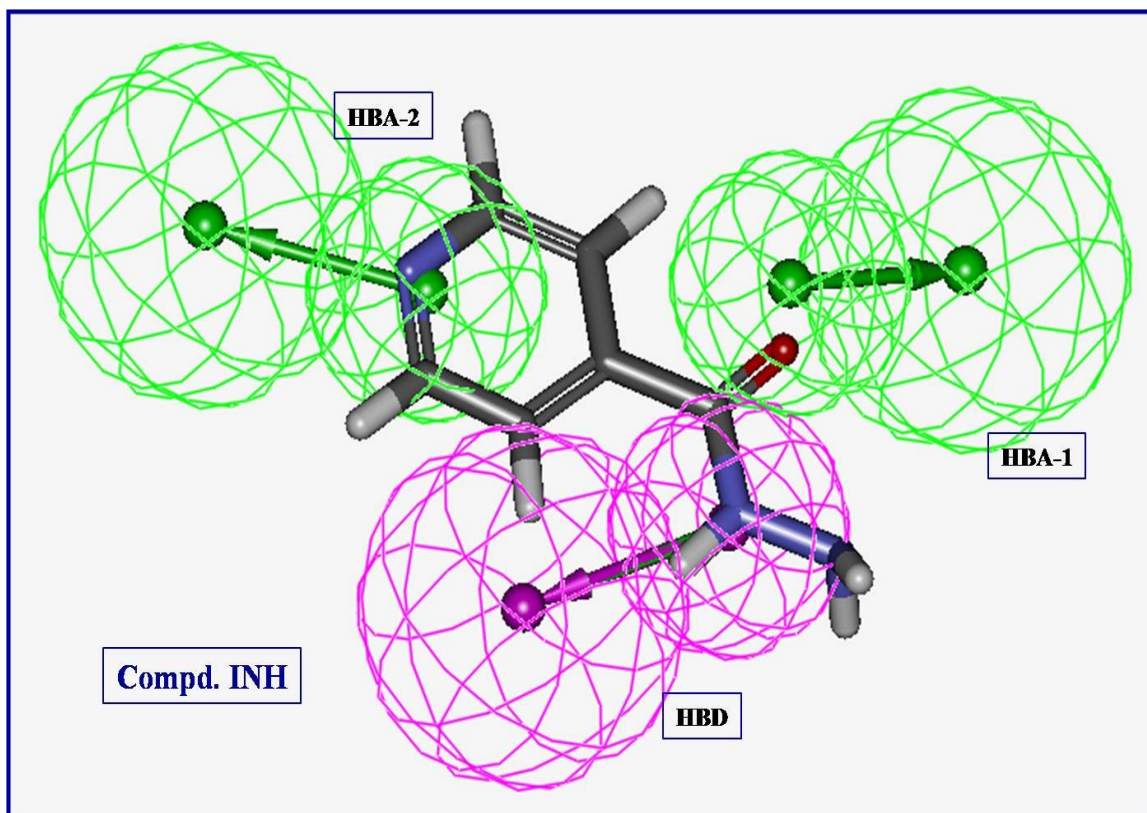
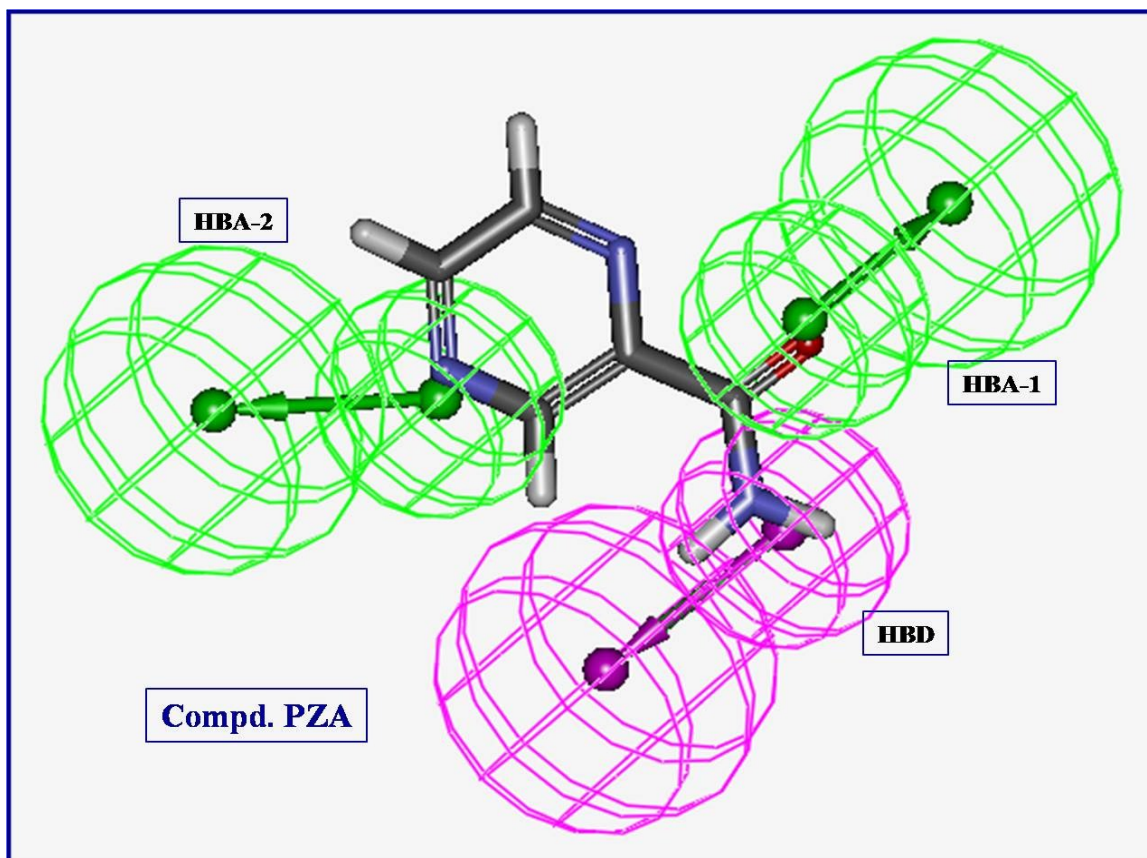
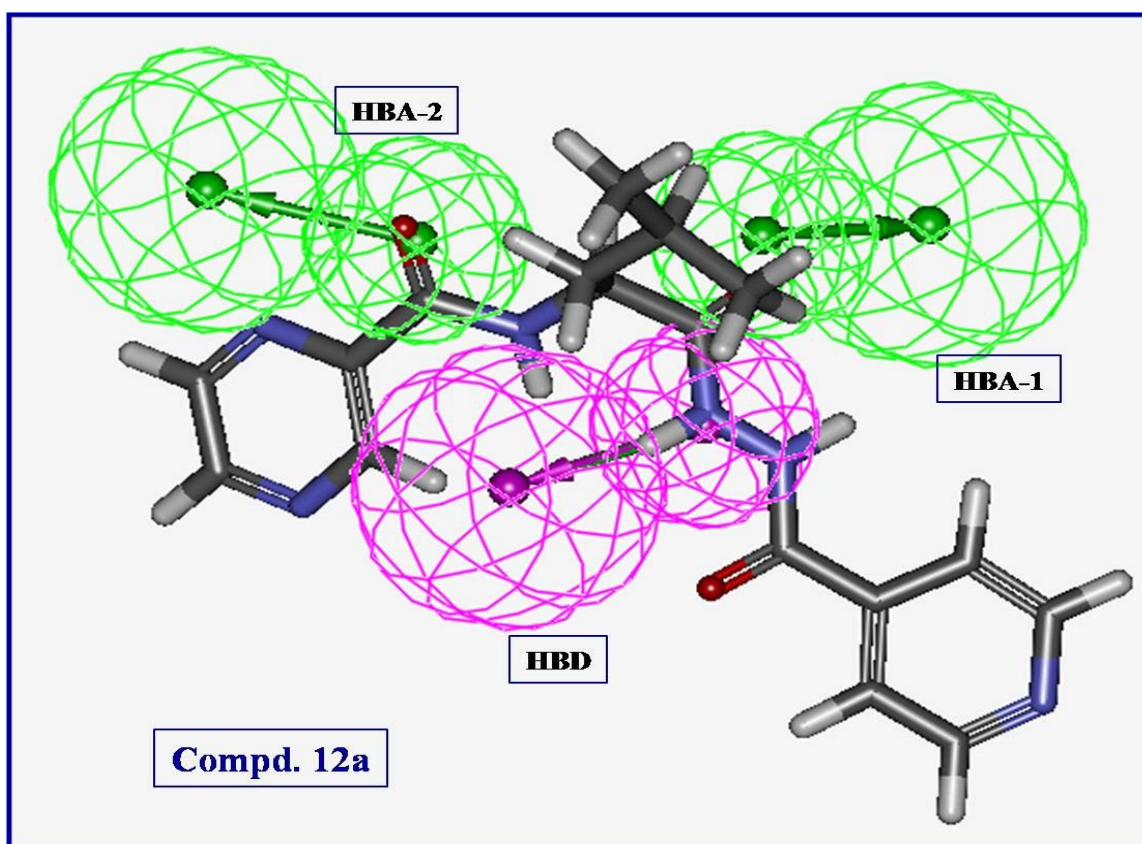
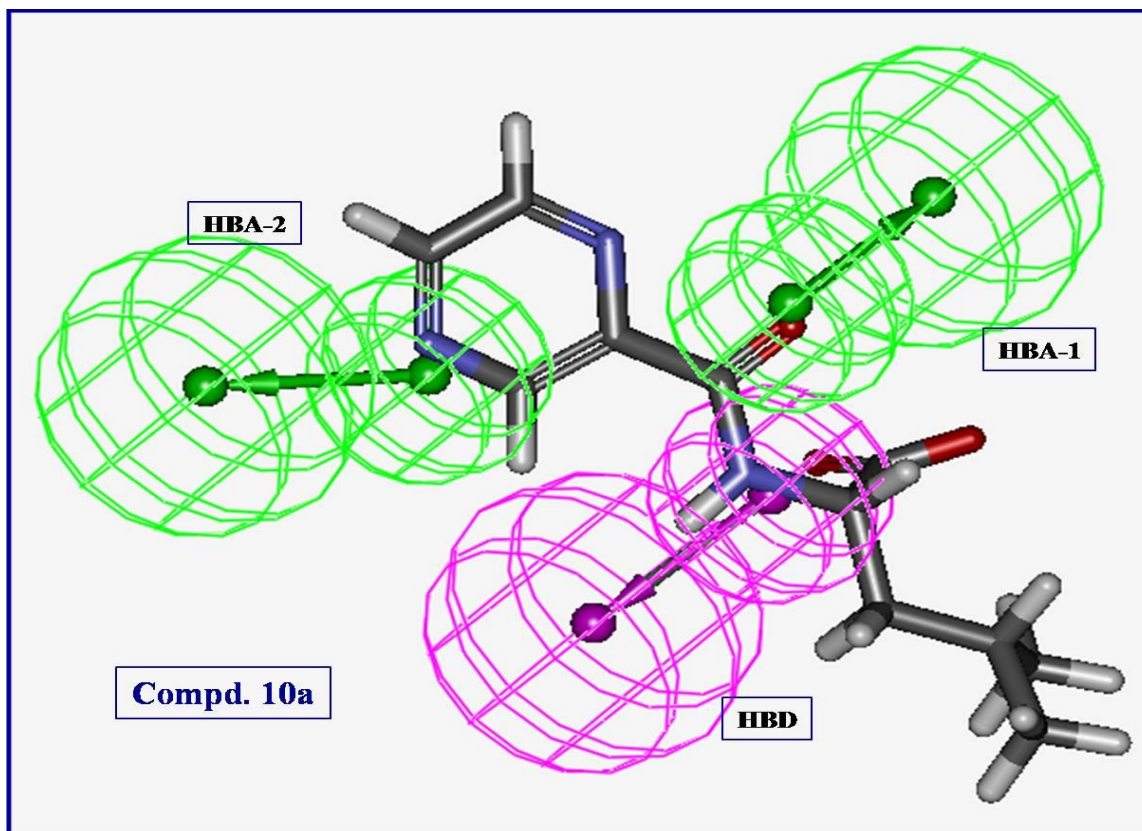
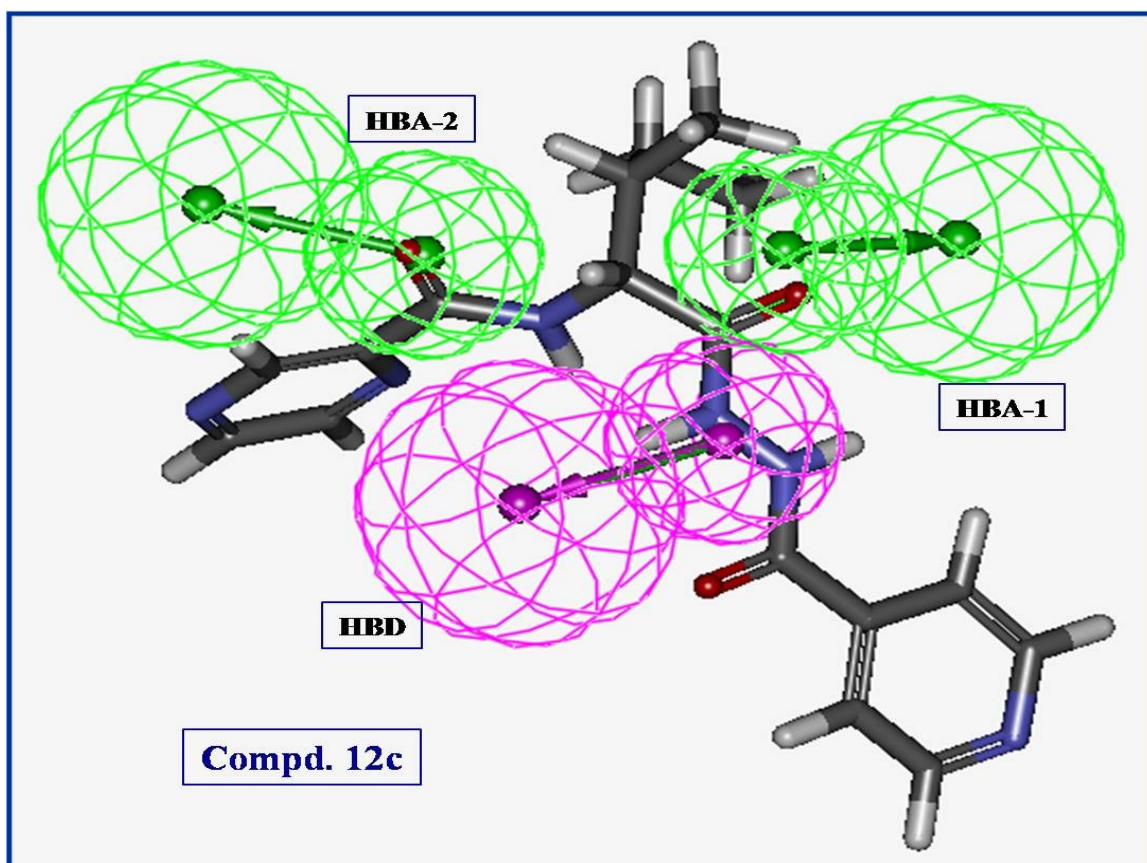
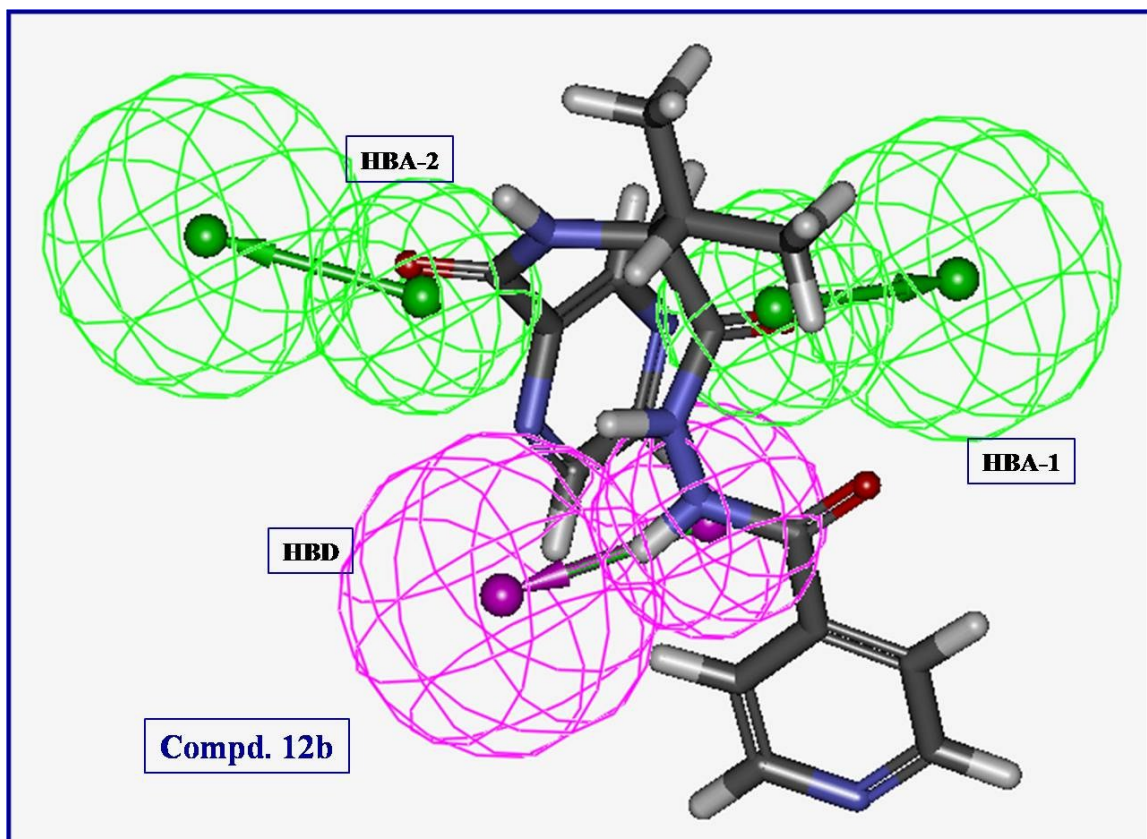
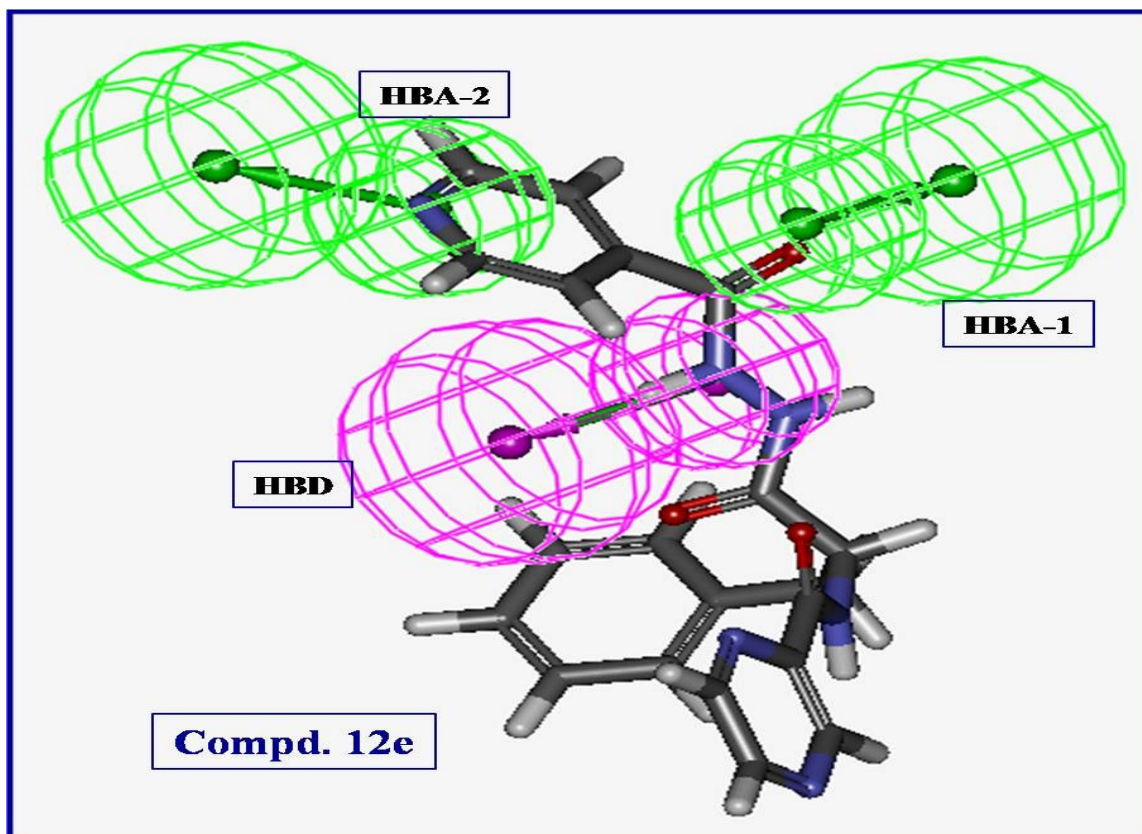
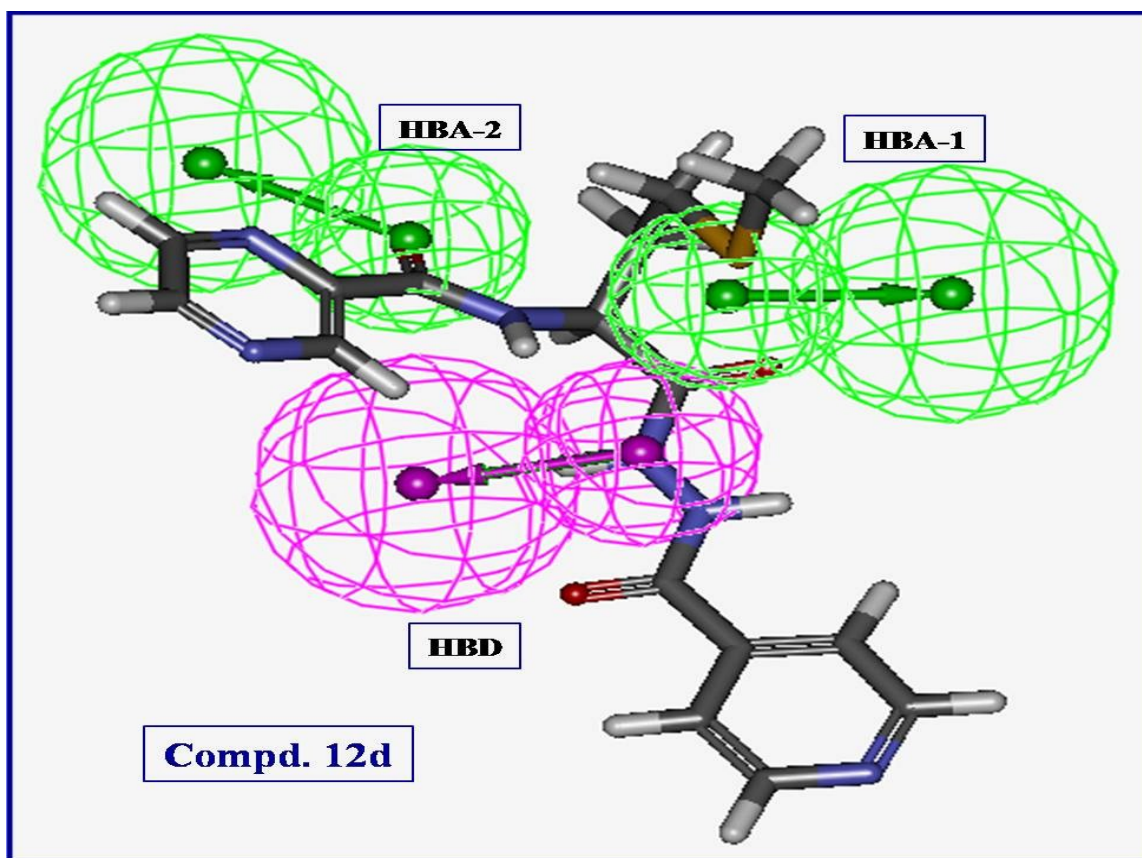


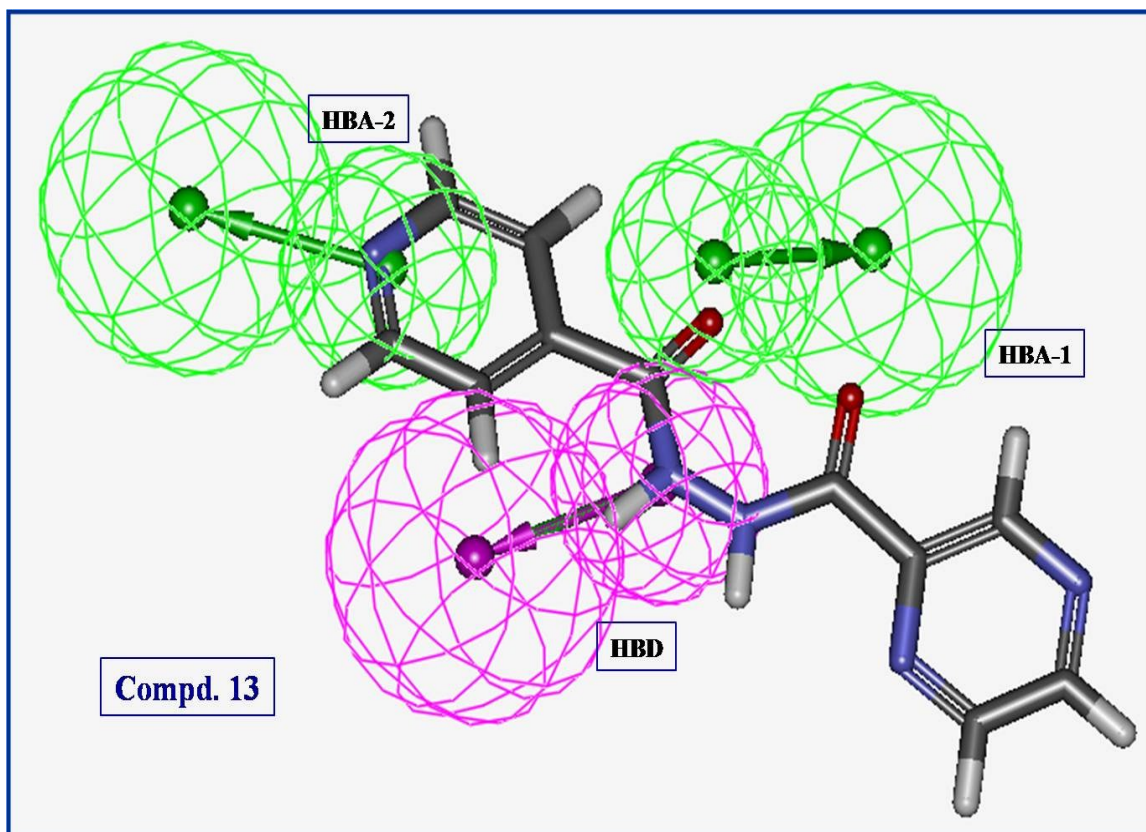
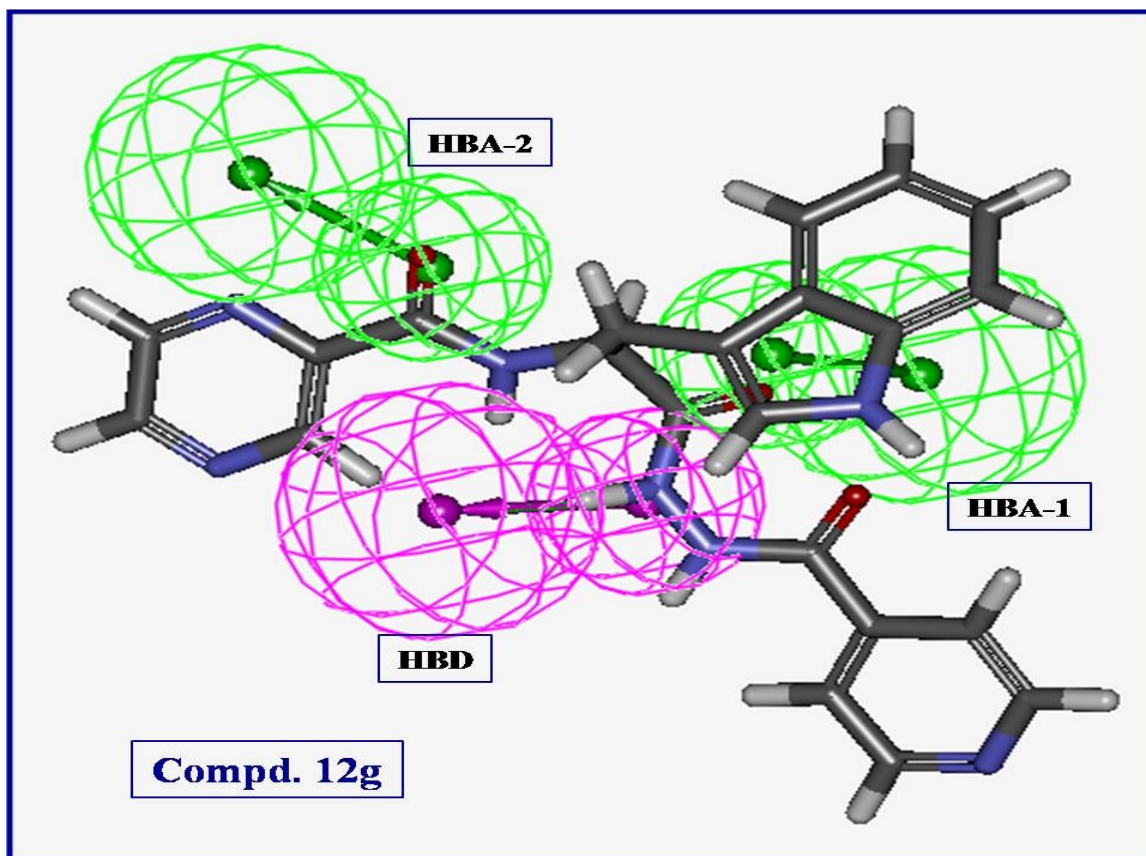
Fig. S1. (A) Constraint distances “HBA-1 – HBA-2 = 4.800, HBA-1 – HBD = 3.026, HBA-2 – HBD = 4.909 Å” and (B) constraint angles “HBA-1 – HBA-2 – HBD = 36.29°” of the generated 3D-pharmacophore for the synthesized bio-active compounds against *Mycobacterium marinum* which contains two hydrogen bonding acceptors (HBA-1, HBA-2; green) and one hydrogen bonding donor (HBD; purple).











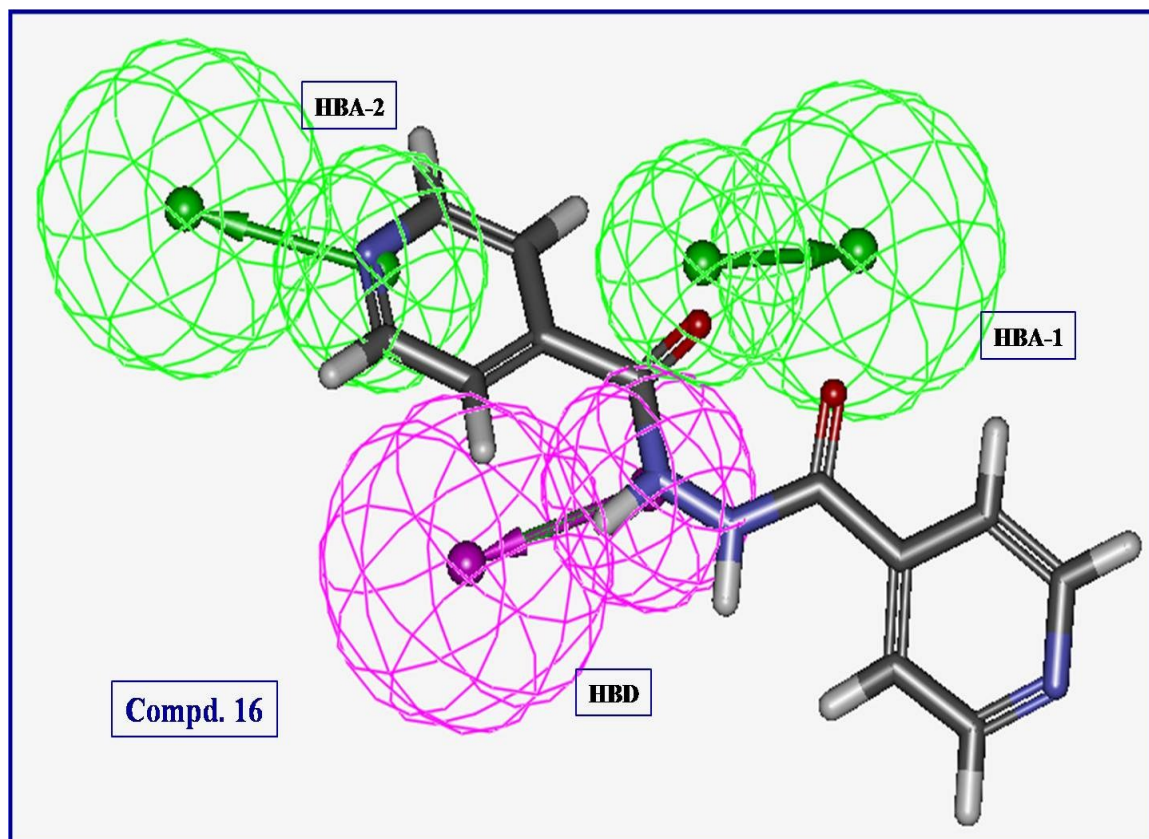


Fig. S2. 3D-pharmacophore mapped on the synthesized bio-active compounds against *Mycobacterium marinum*.

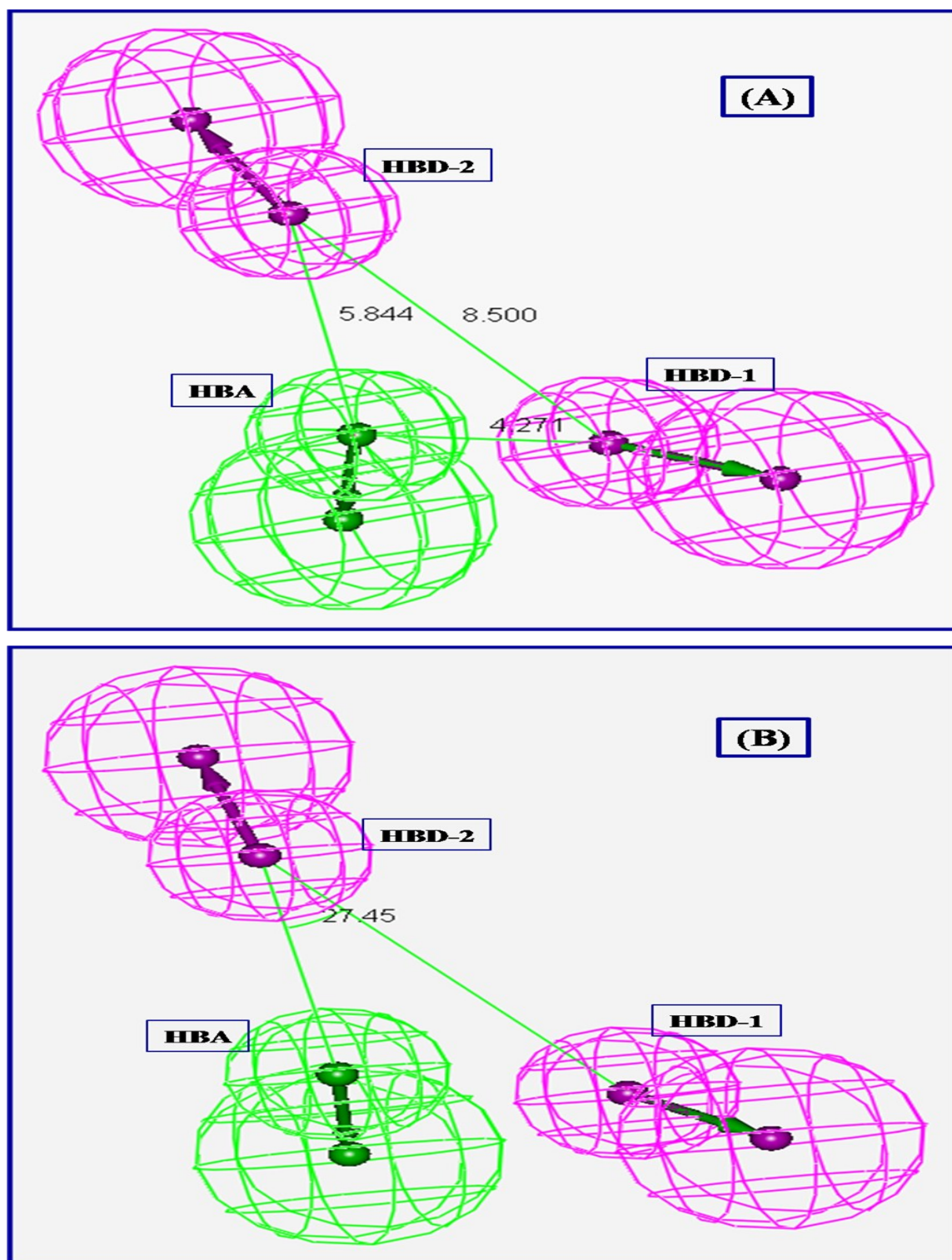
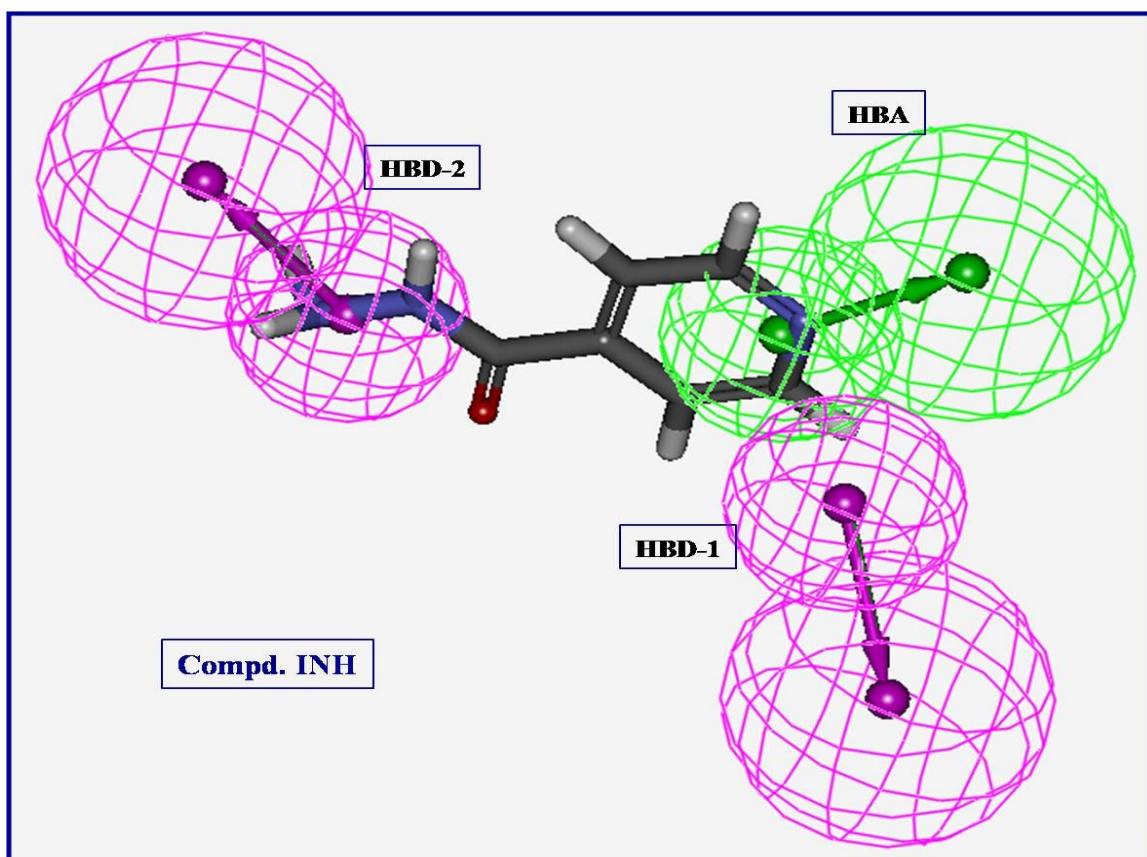
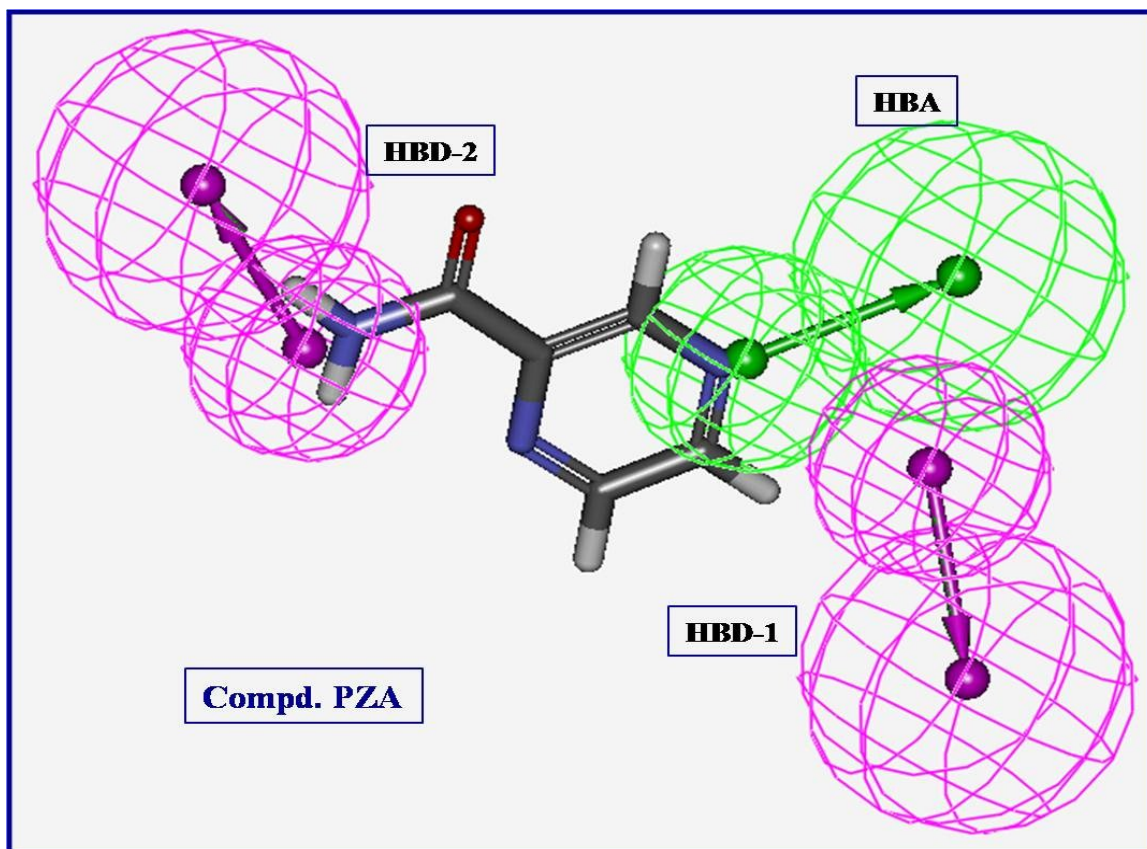
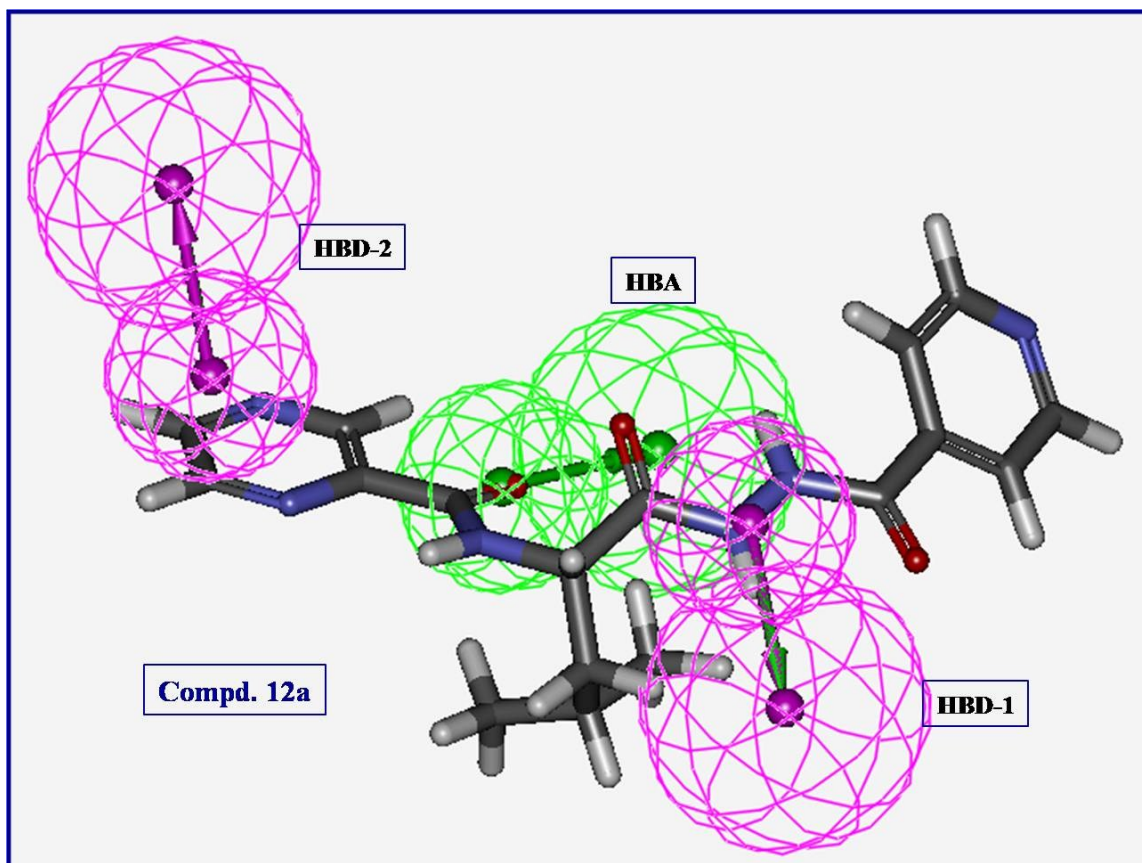
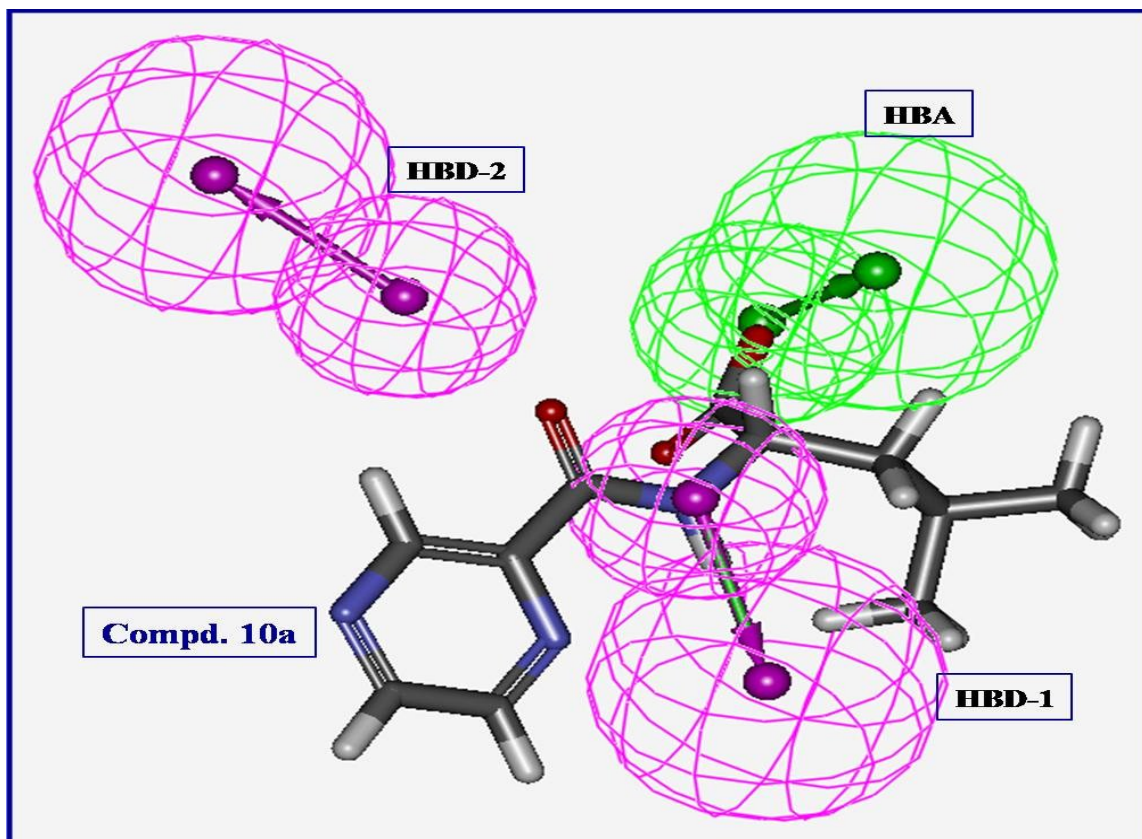
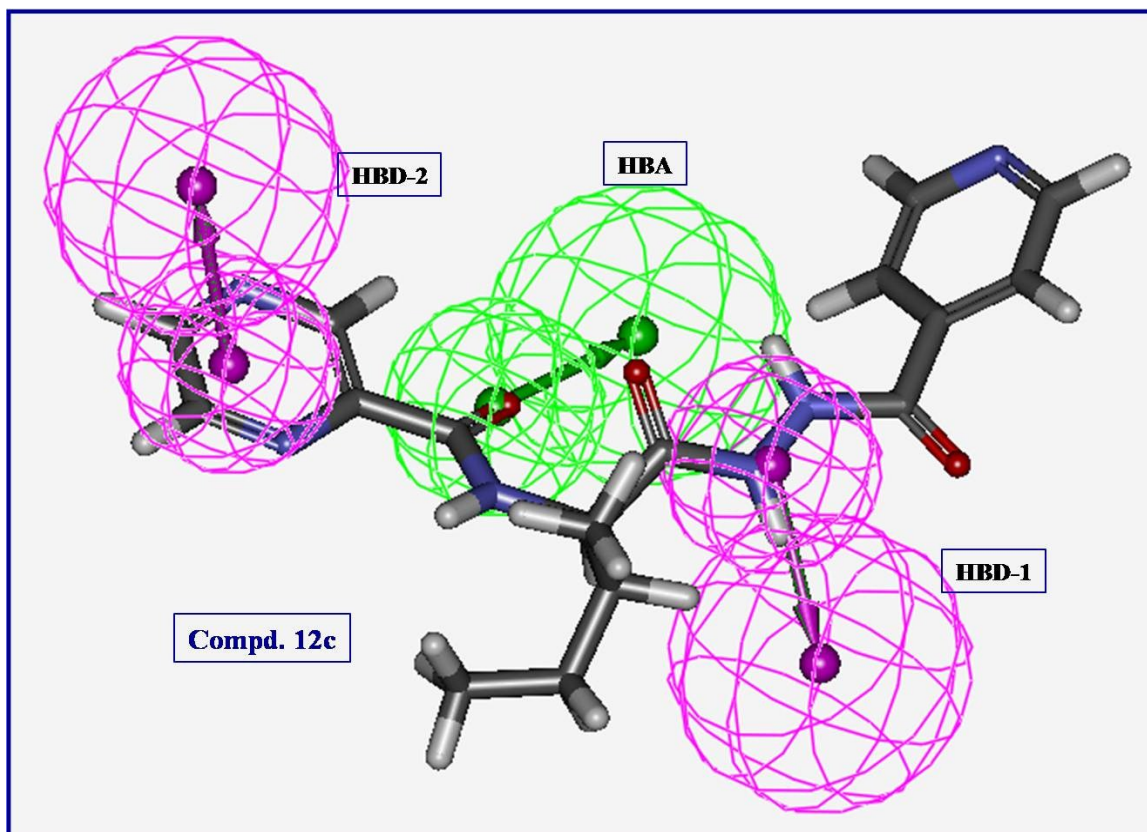
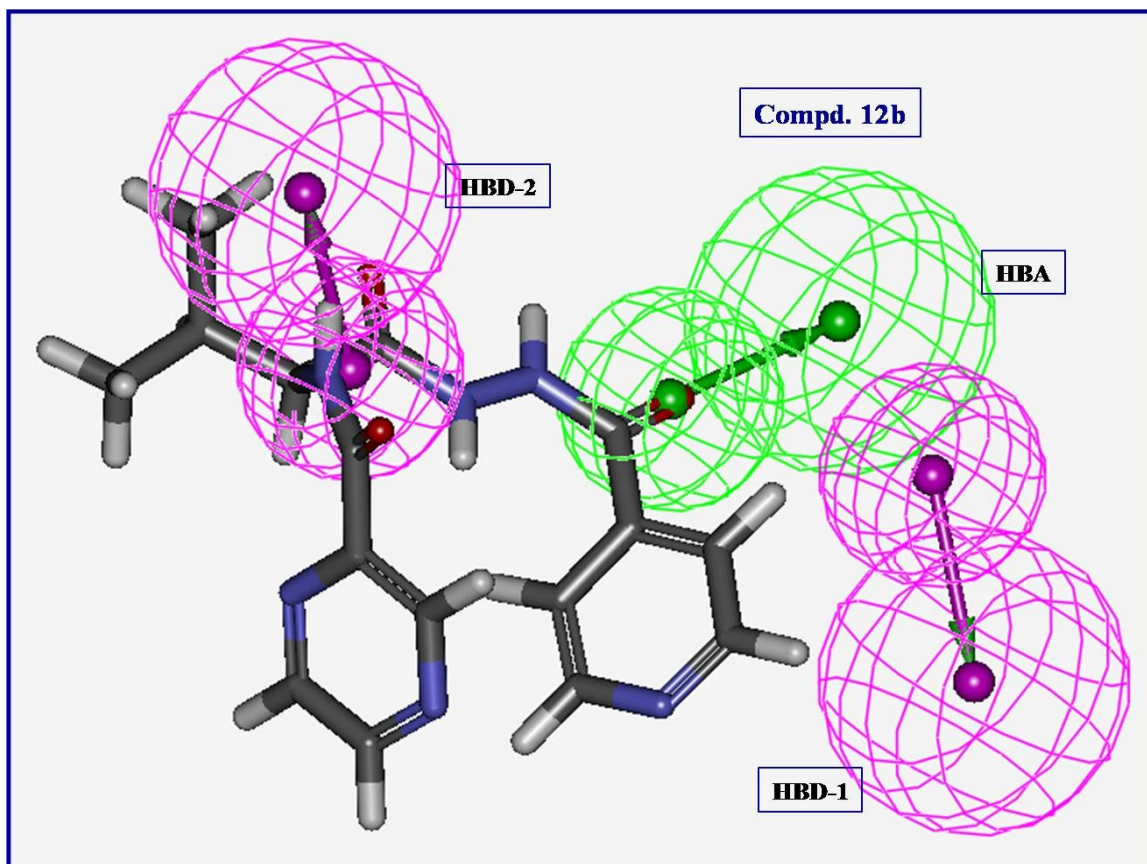
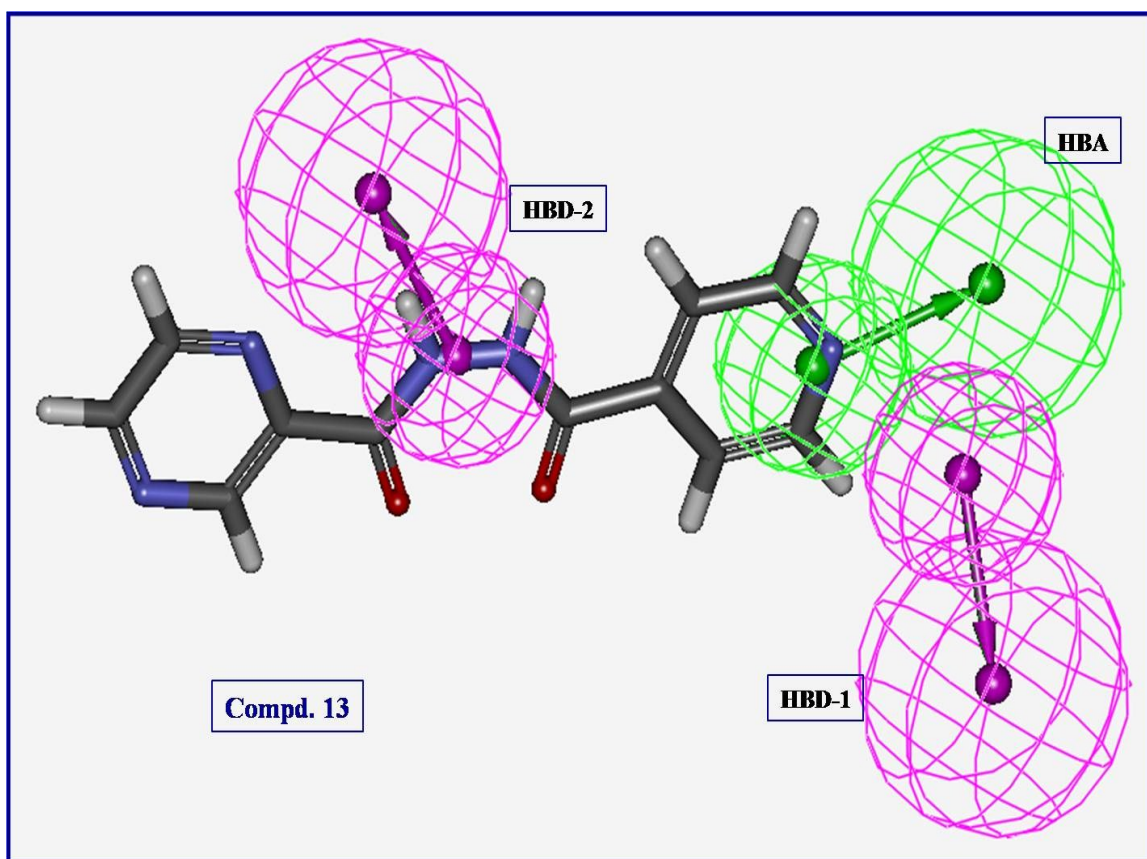
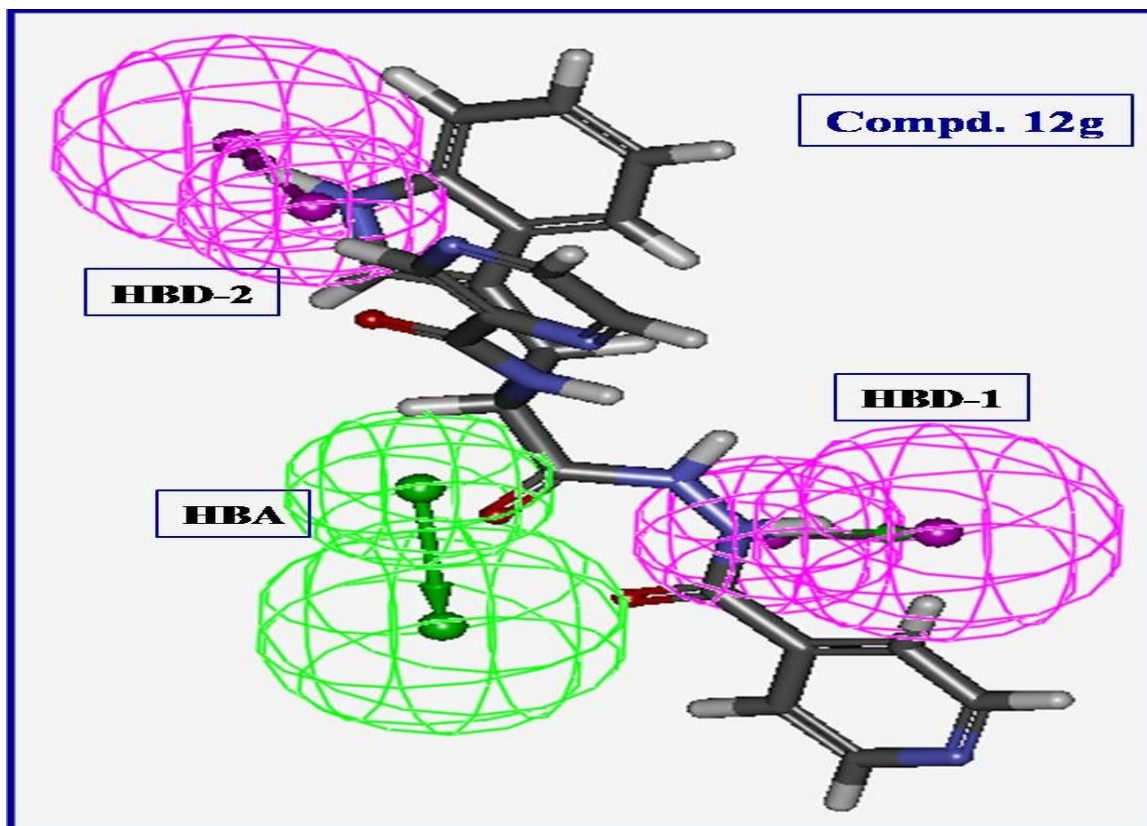


Fig. S3. (A) Constraint distances “HBD-1 – HBD-2 = 8.500, HBD-1 – HBA = 4.271, HBD-2 – HBA = 5.844 Å” and (B) constraint angles “HBD-1 – HBD-2 – HBA = 27.45°” of the generated 3D-pharmacophore for the synthesized bio-active compounds against *Mycobacterium fortuitum* which contains two hydrogen bonding donors (HBD-1, HBD-2; purple) and one hydrogen bonding acceptor (HBA; green).









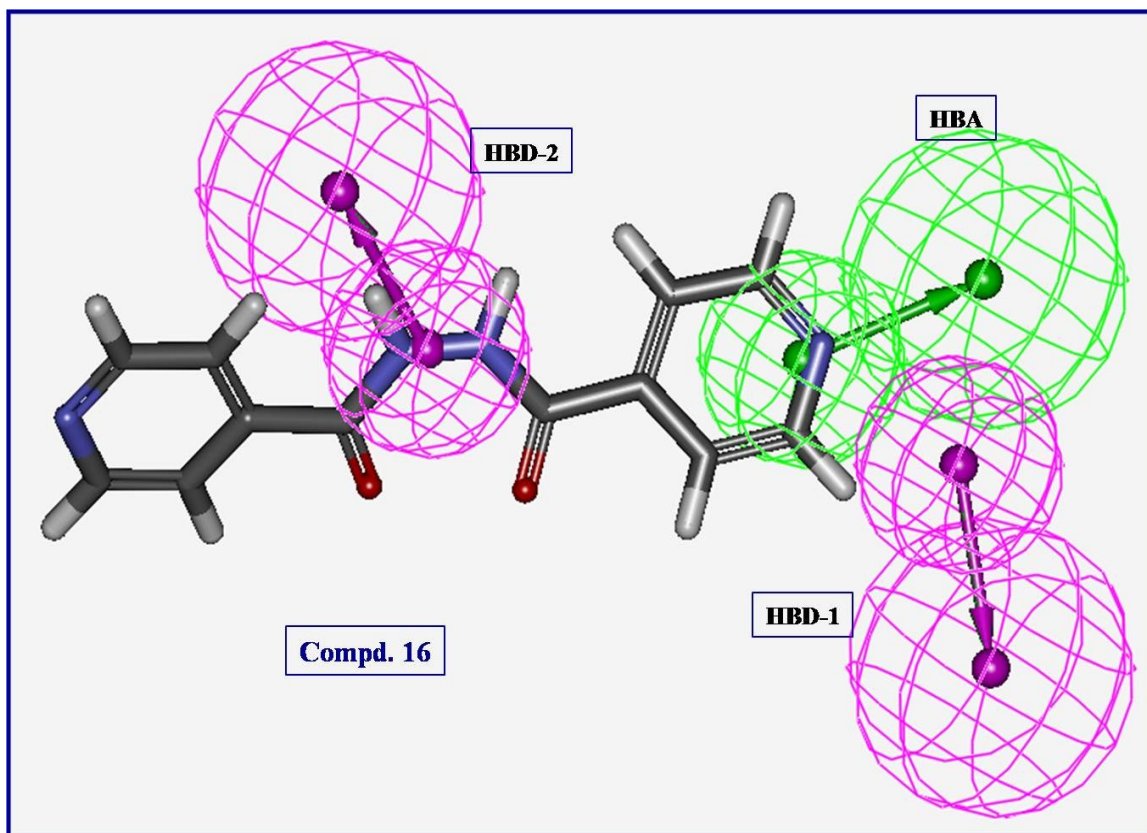


Fig. S4. 3D-pharmacophore mapped on the synthesized bio-active compounds against *Mycobacterium fortuitum*.

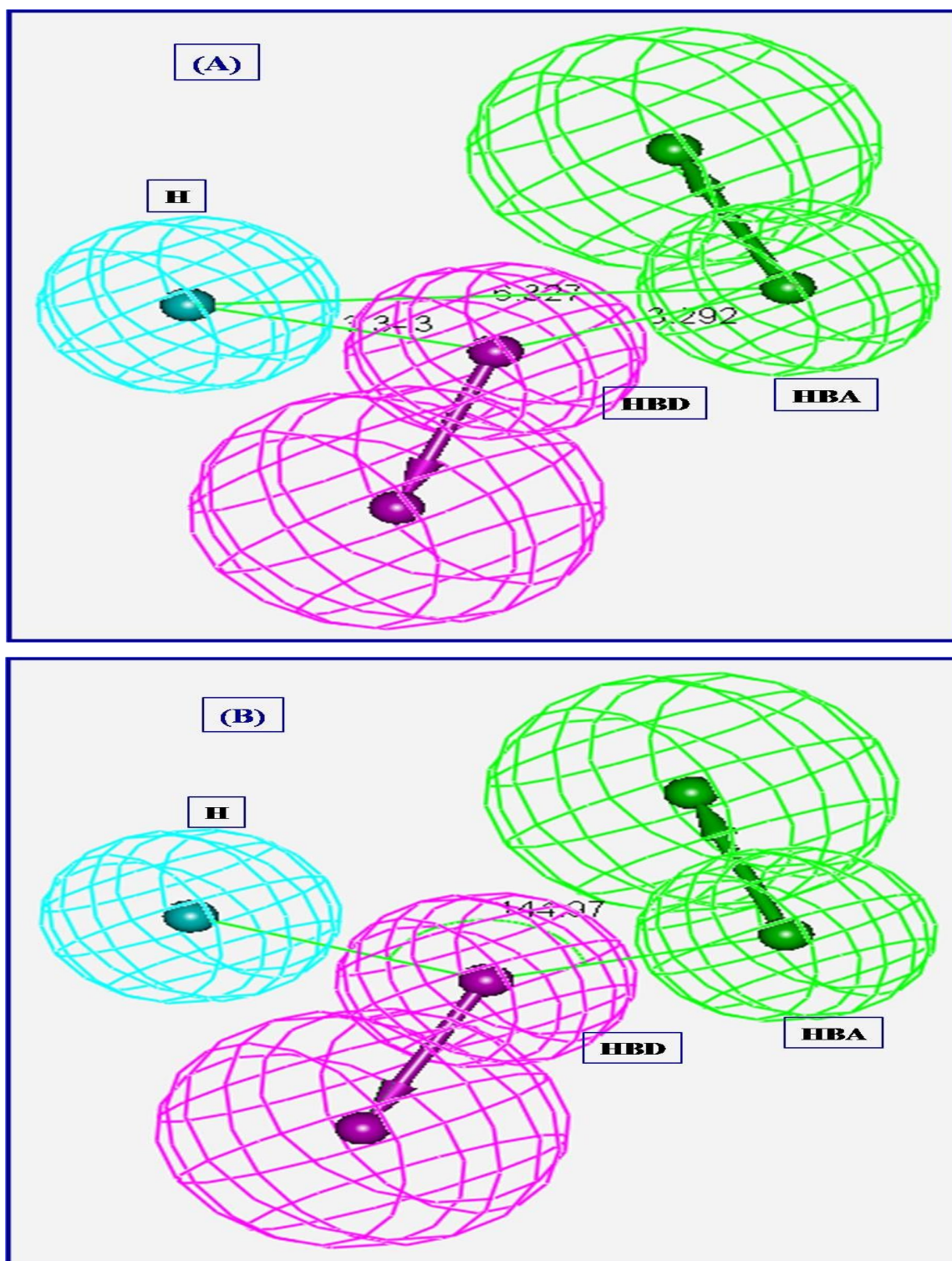
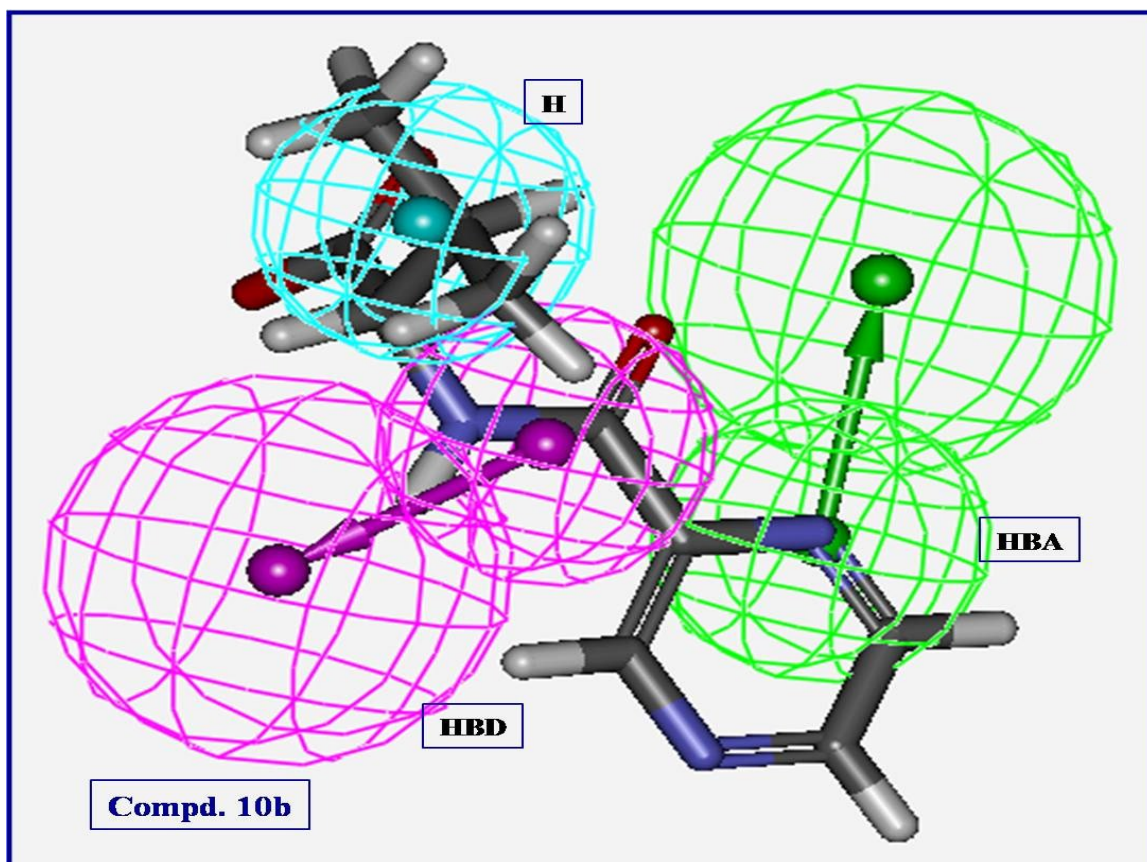
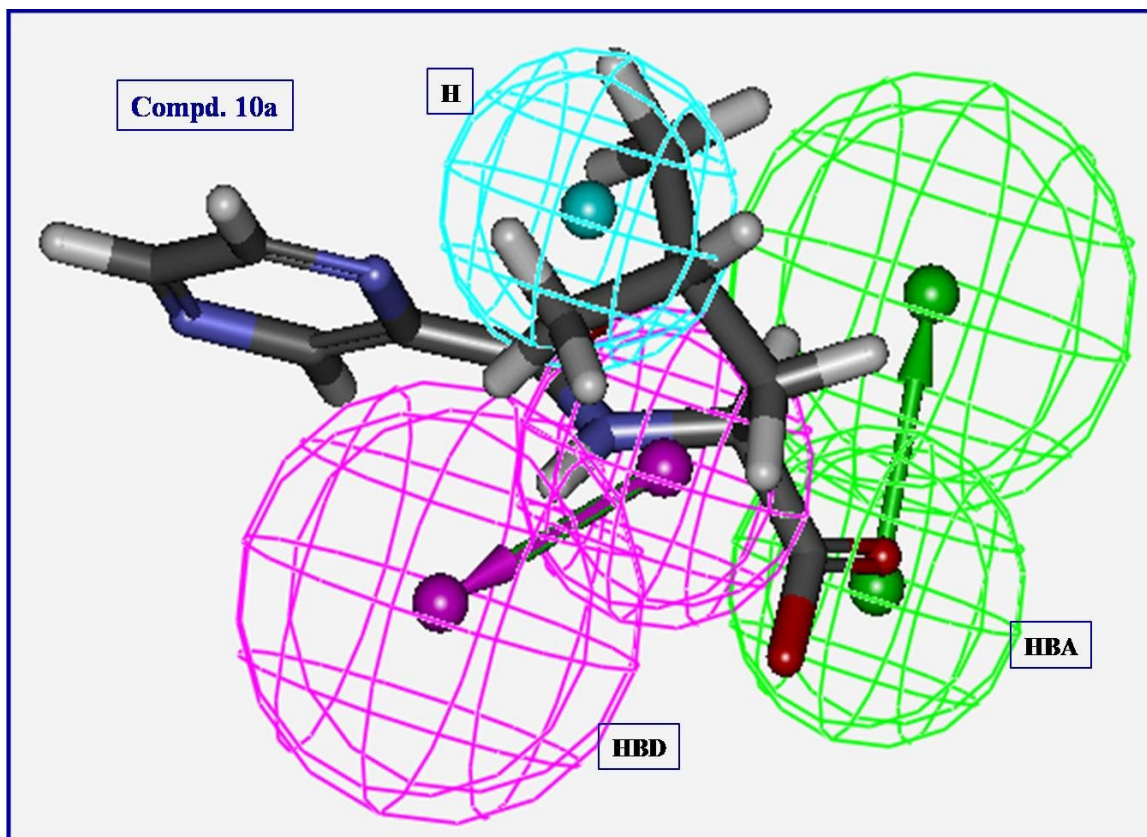
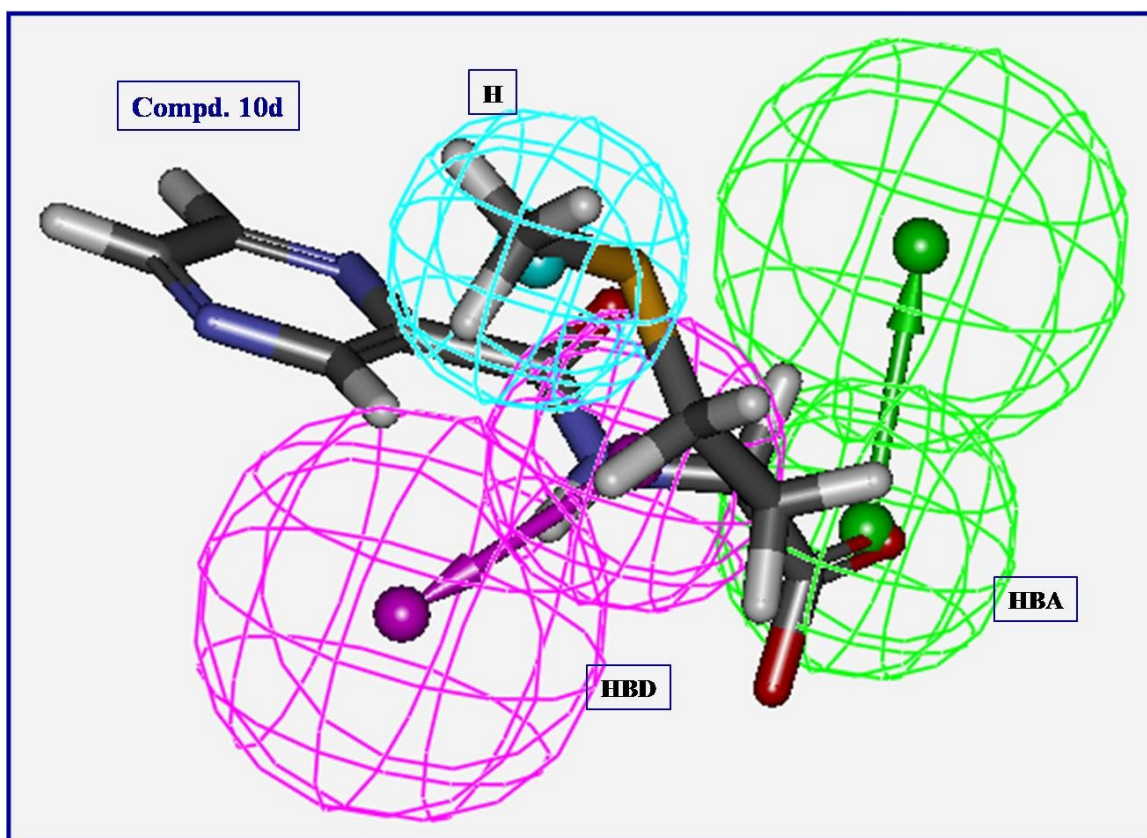
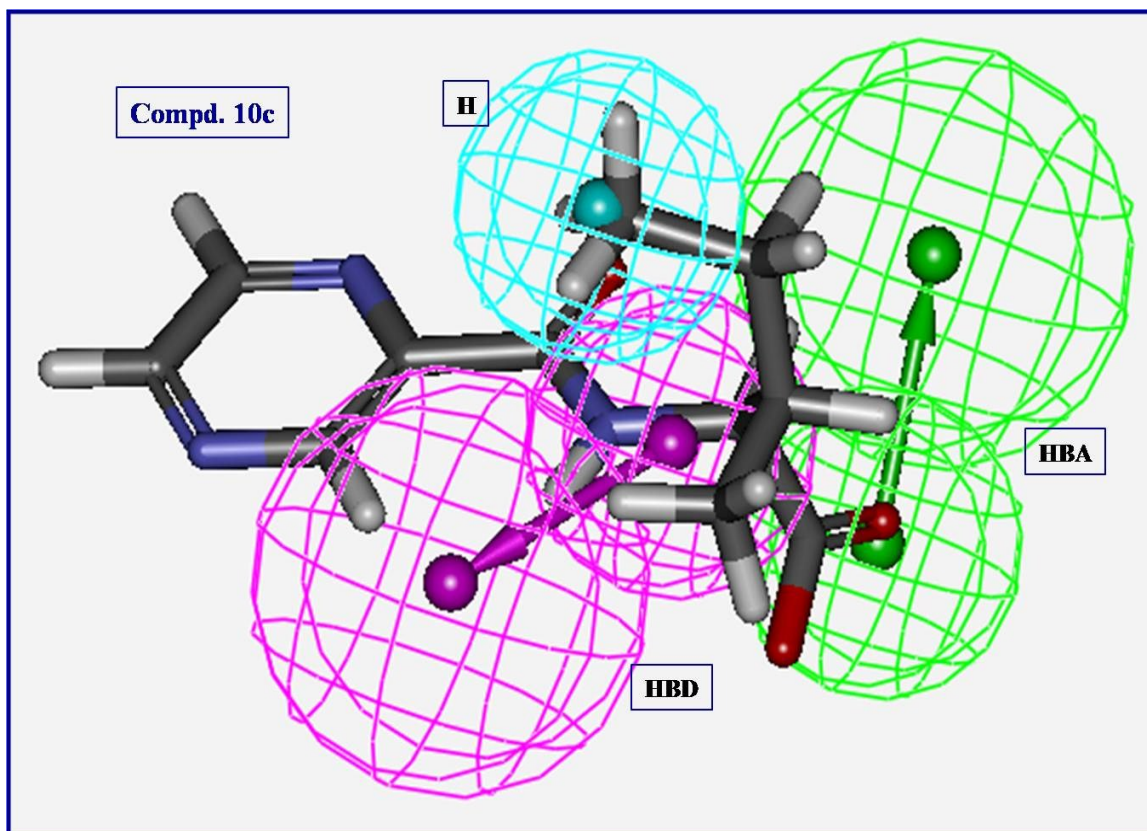
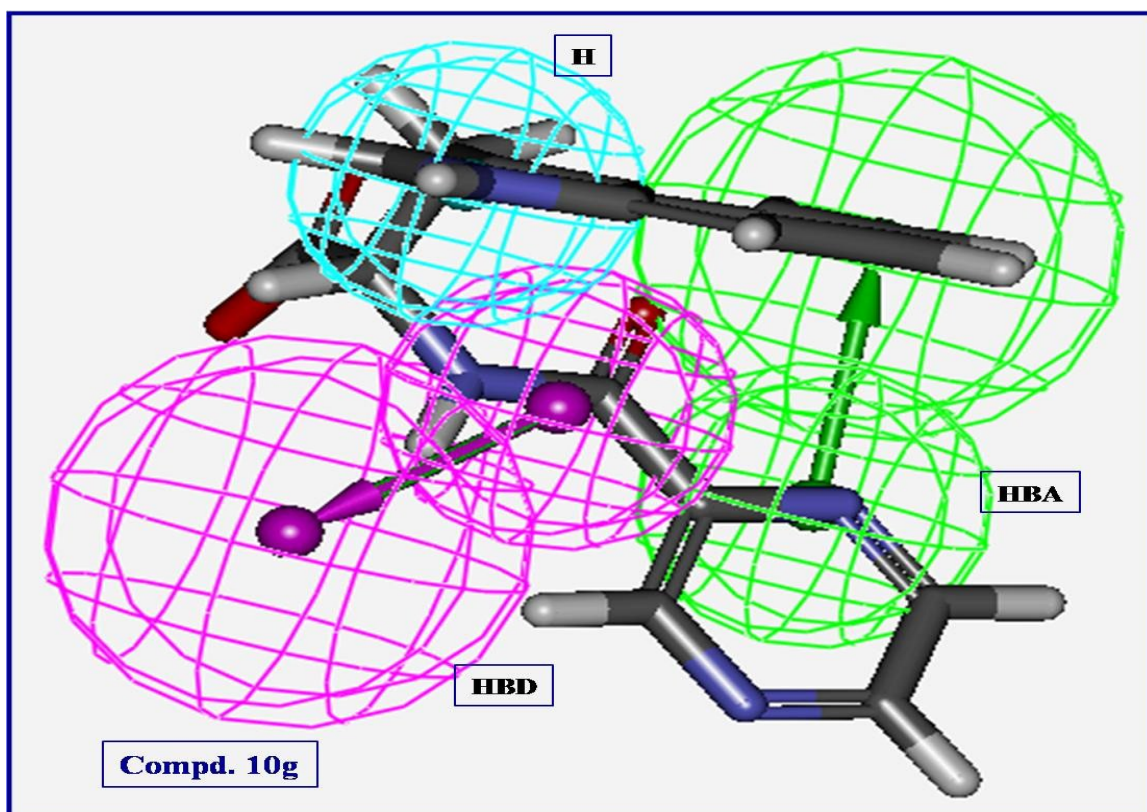
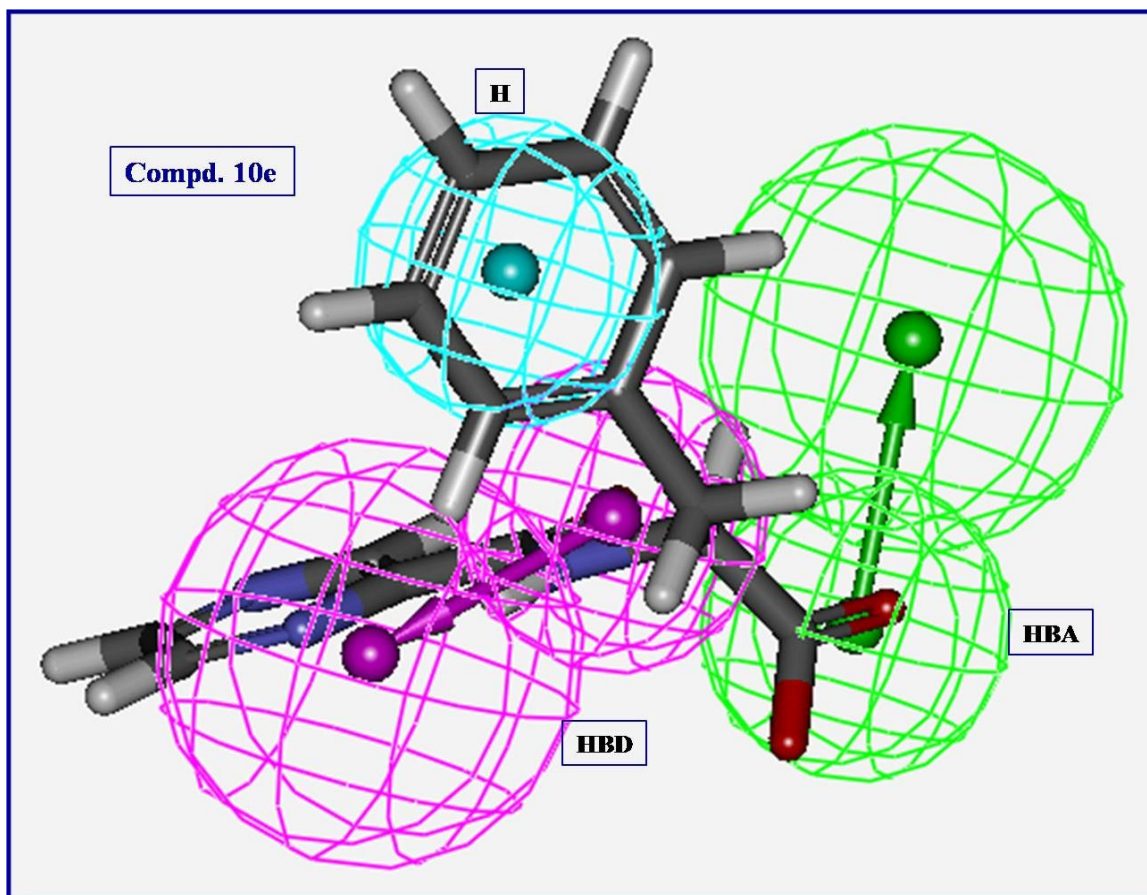
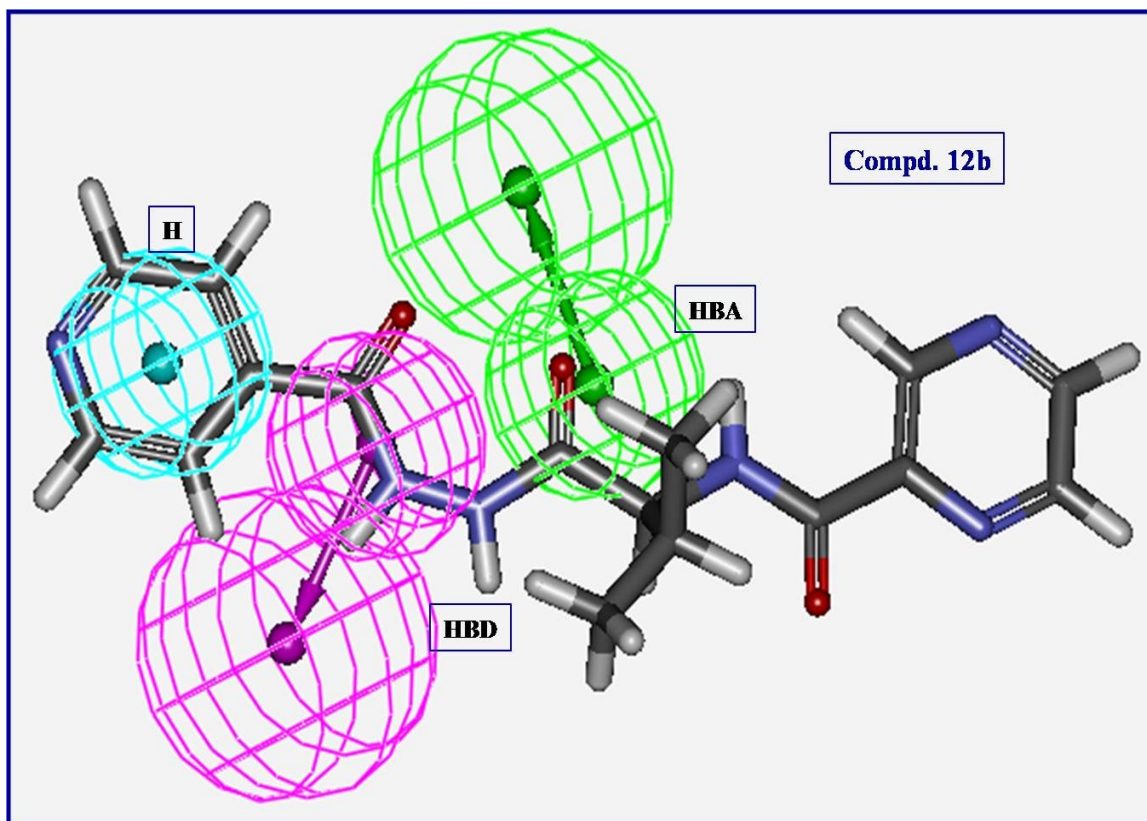
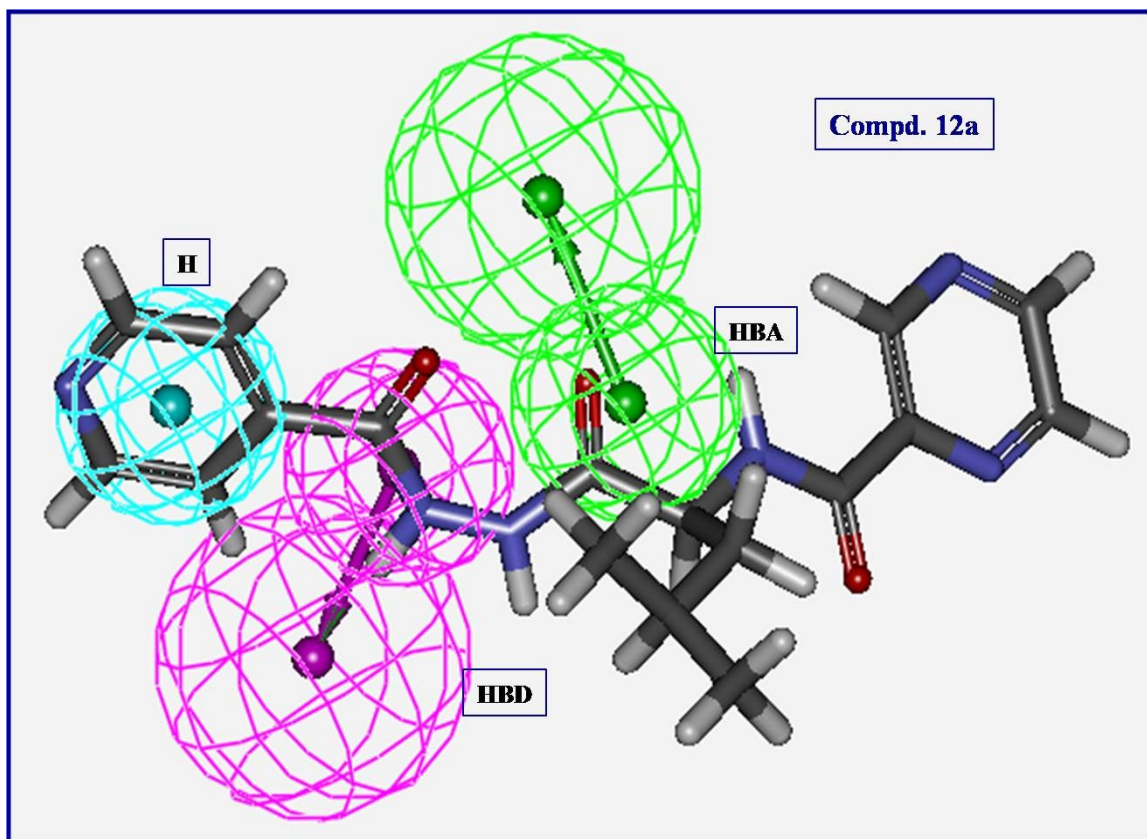


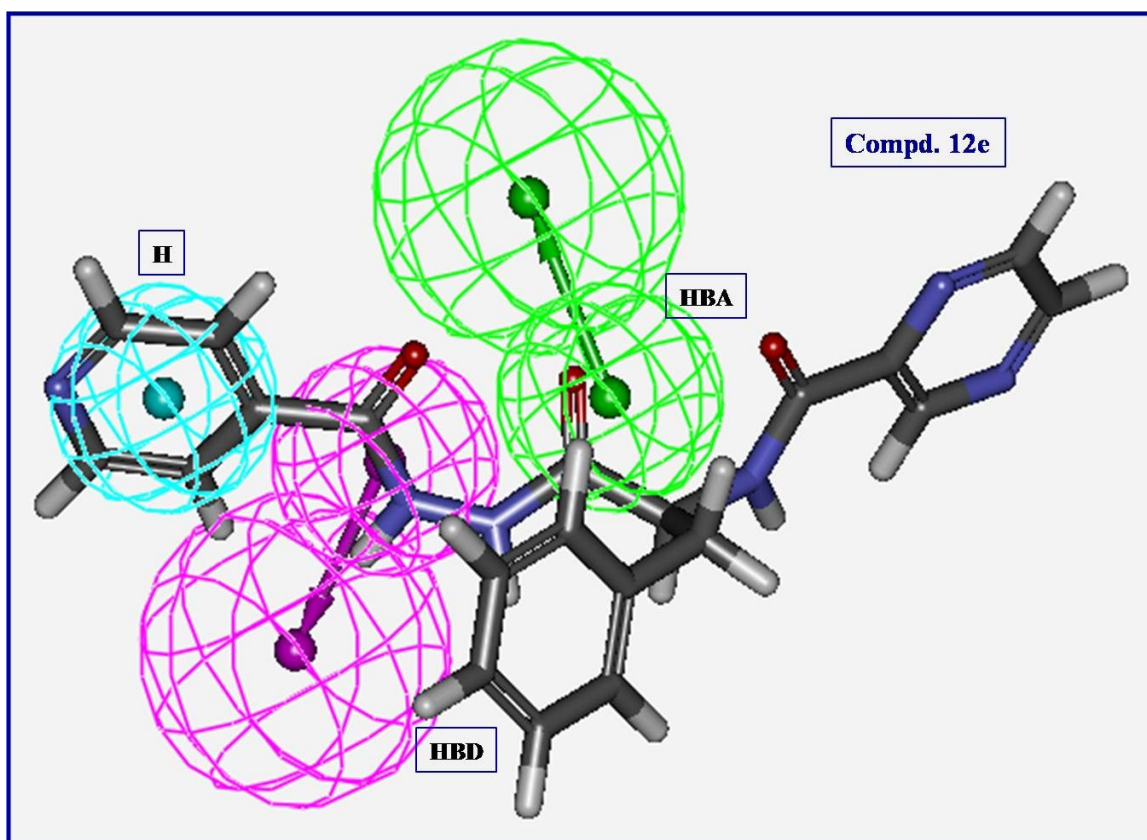
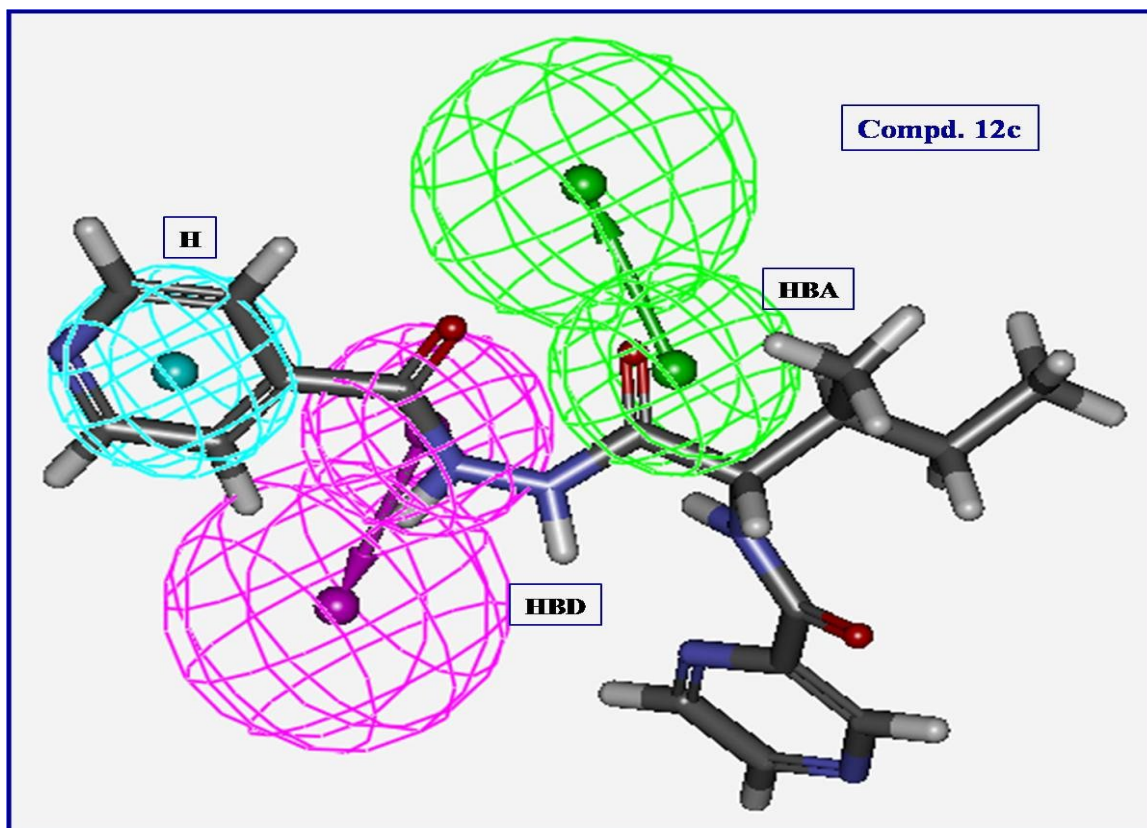
Fig. S5. (A) Constraint distances “HBA – HBD = 3.292, HBA – H = 6.327, HBD – H = 3.343 Å” and (B) constraint angles “HBA – HBD – H = 144.97 °” of the generated 3D-pharmacophore for the synthesized bio-active compounds against *Mycobacterium tuberculosis* which contains hydrogen bonding acceptor (HBA; green), hydrogen bonding donor (HBD; purple) and hydrophobic (H; light blue).











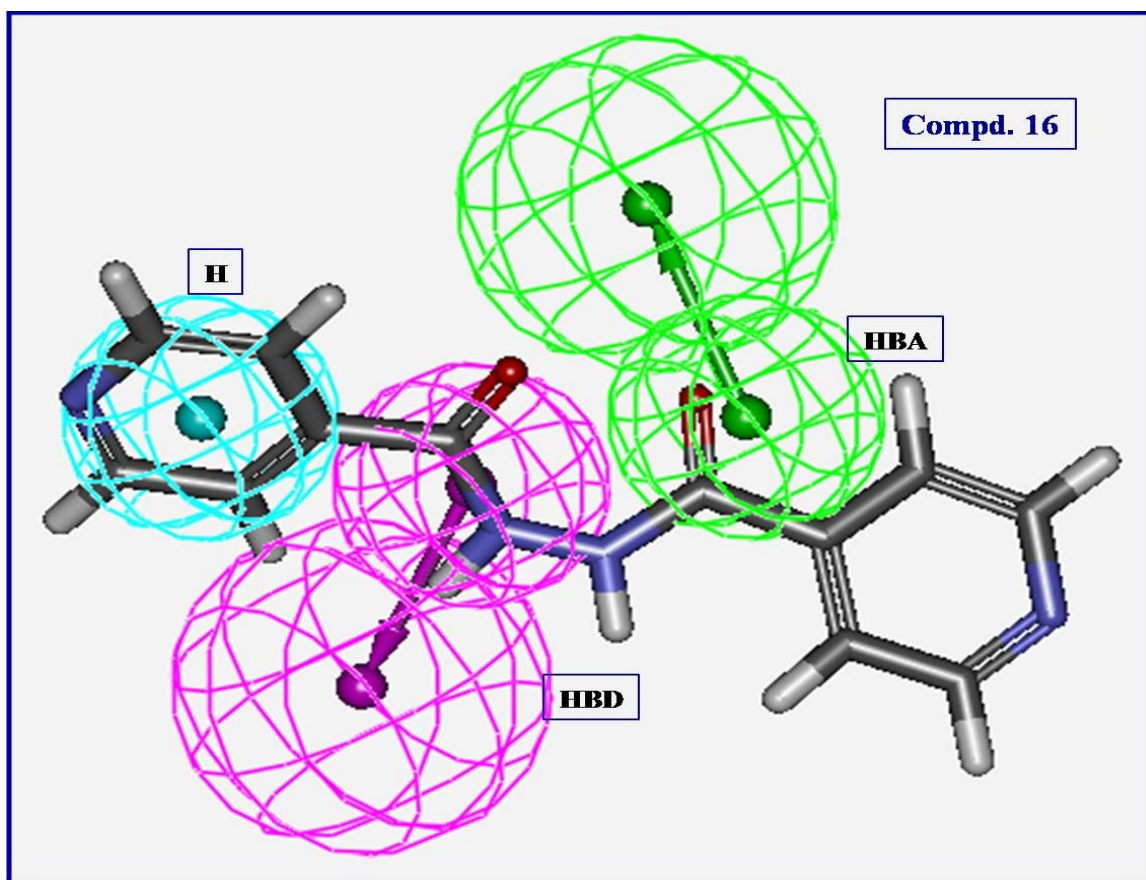
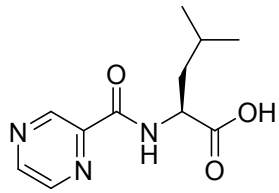
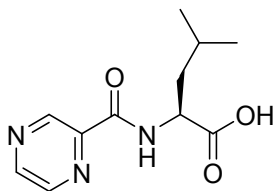
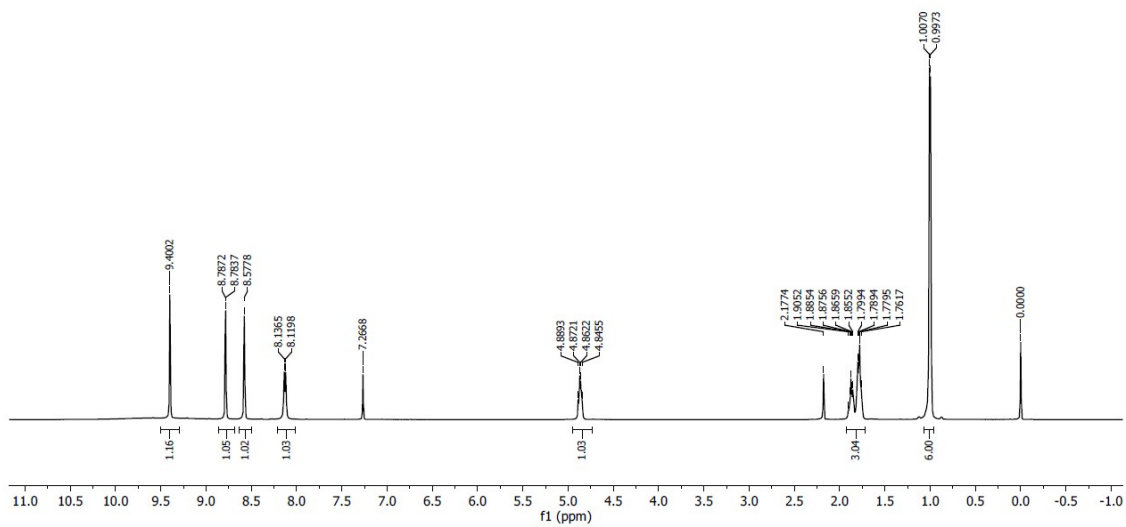


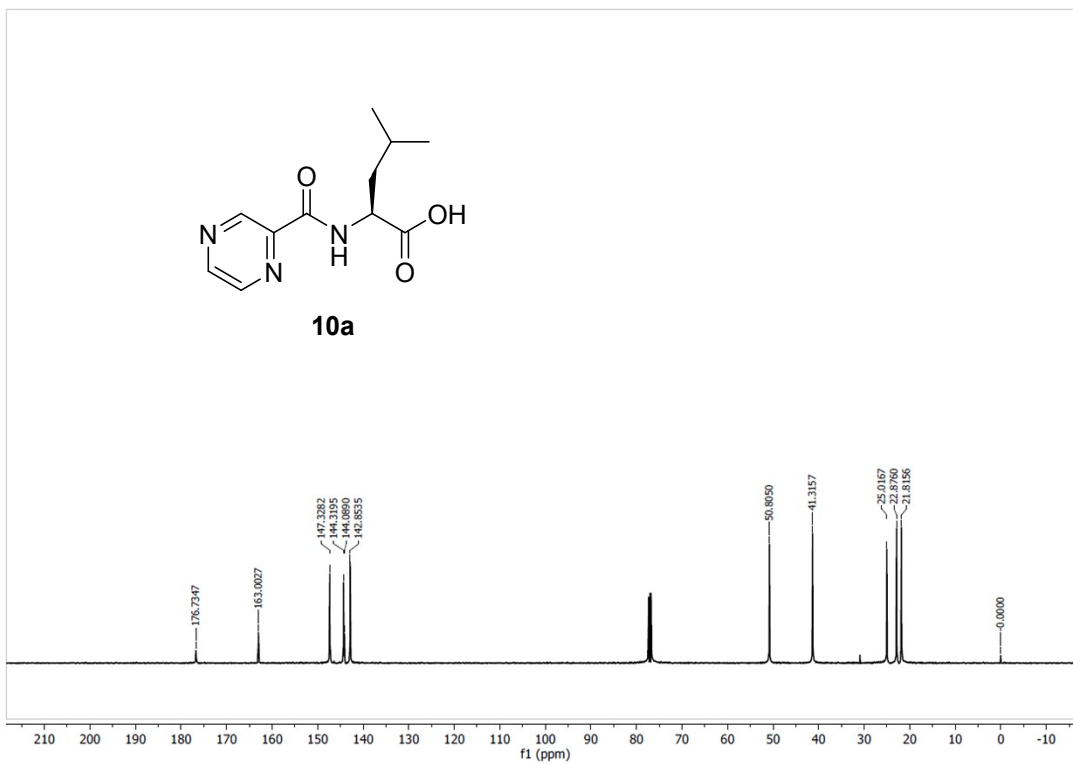
Fig. S6. 3D-pharmacophore mapped on the synthesized bio-active compounds against *Mycobacterium tuberculosis*.

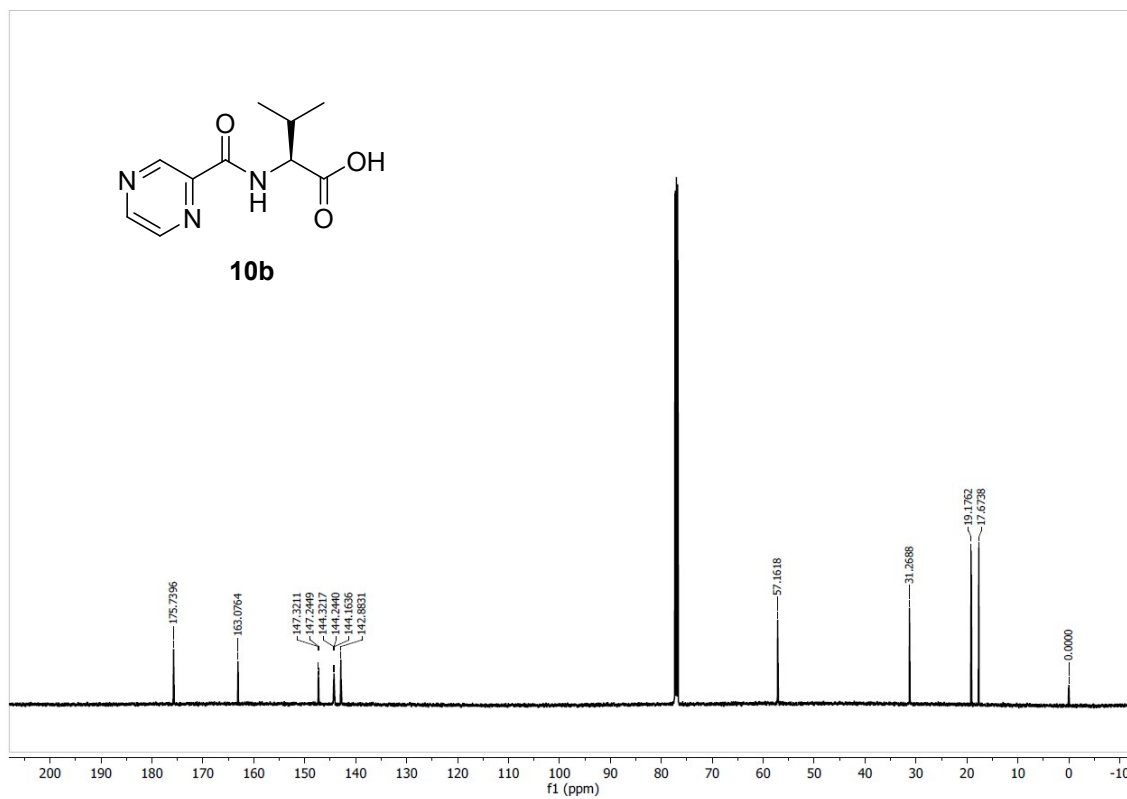
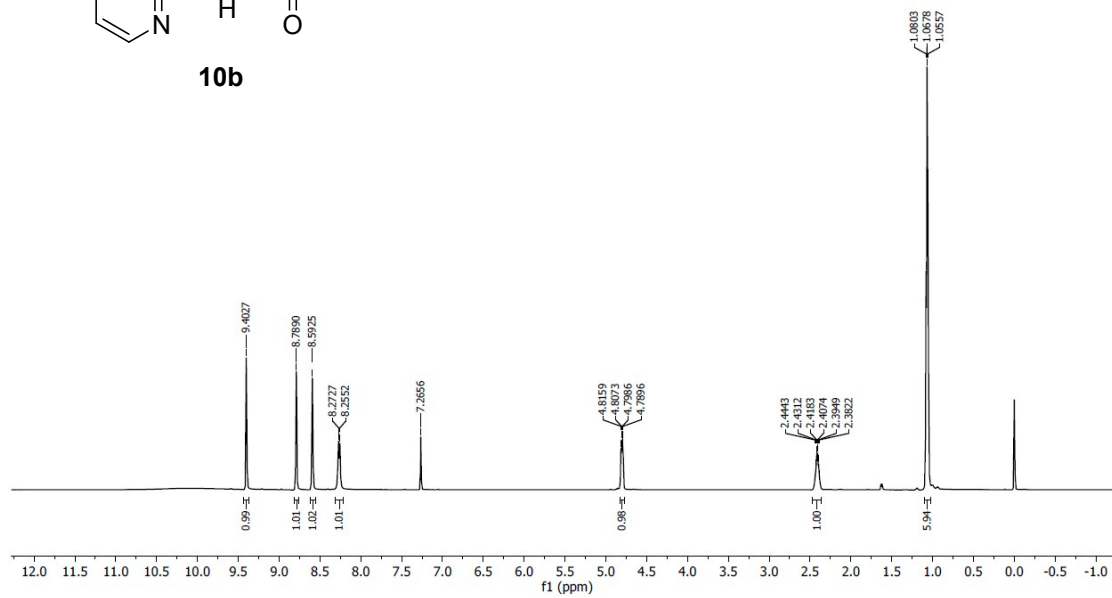
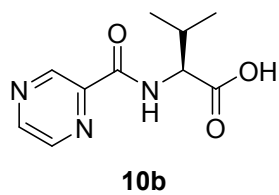


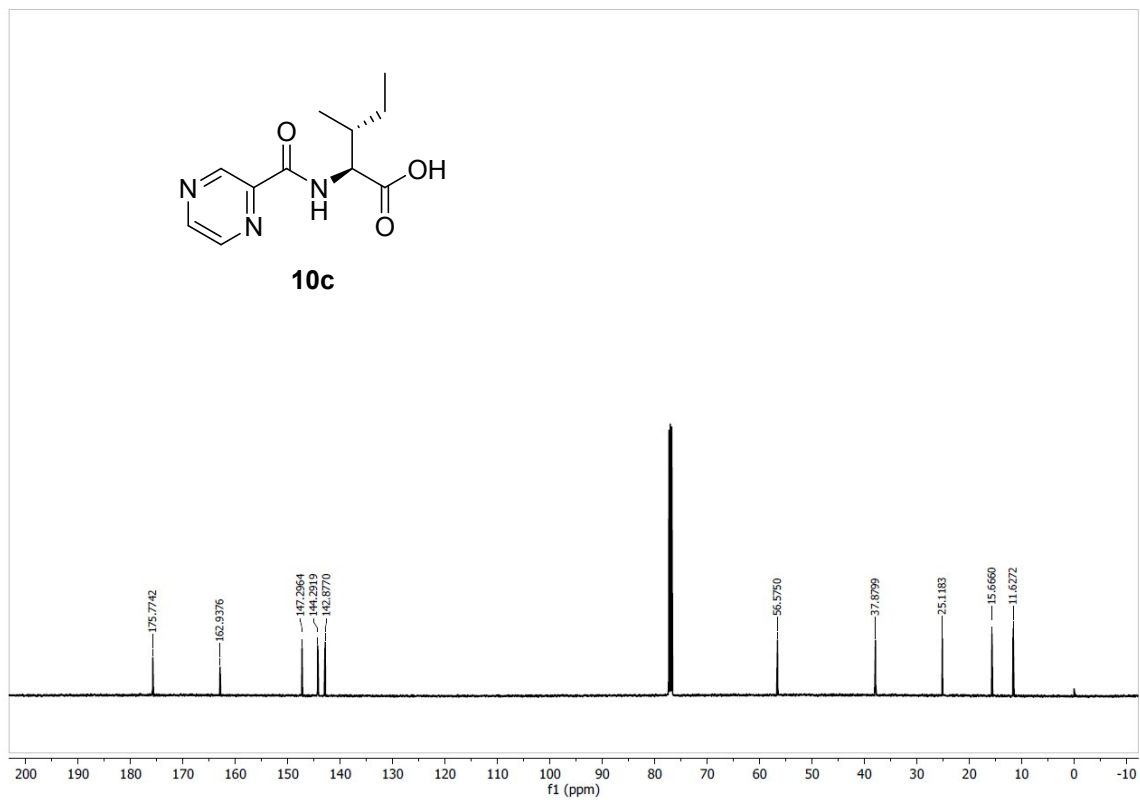
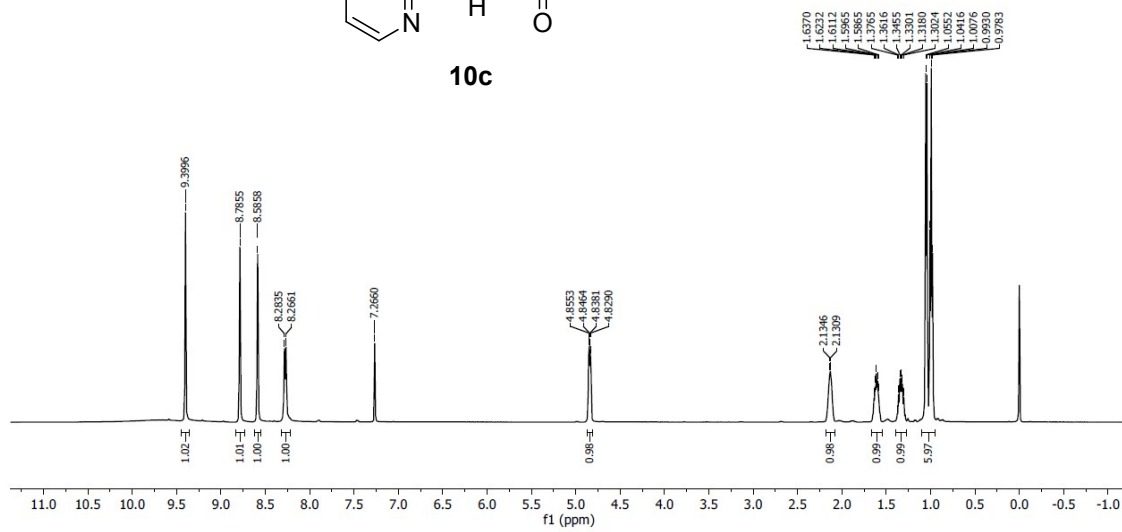
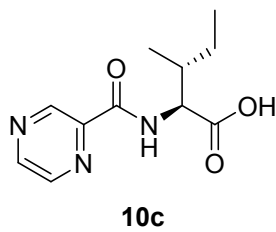
10a

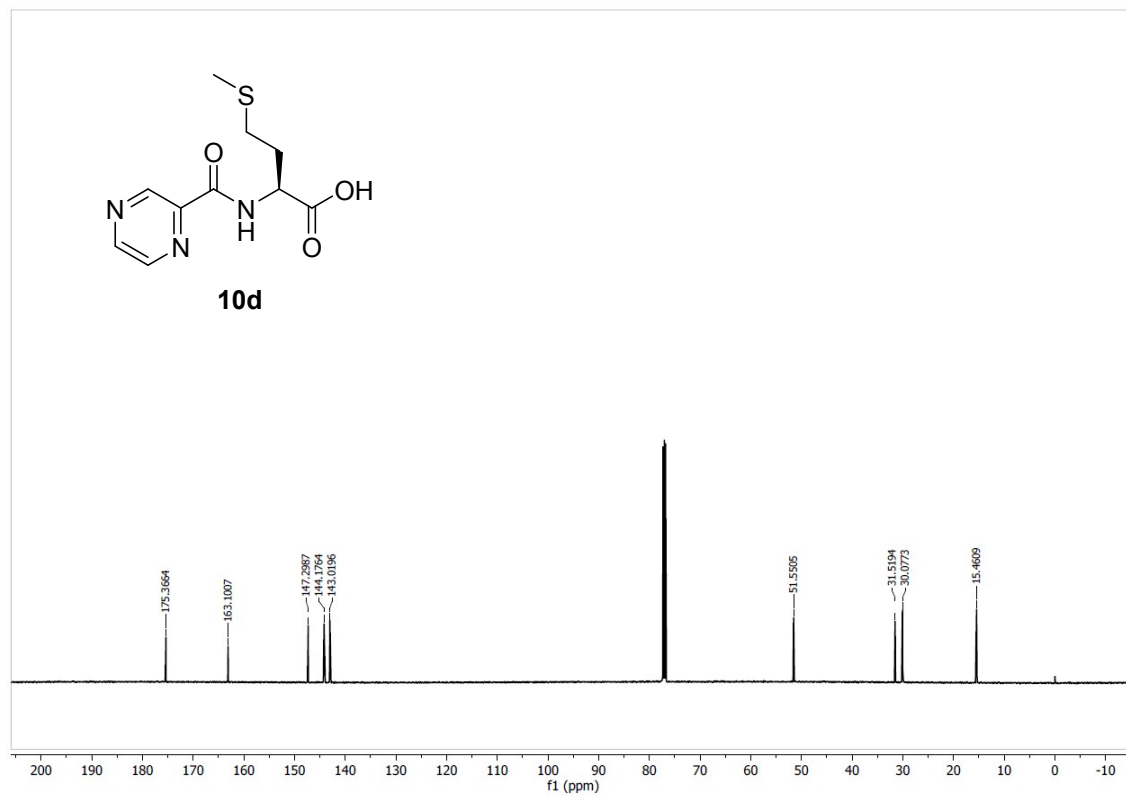
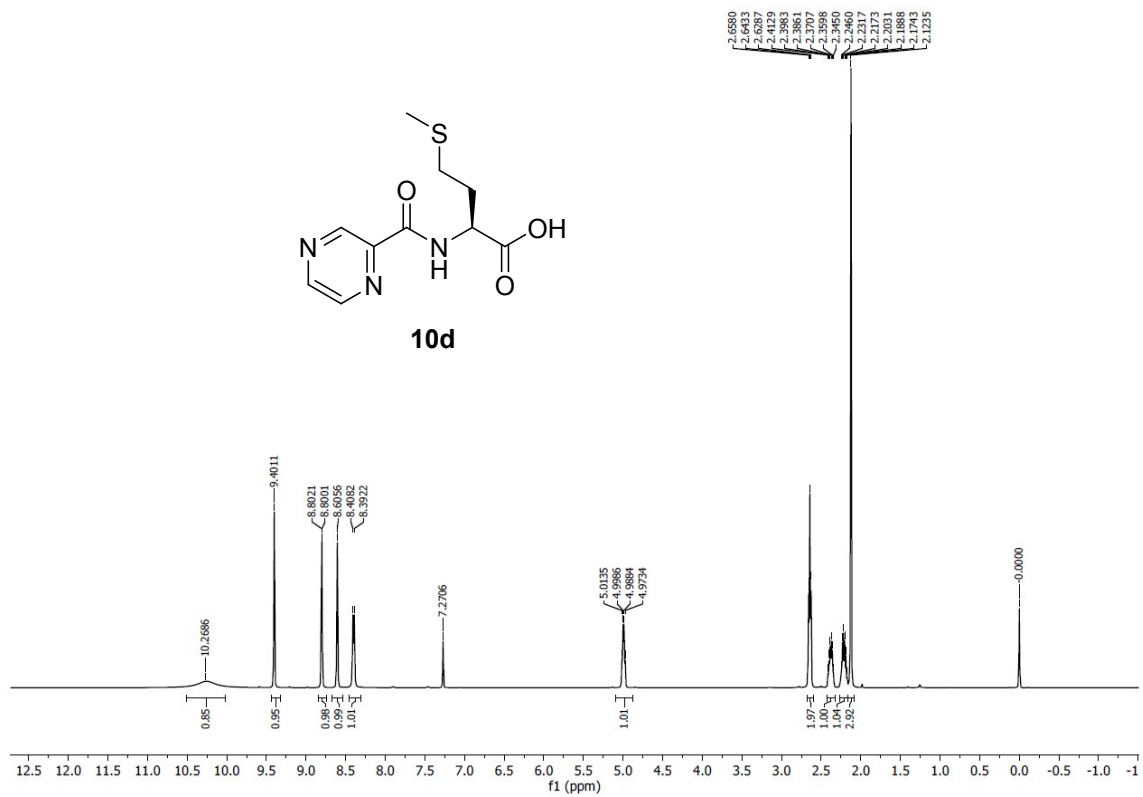


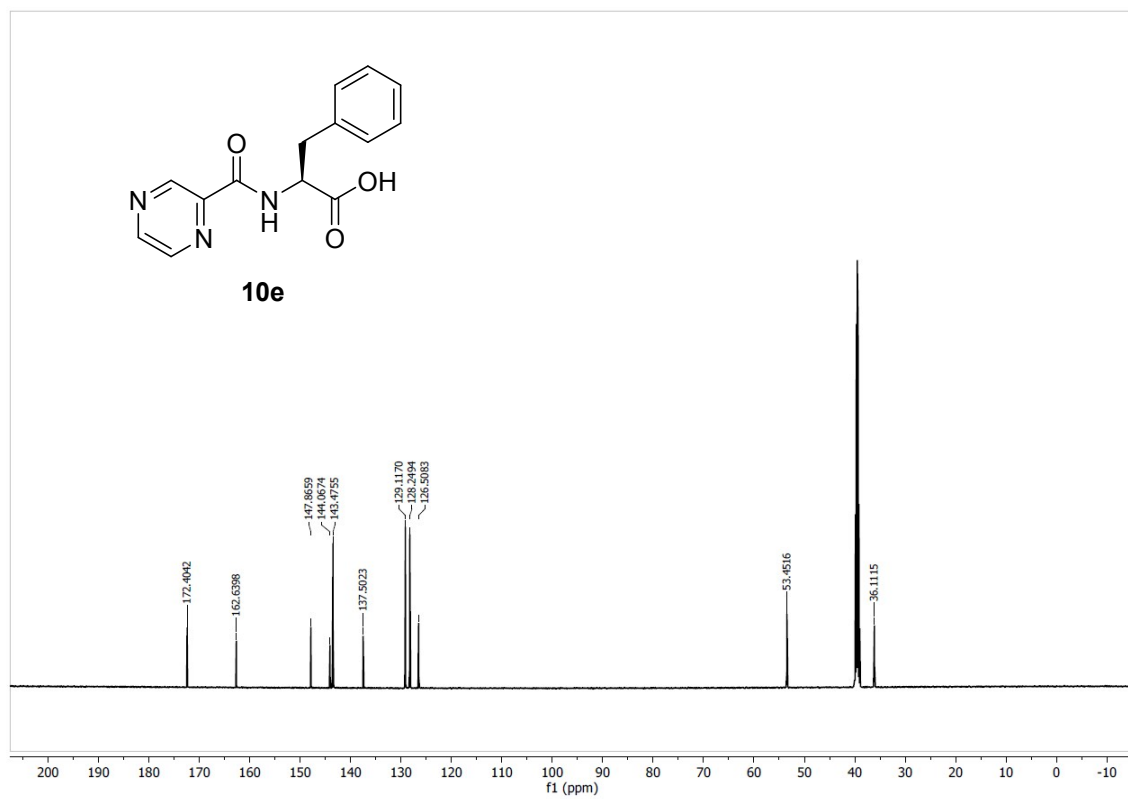
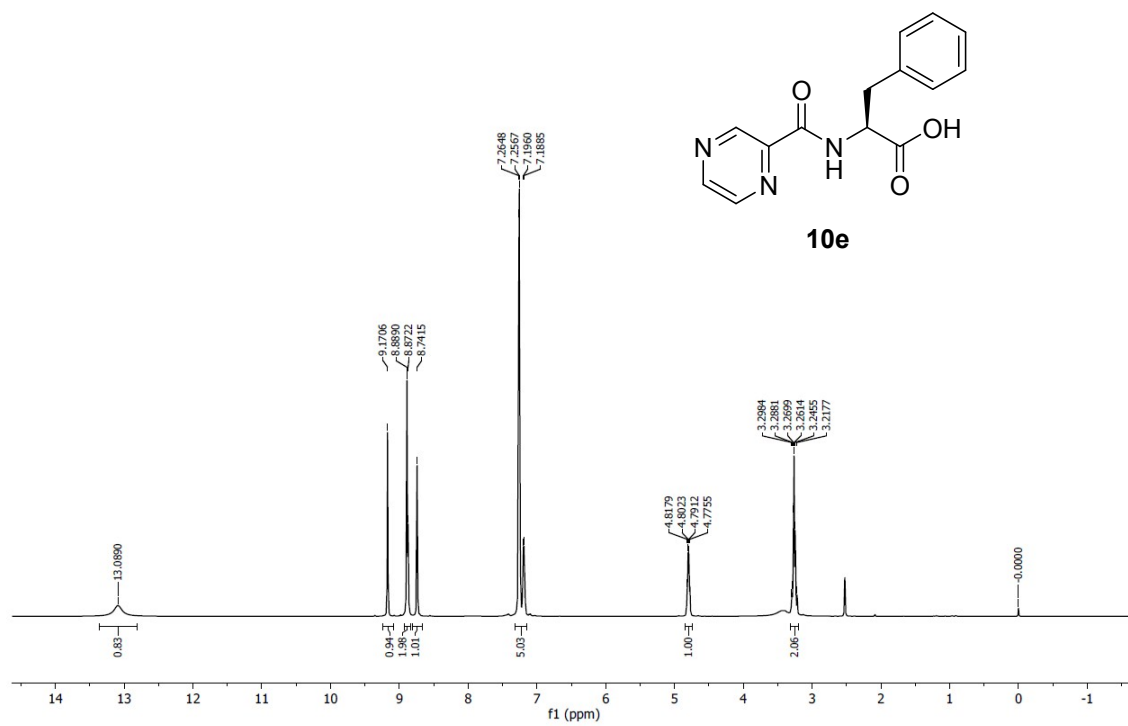
10a

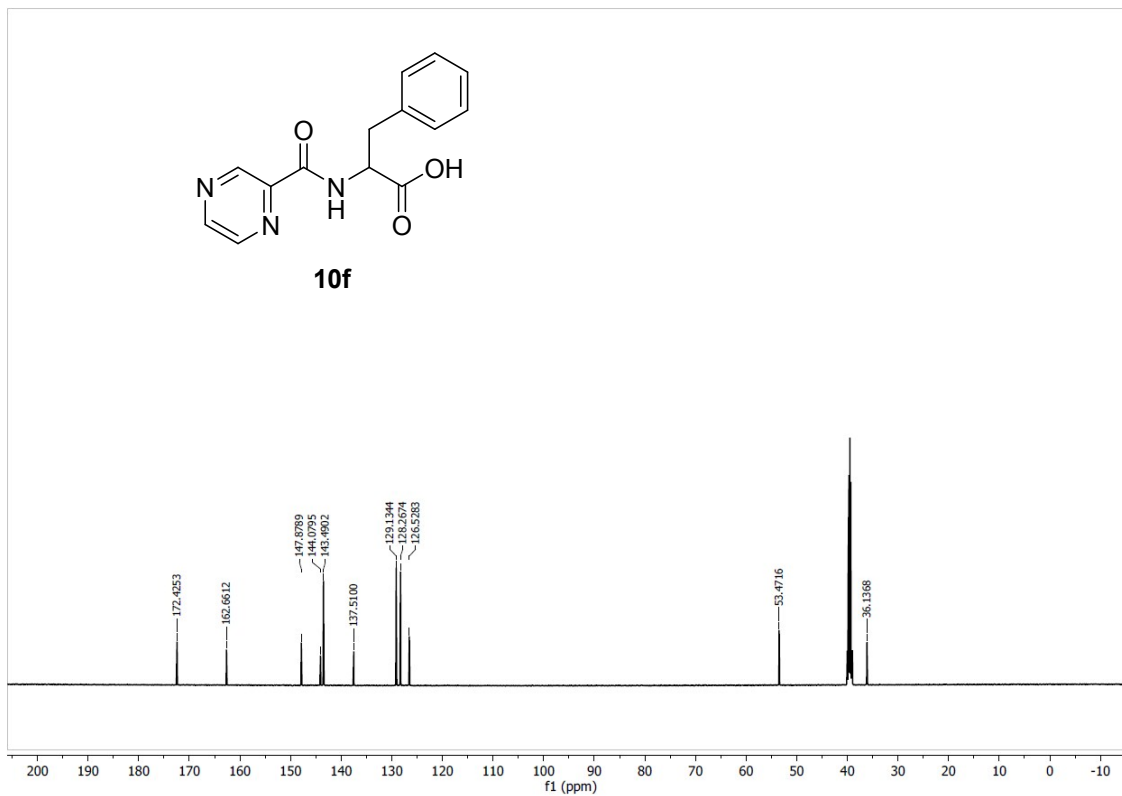
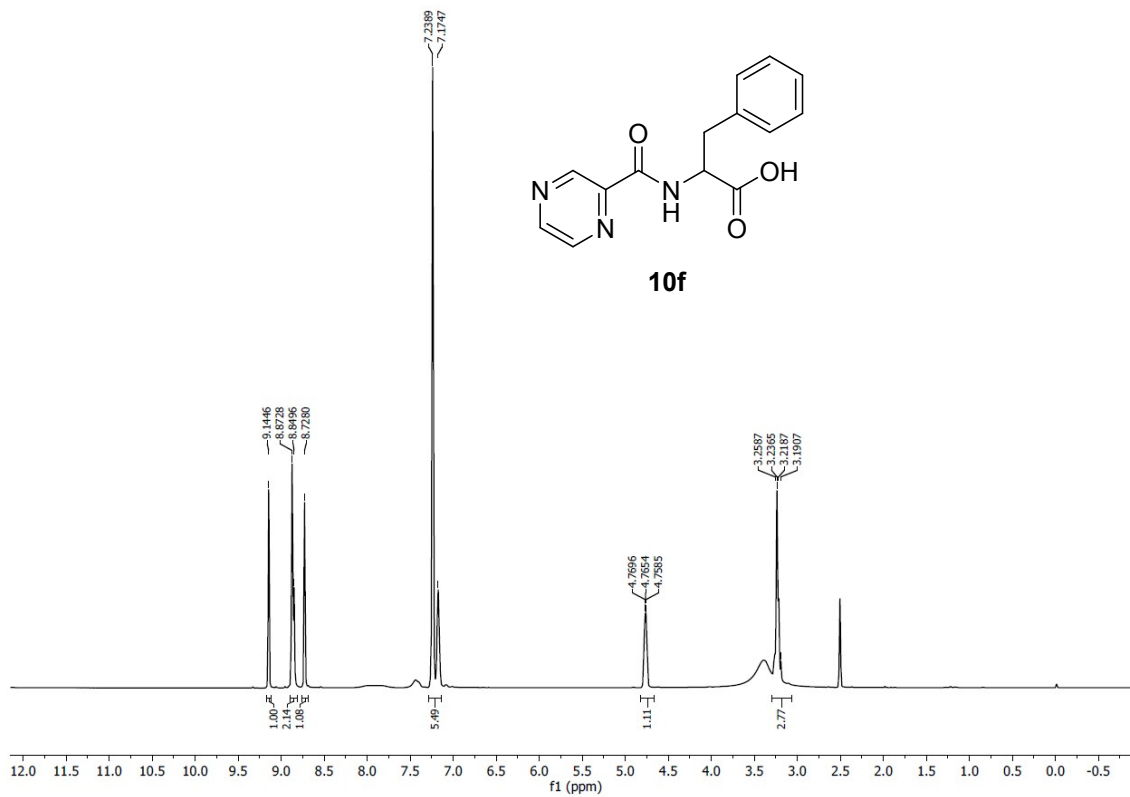


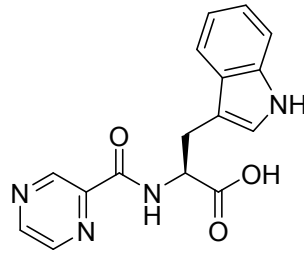




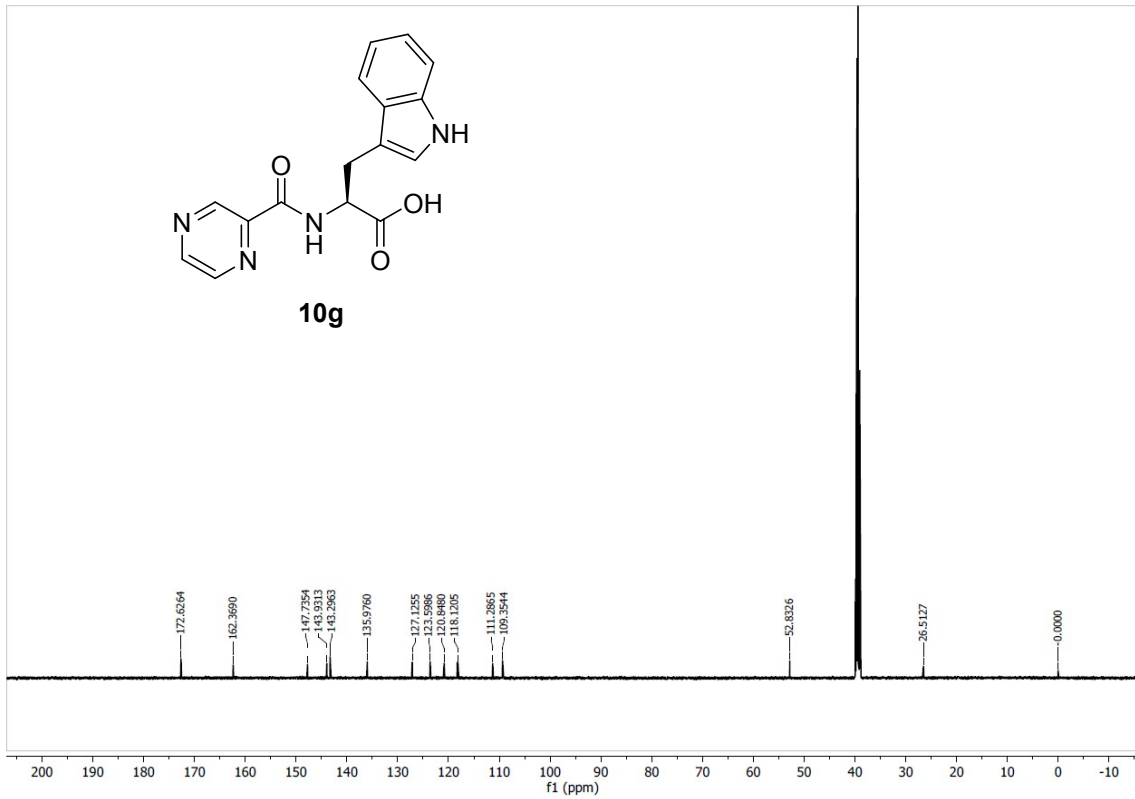
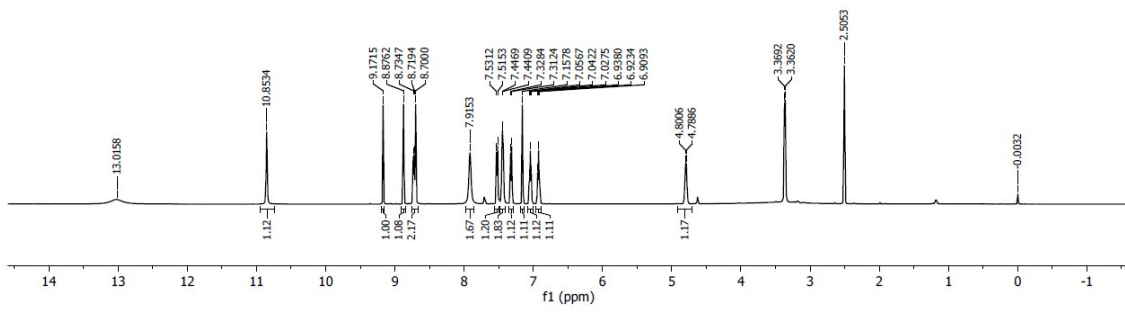


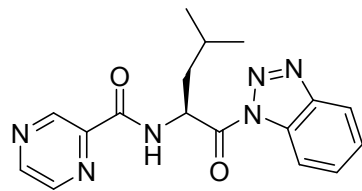




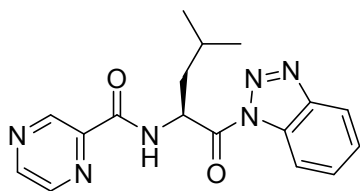
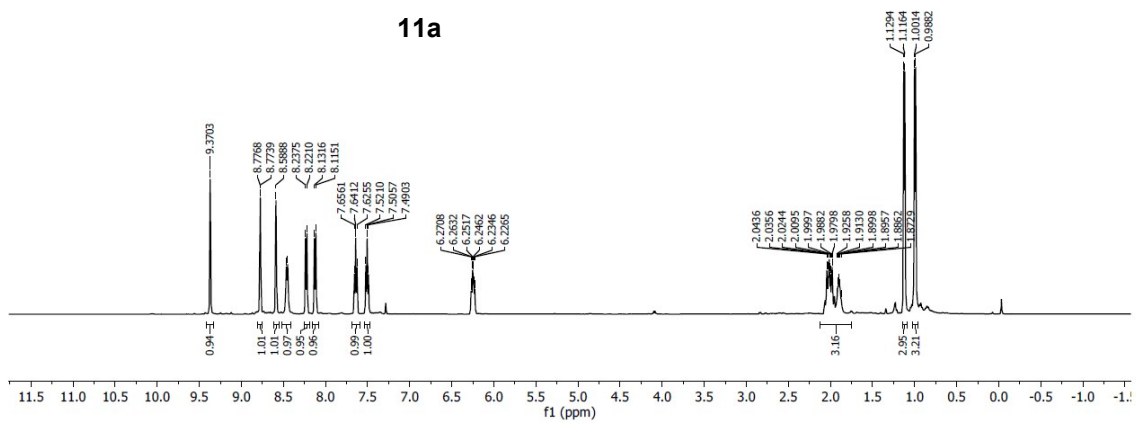


10g

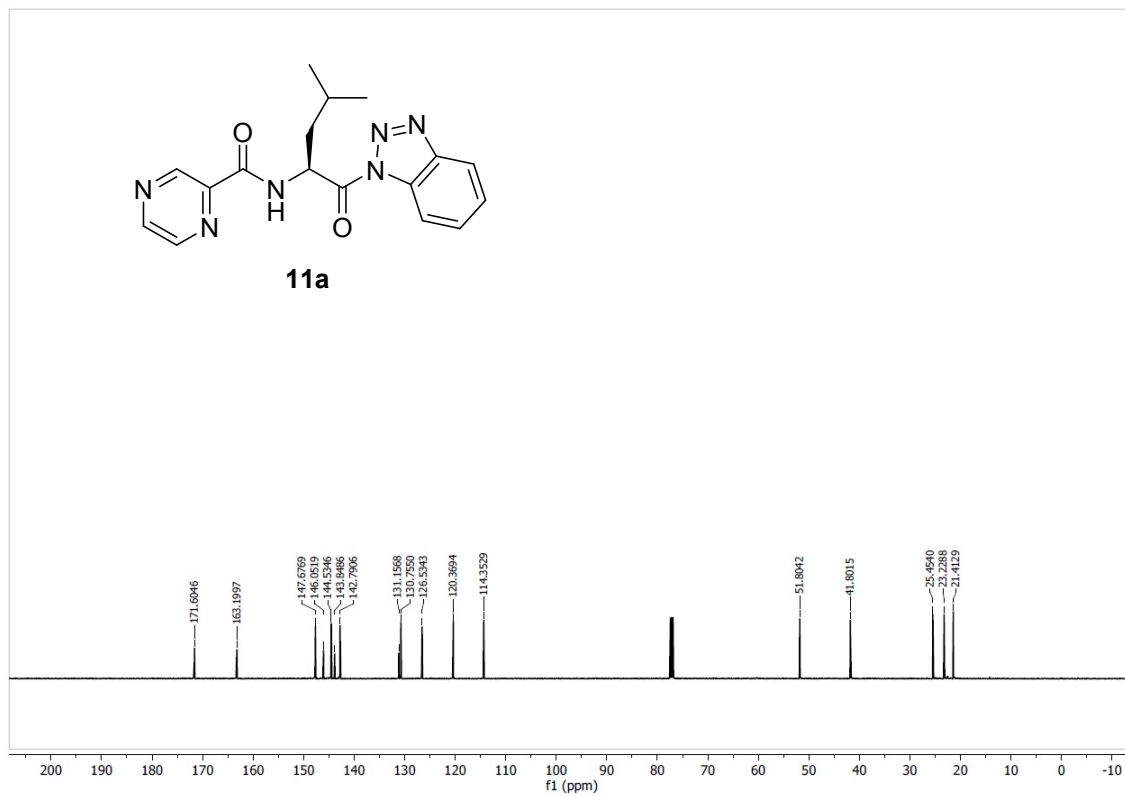


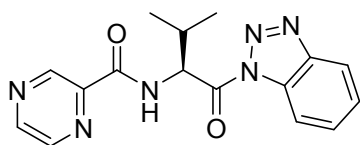


11a

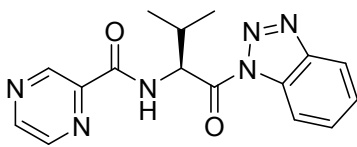
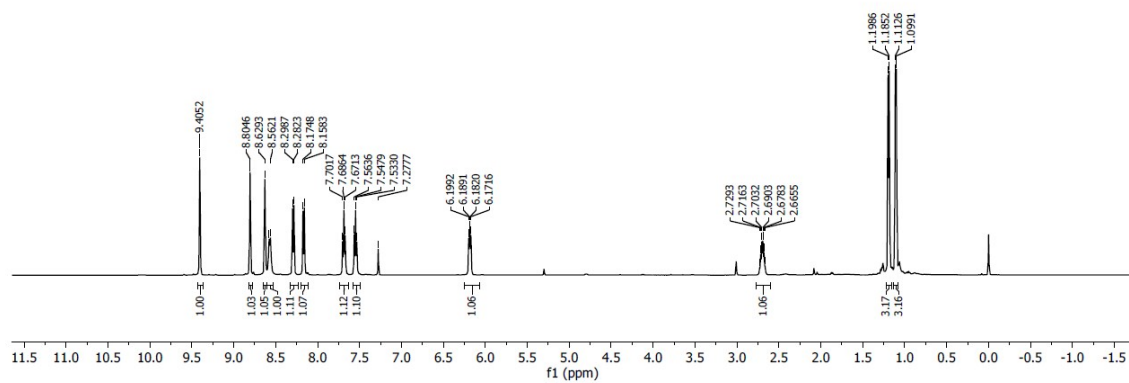


11a

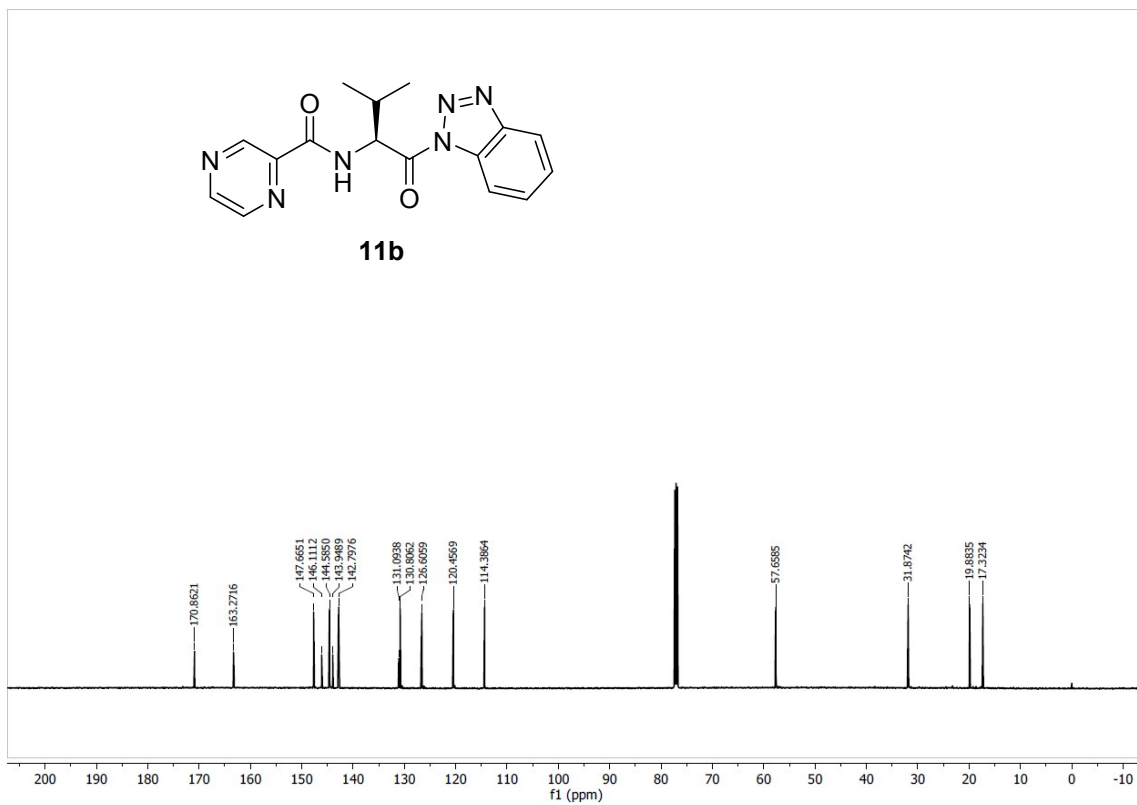


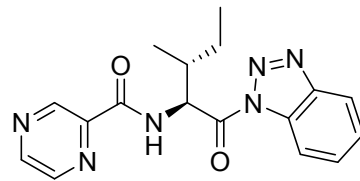


11b

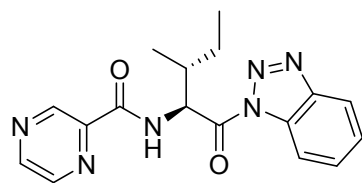
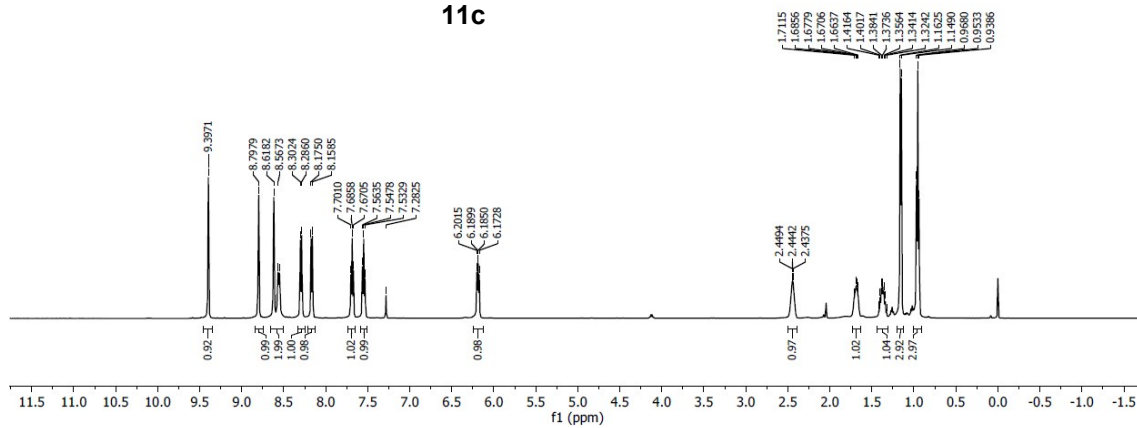


11b

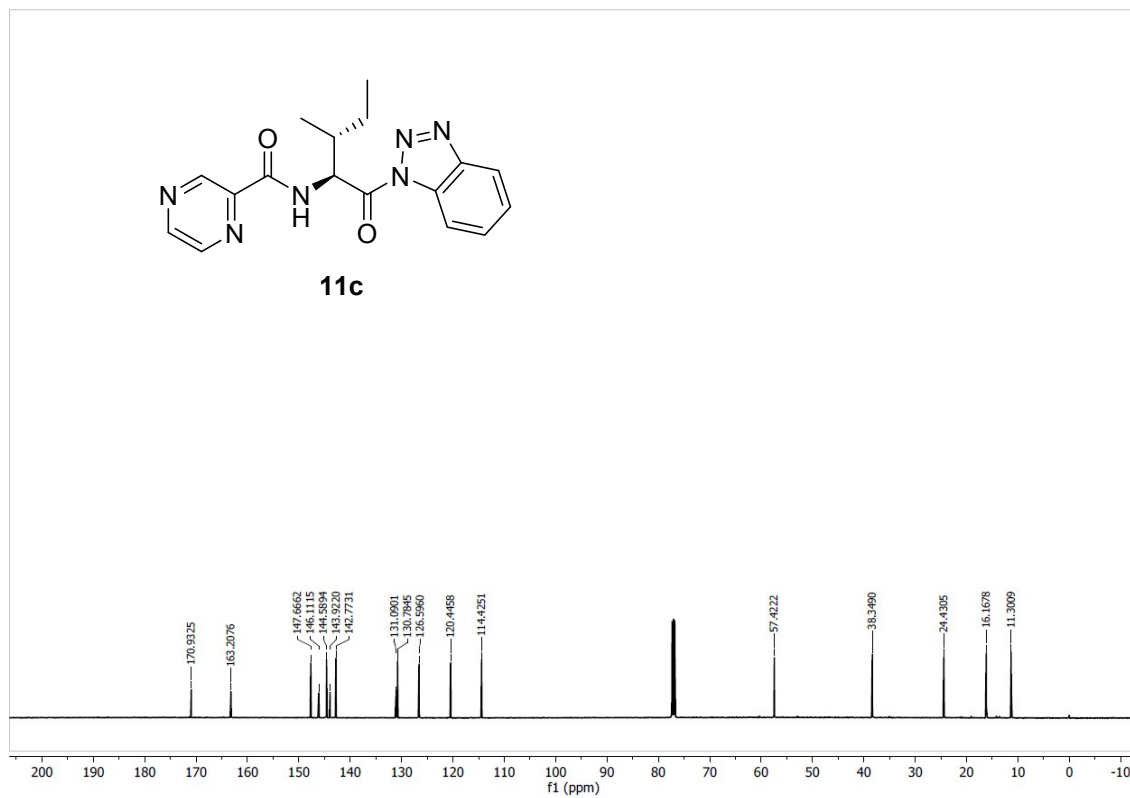


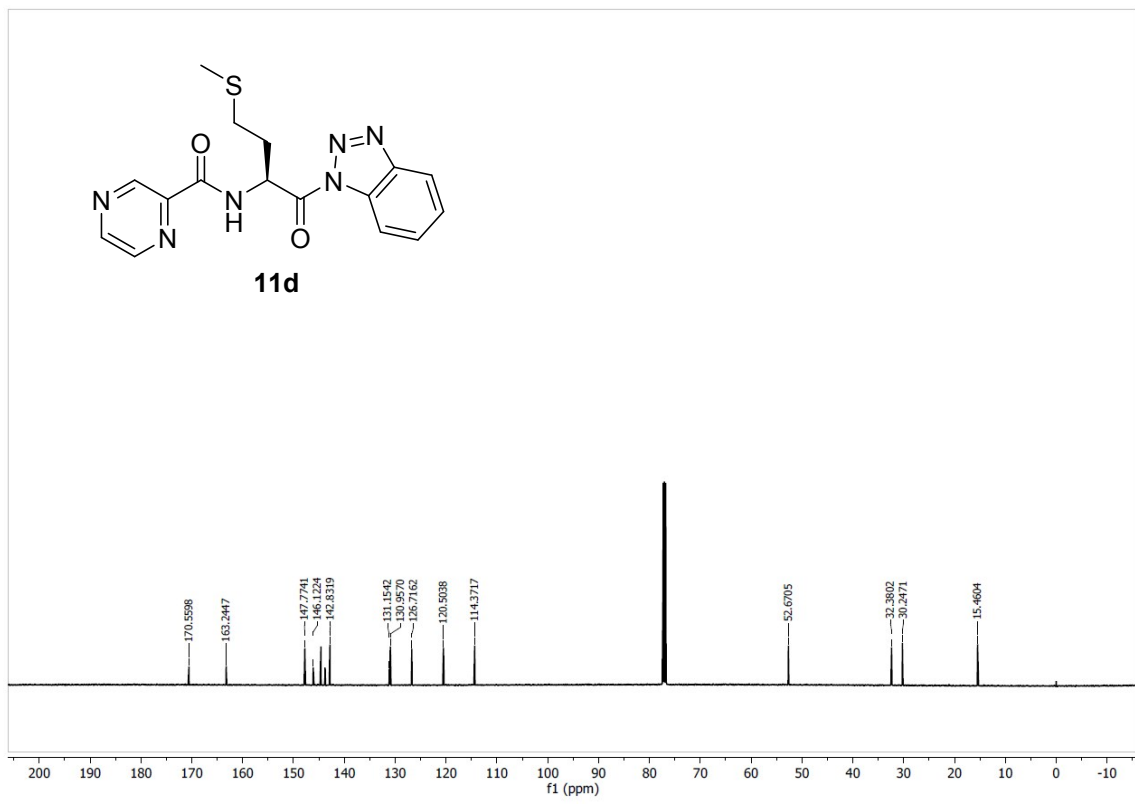
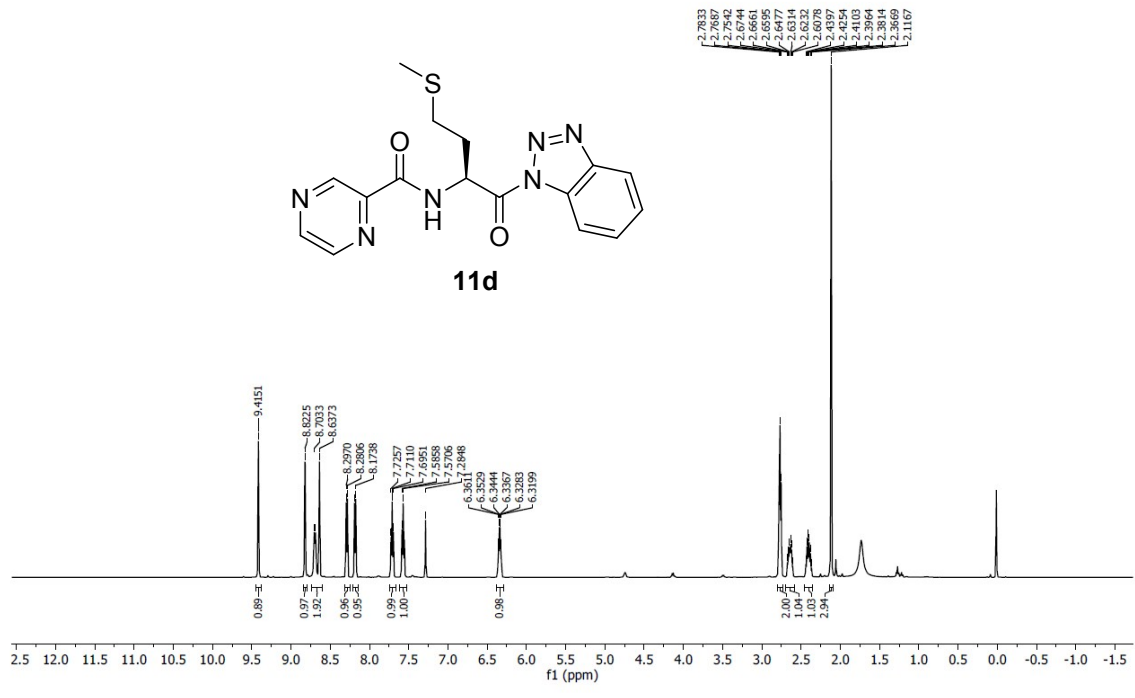


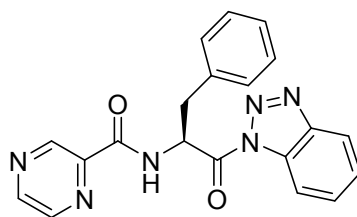
11c



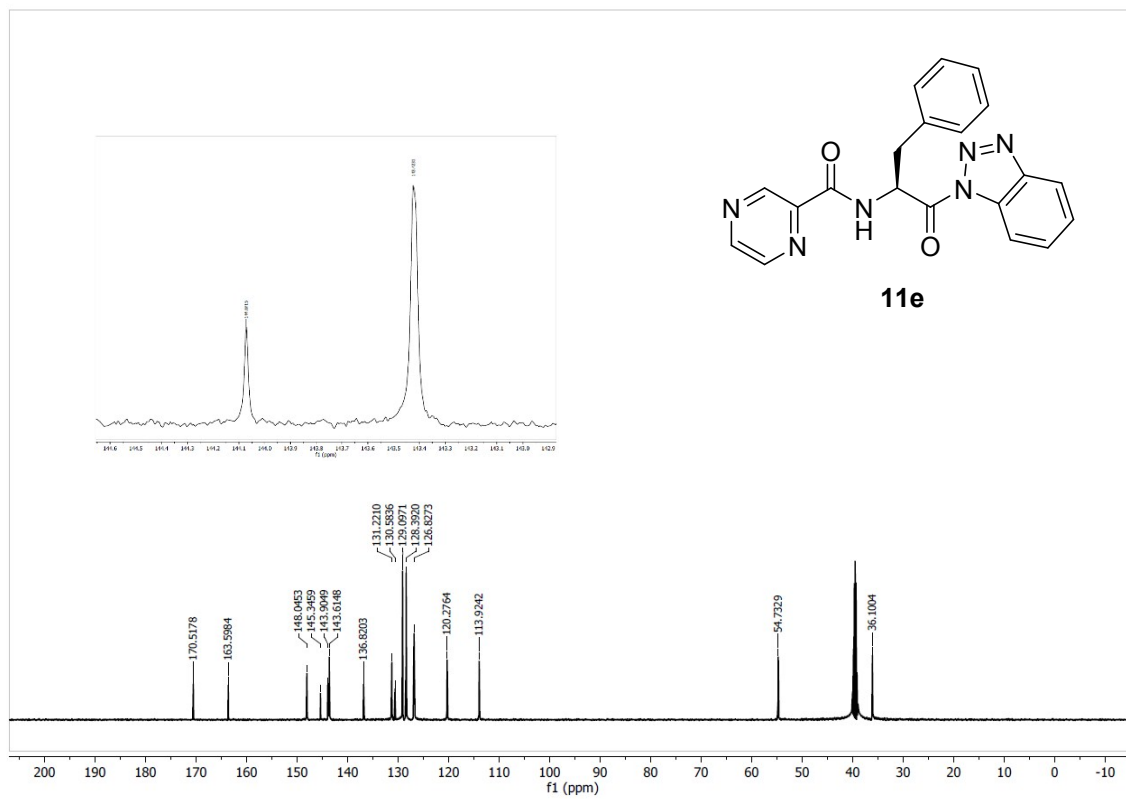
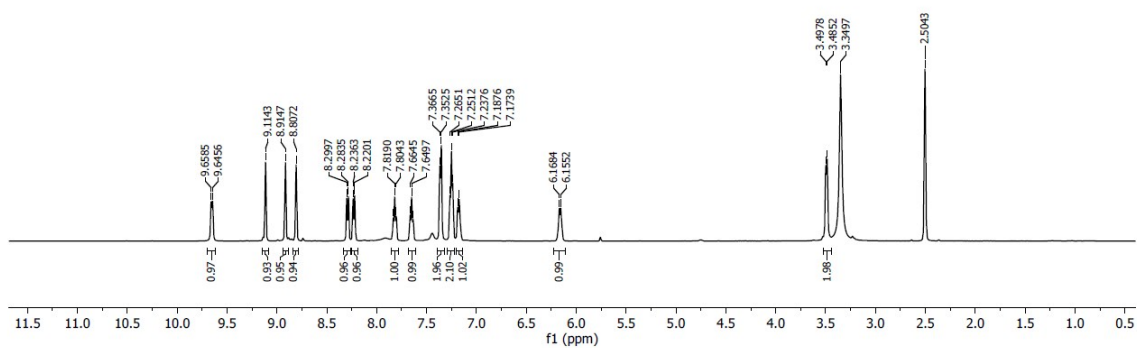
11c

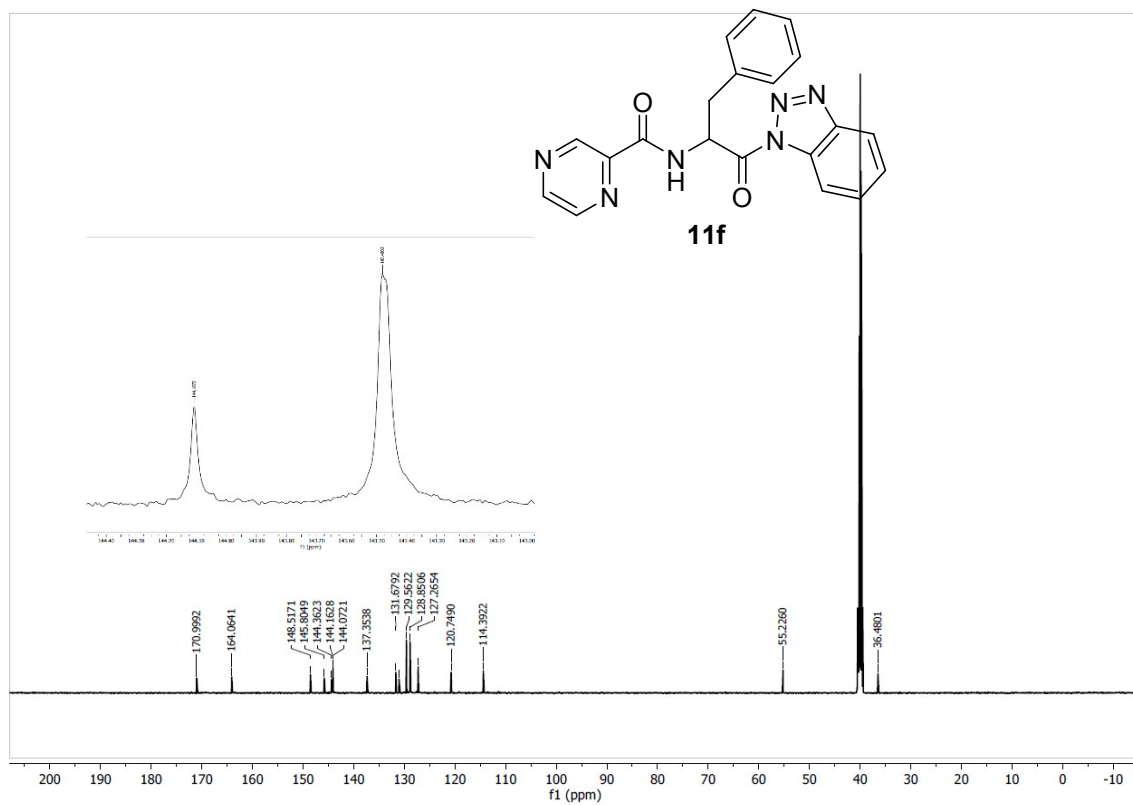
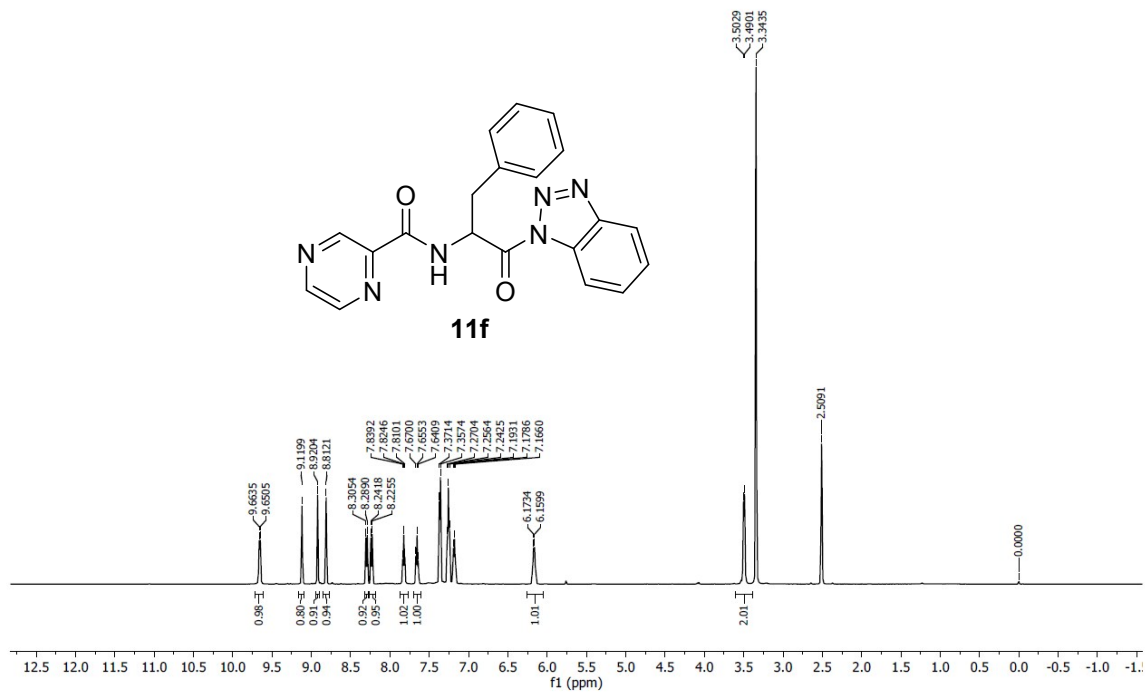


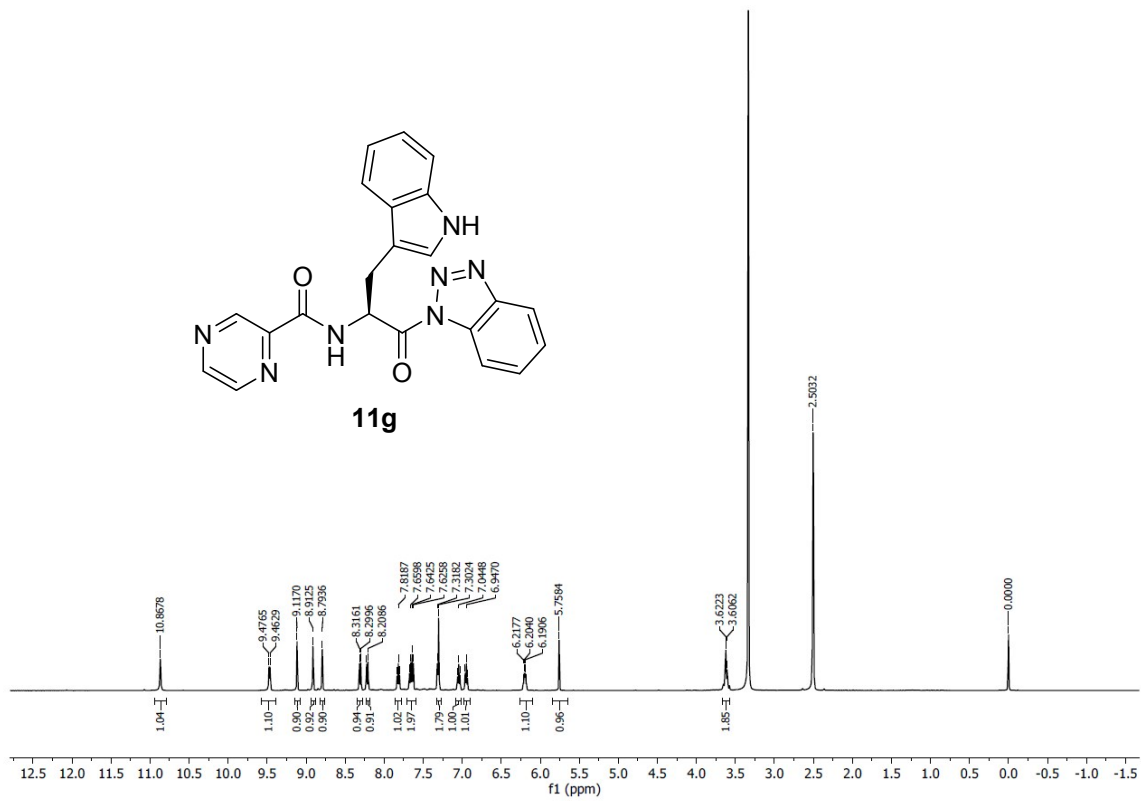
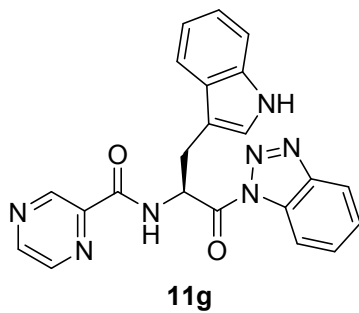


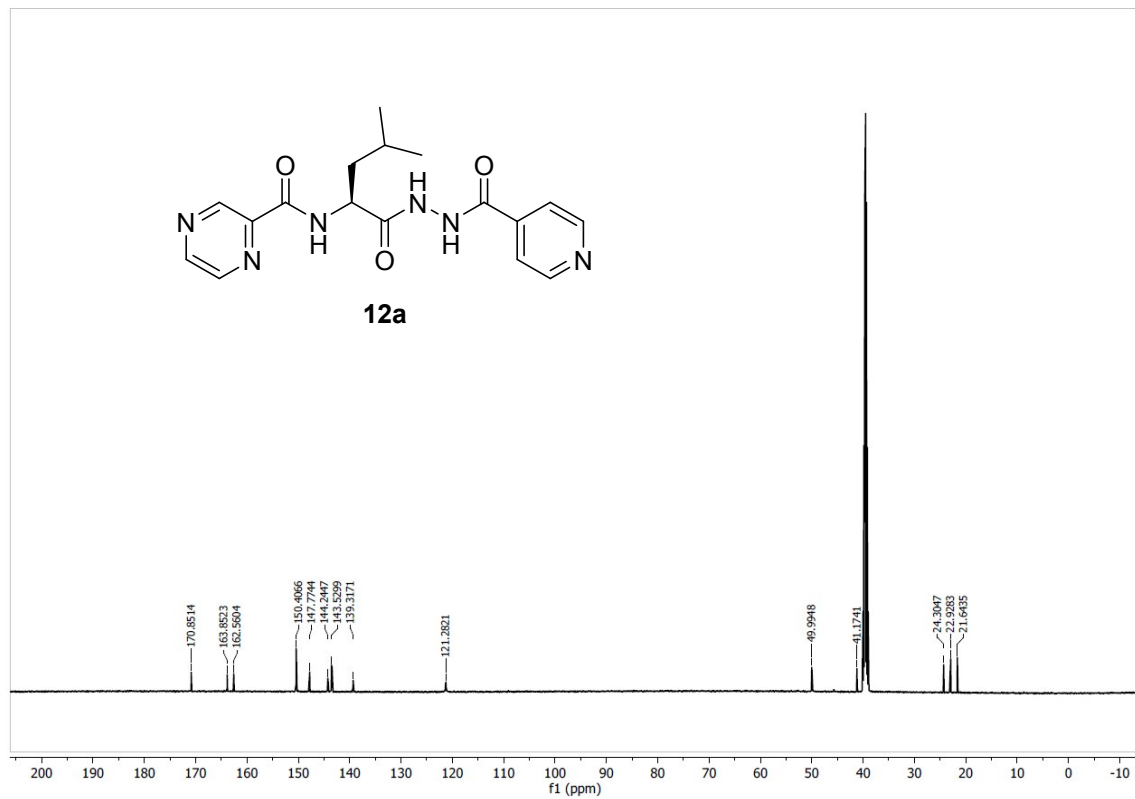
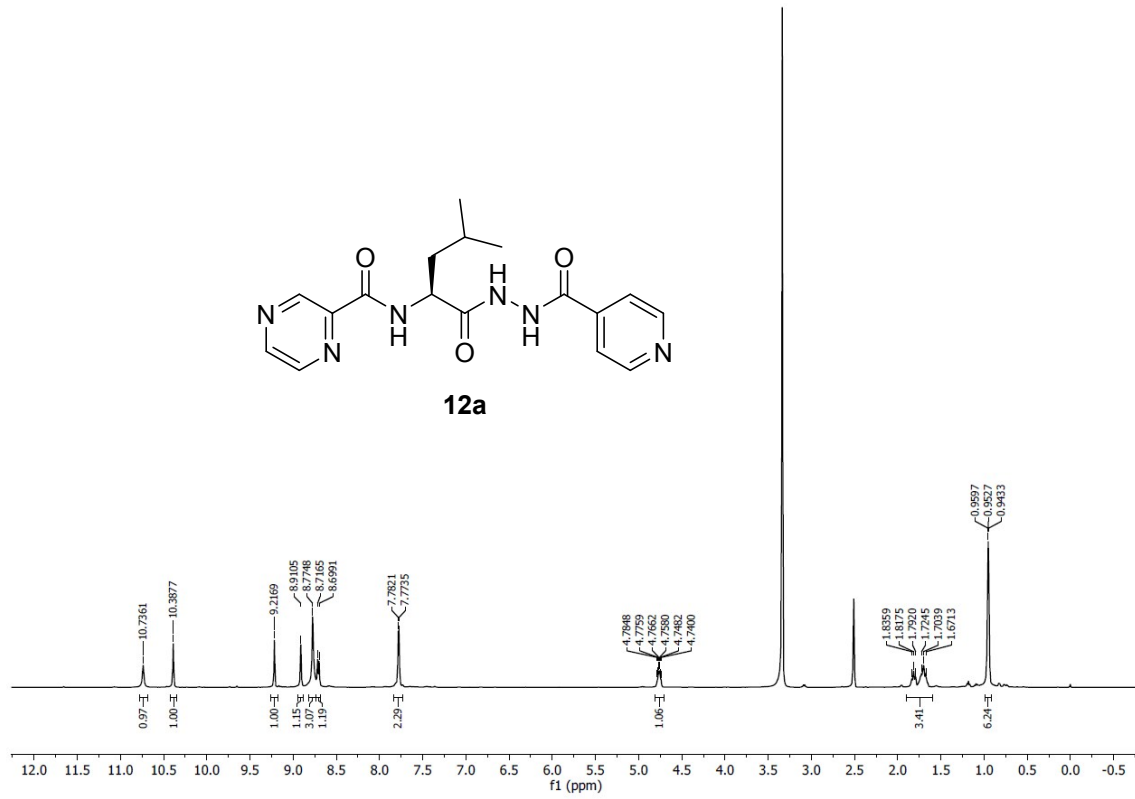


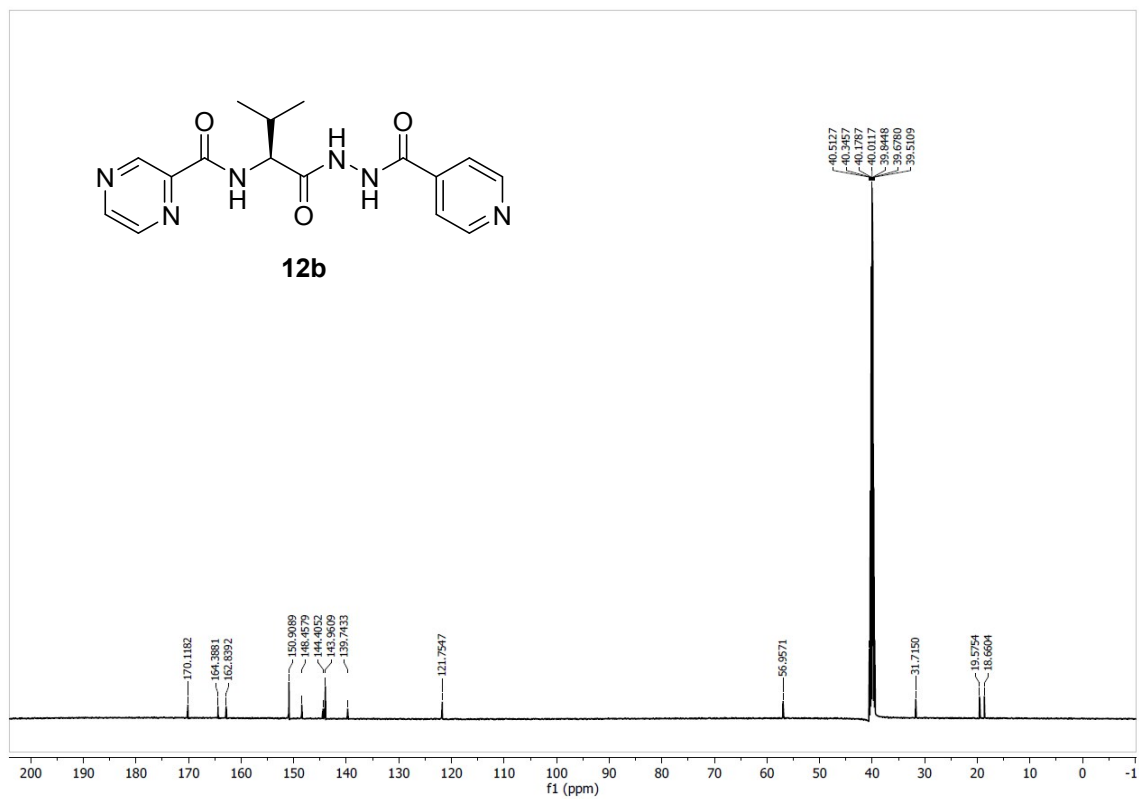
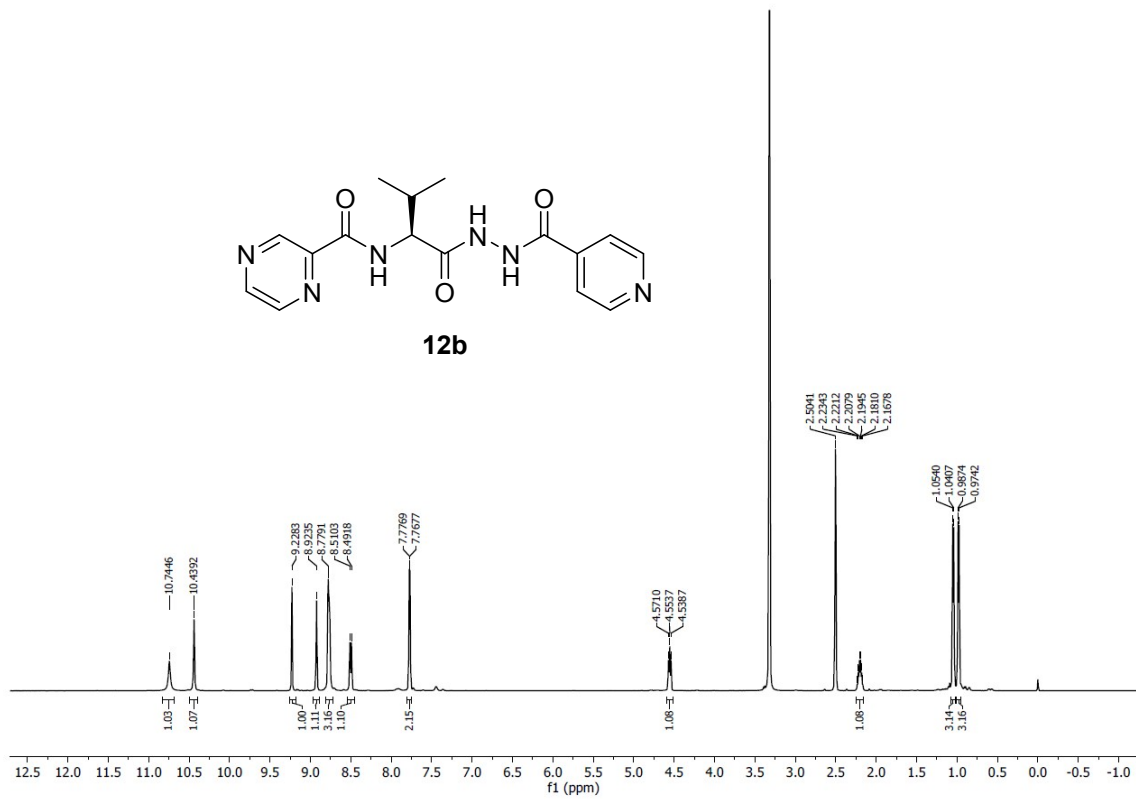
11e

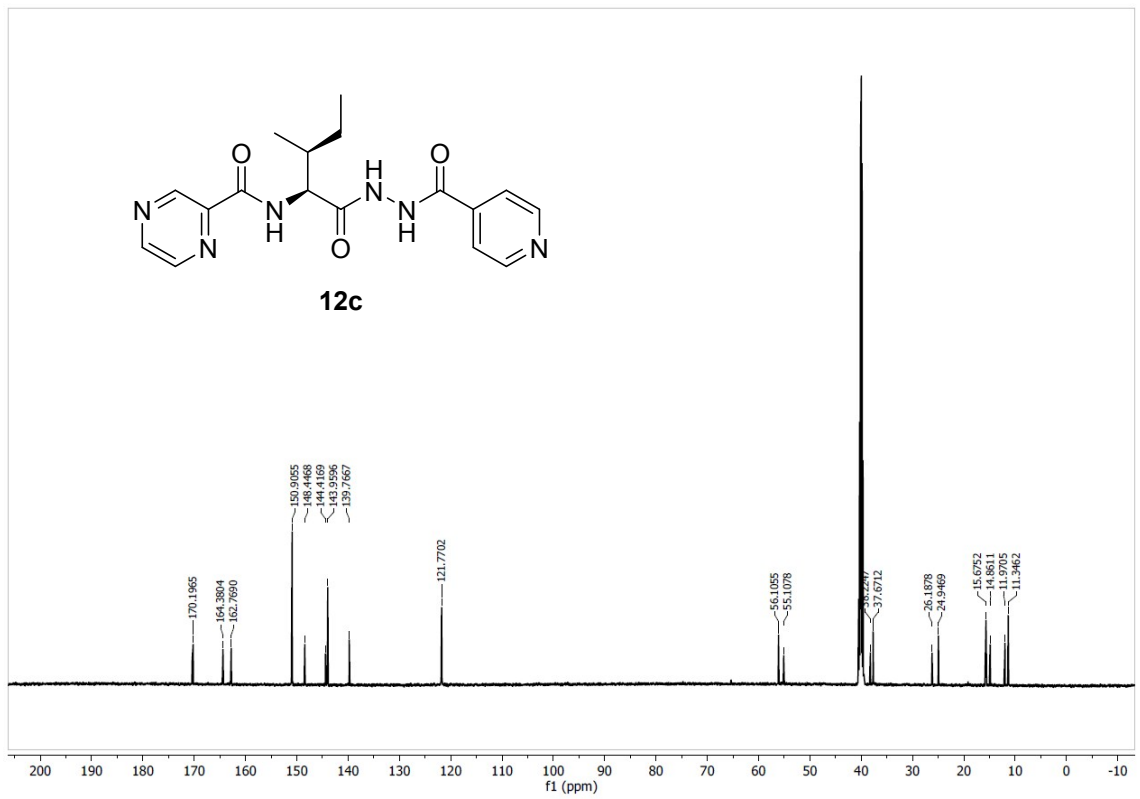
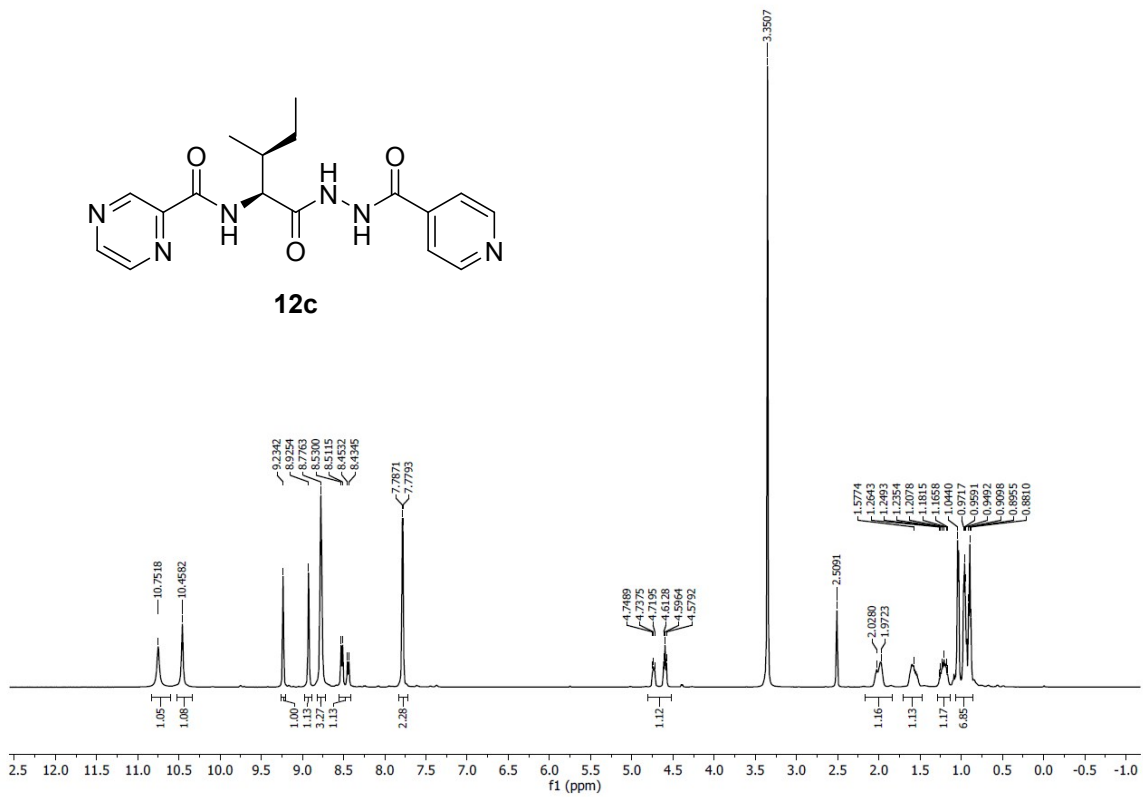


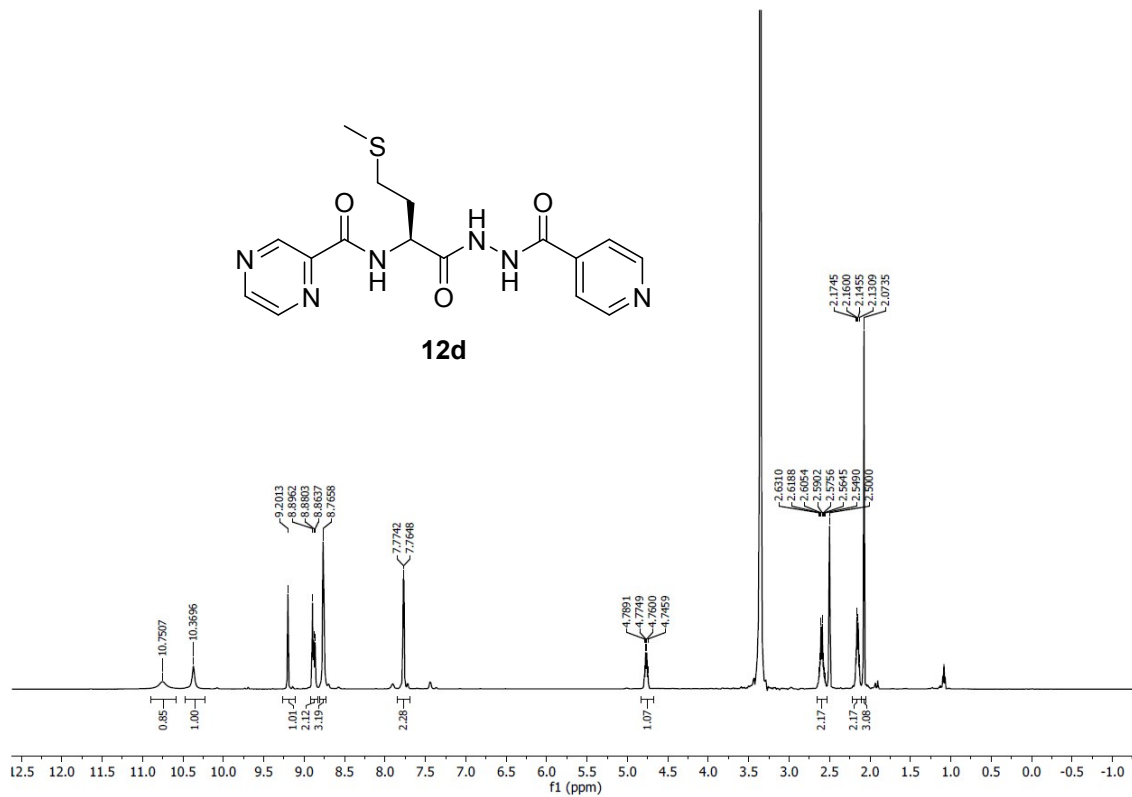


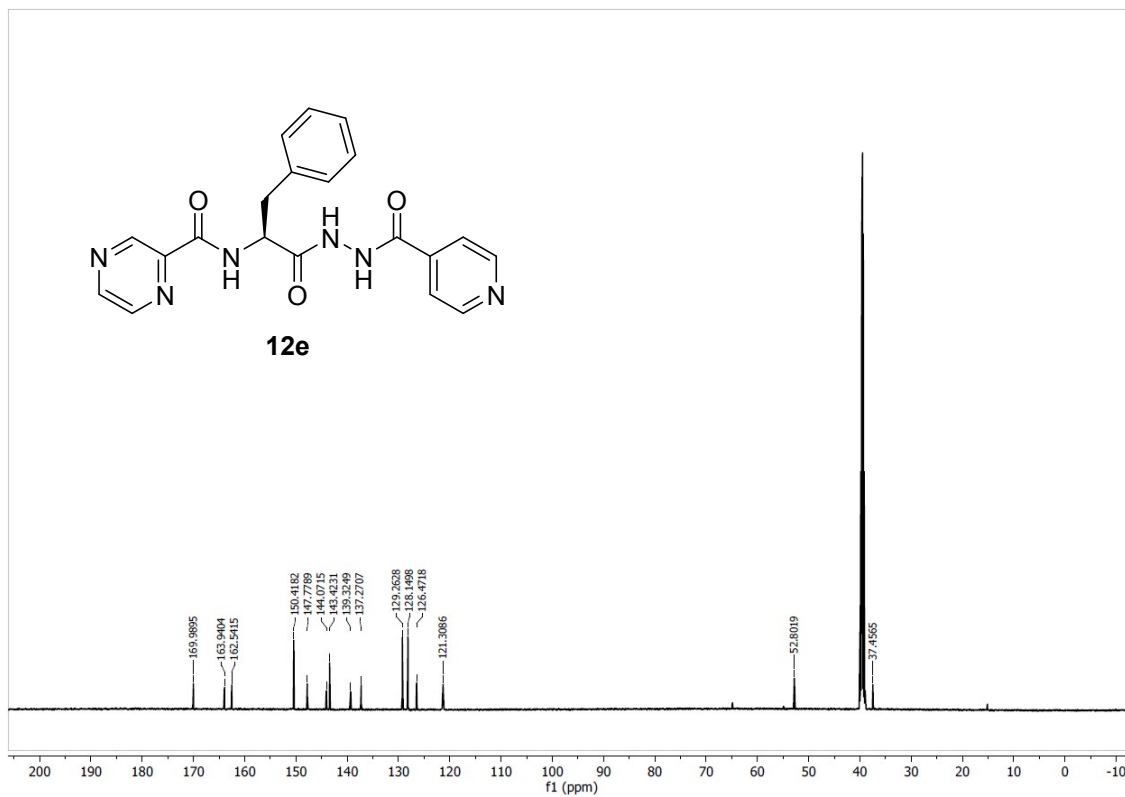
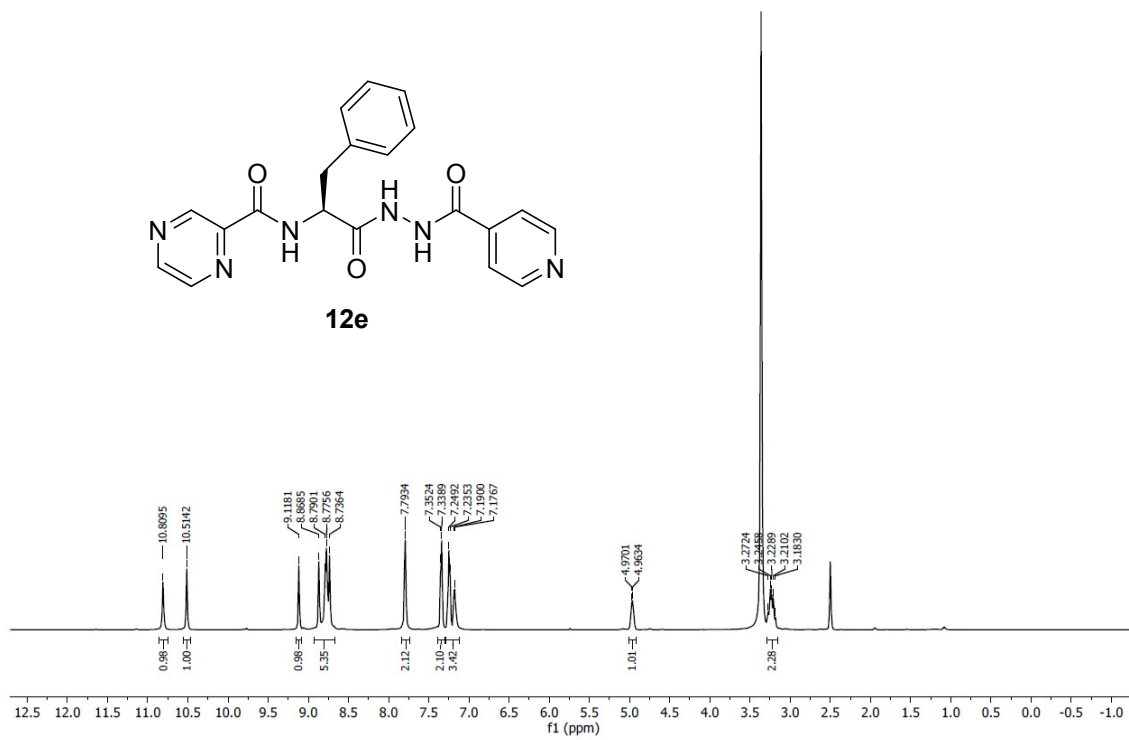
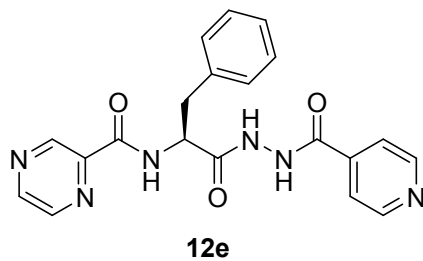


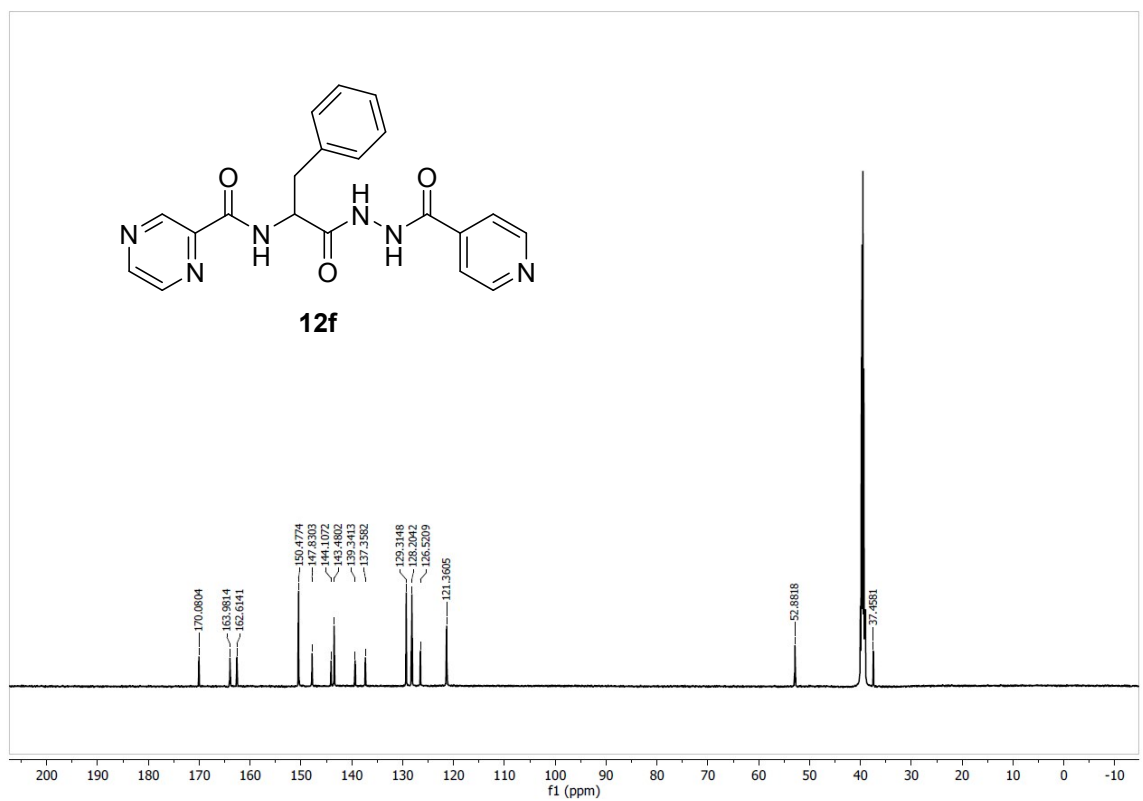
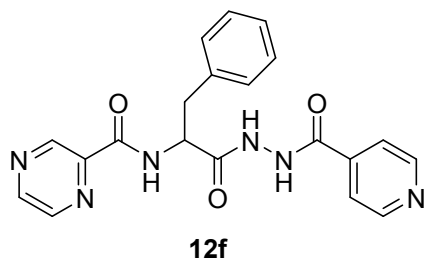
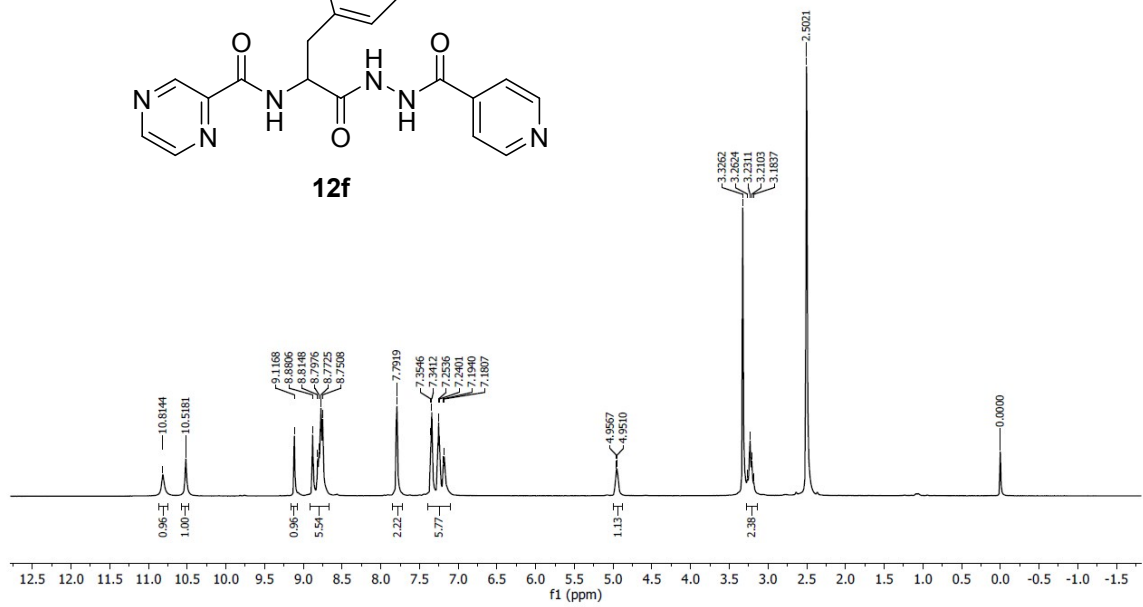
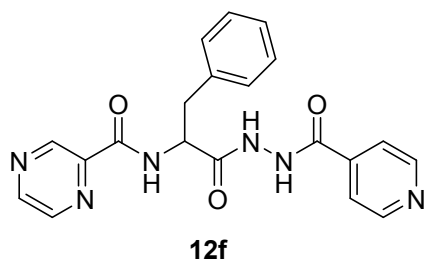


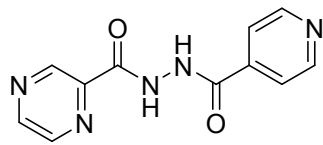




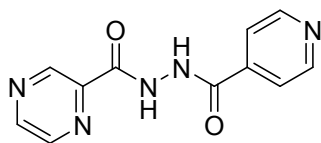
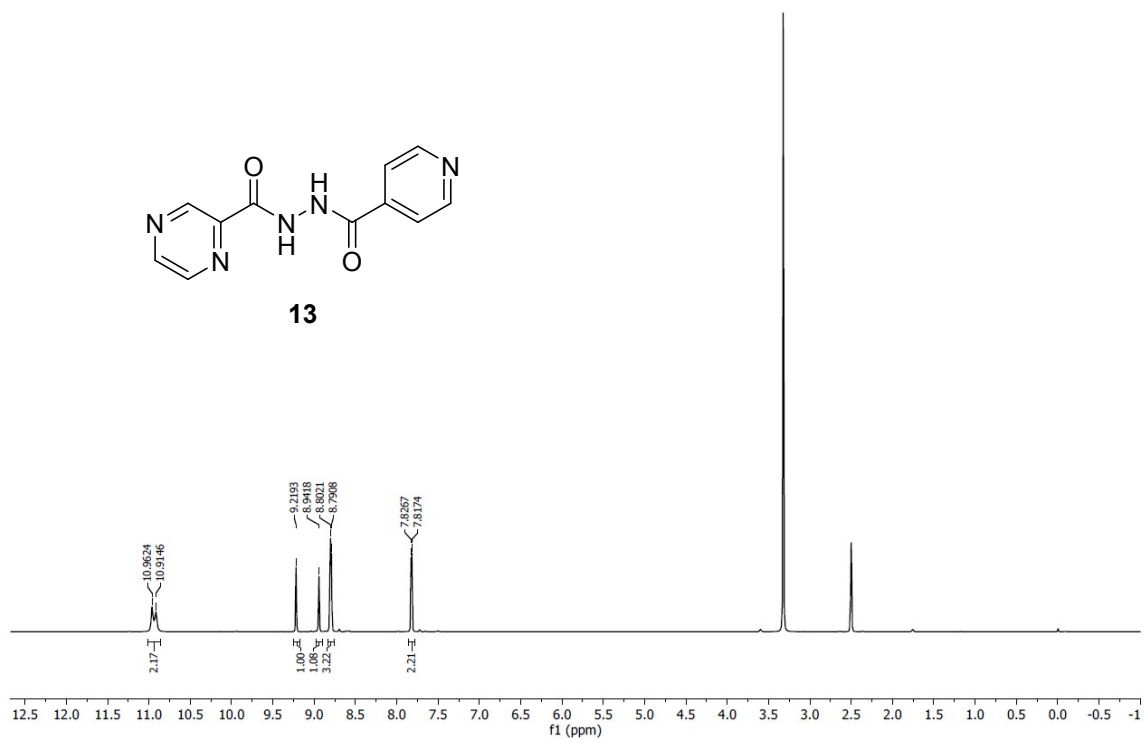




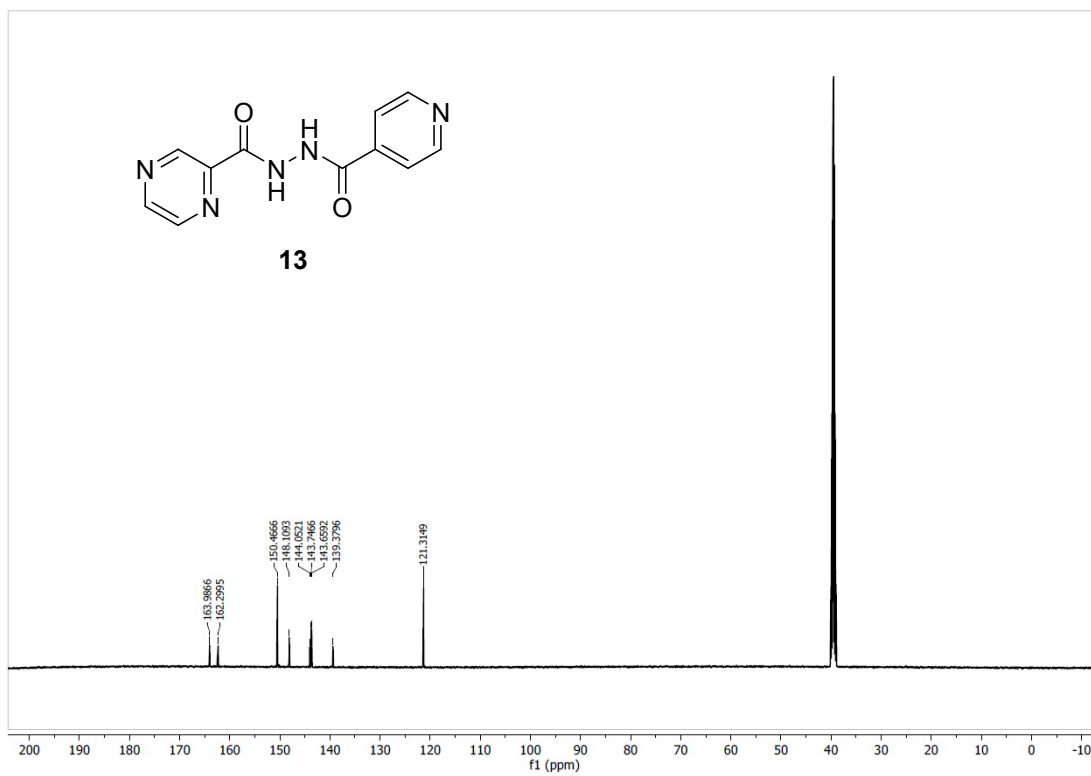


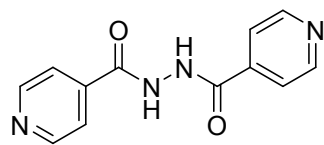


13

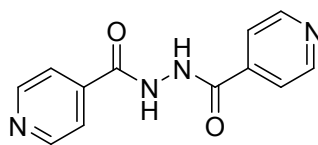
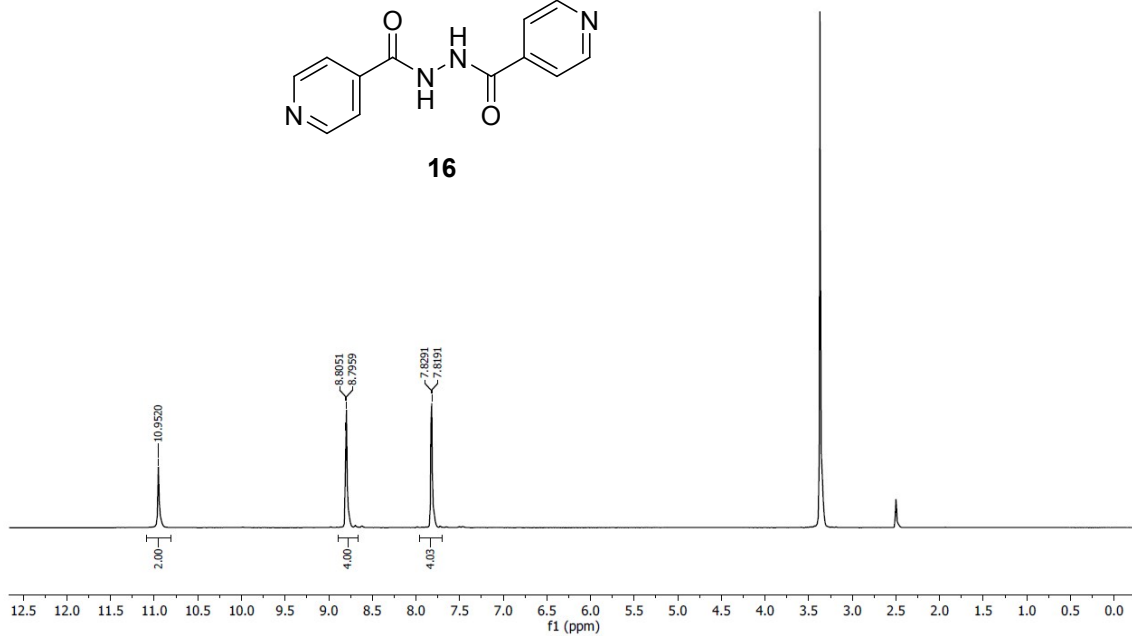


13

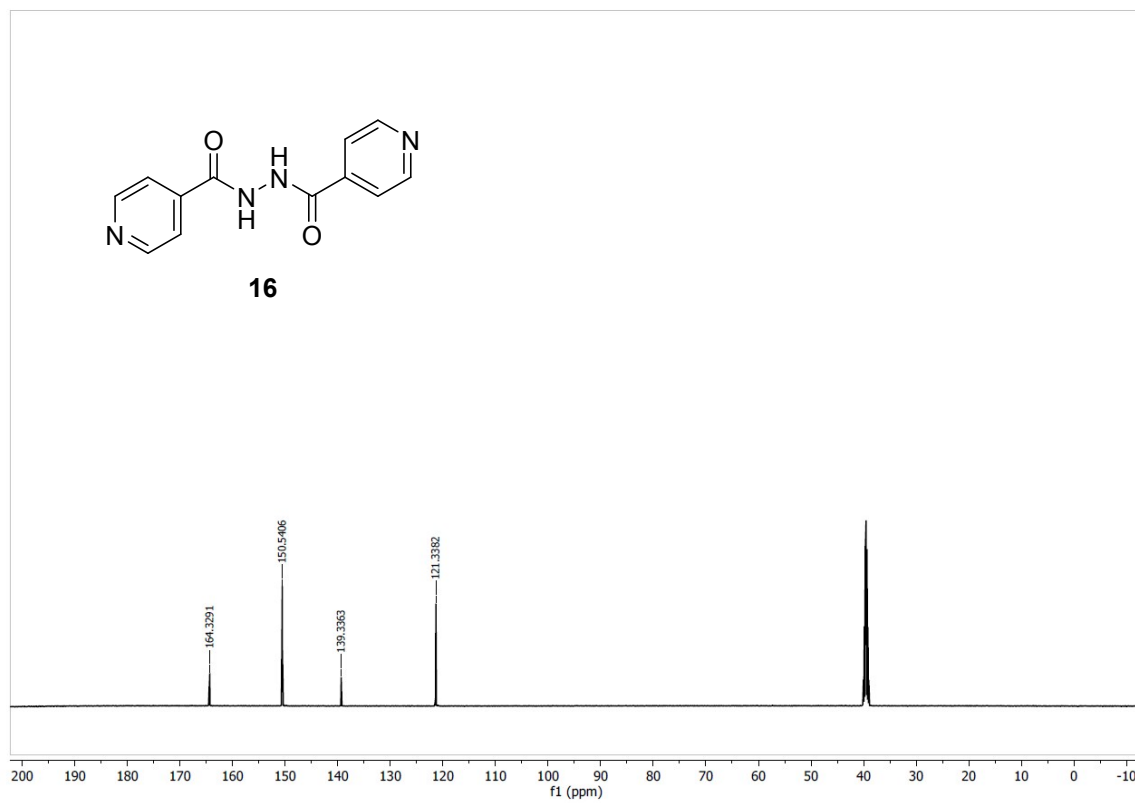


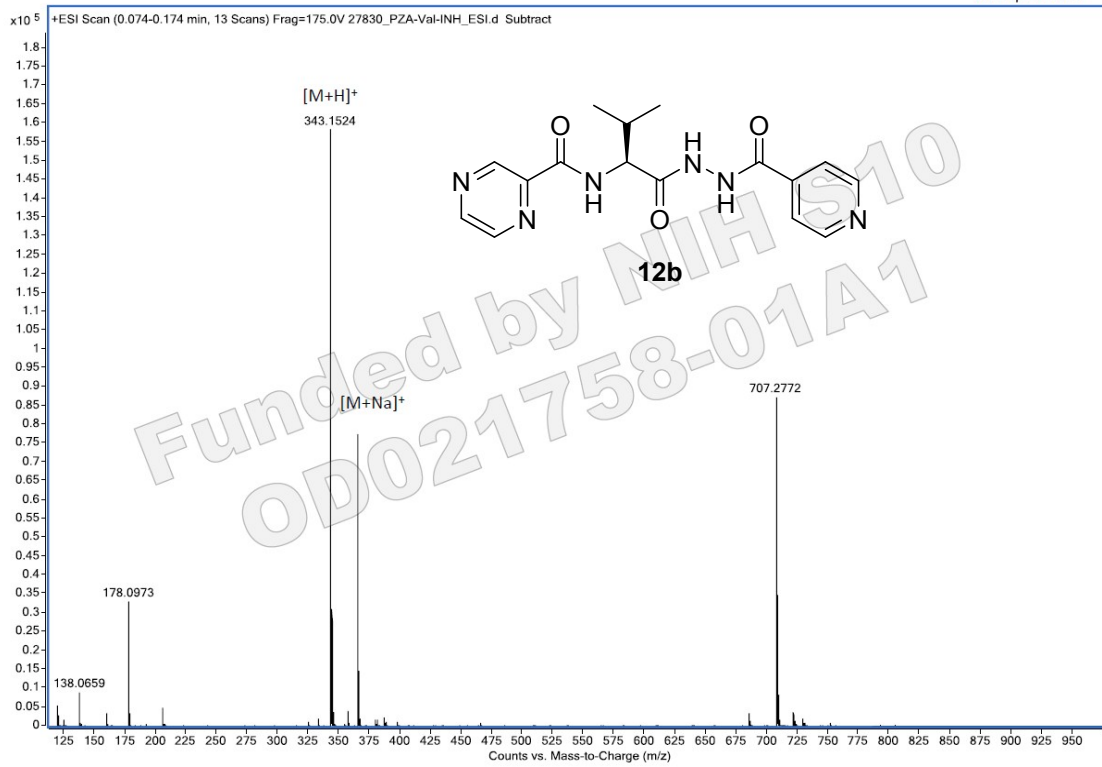


16

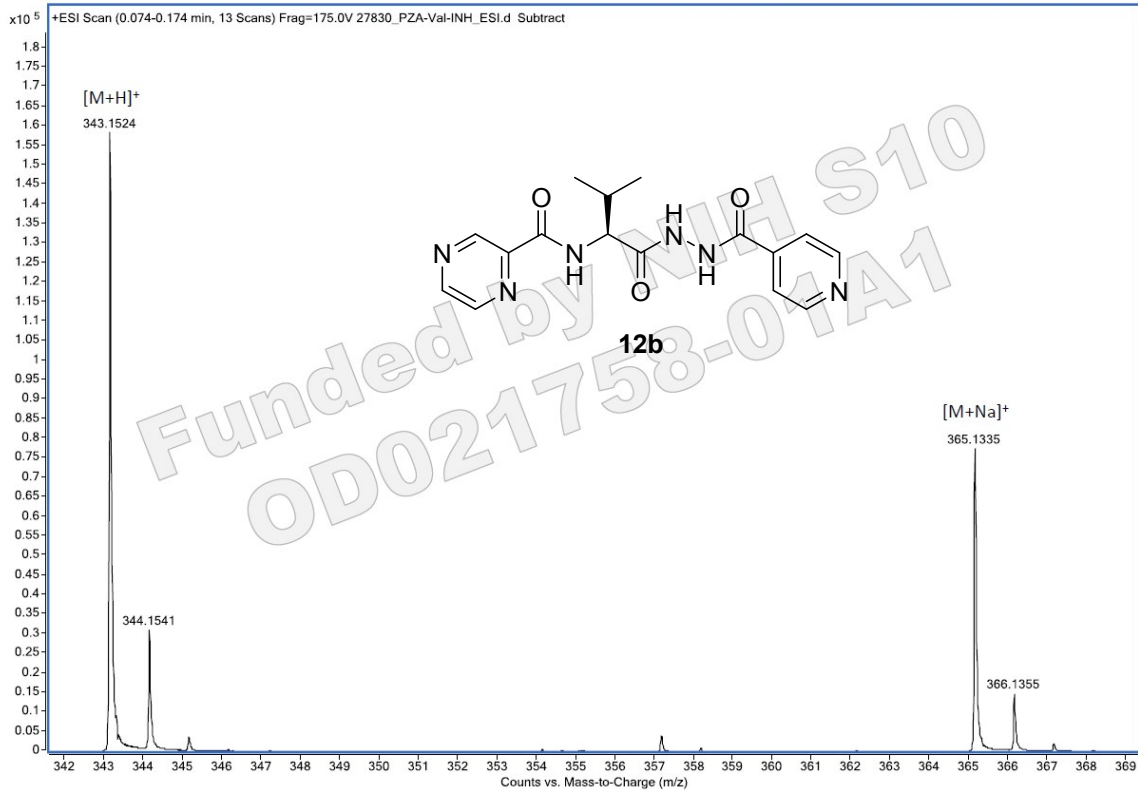


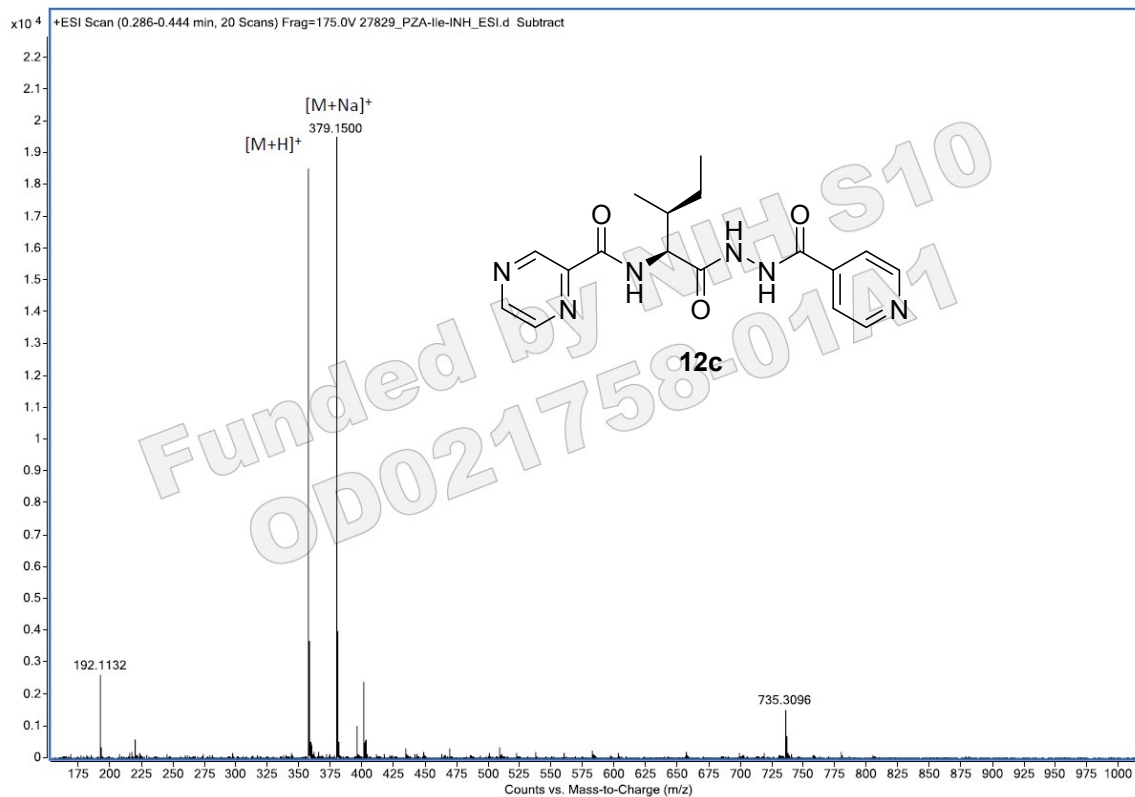
16



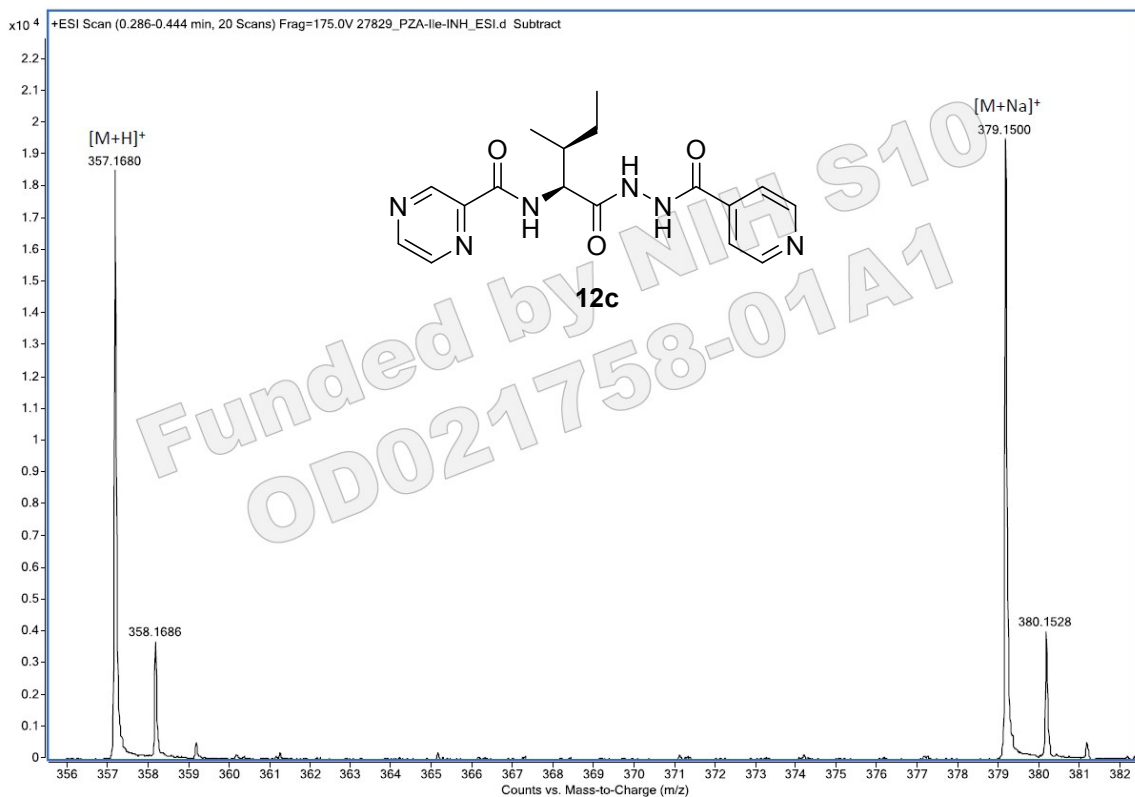


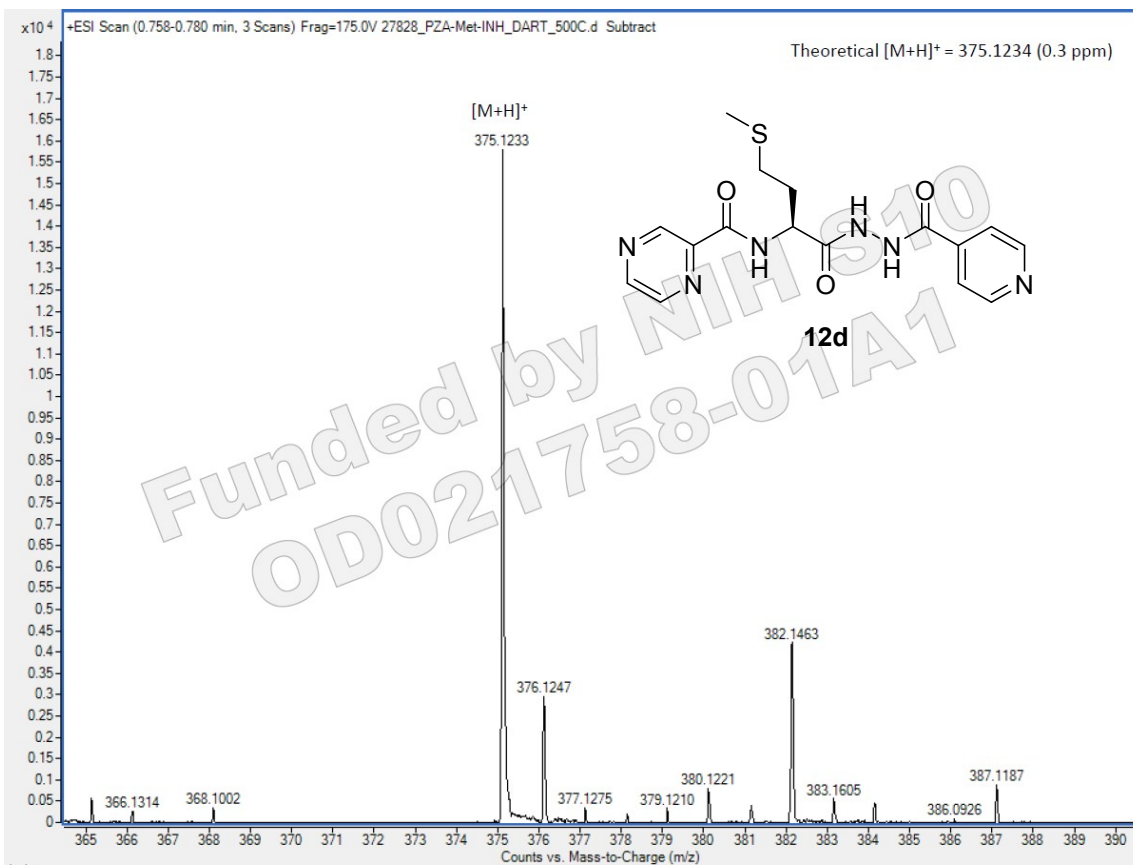
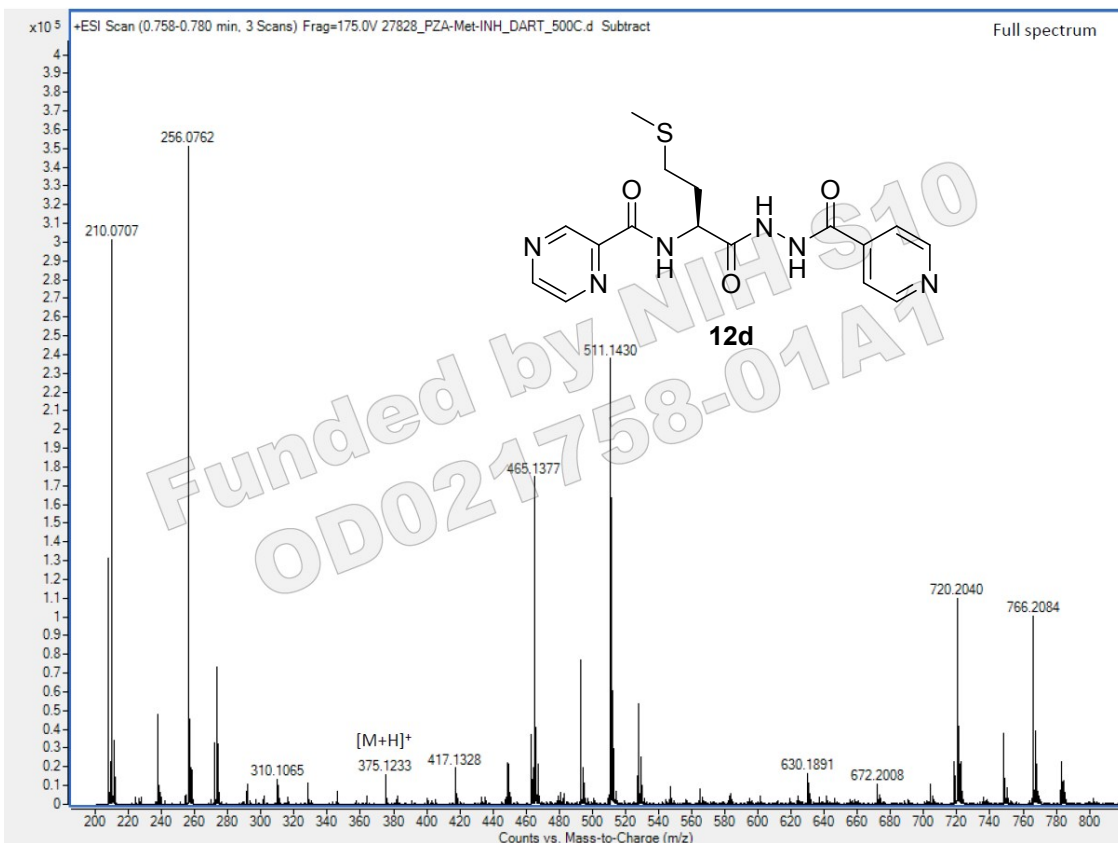
Theoretical $[M+H]^+$ = 343.1513 (3.2 ppm)
Theoretical $[M+Na]^+$ = 365.1335 (0.5 ppm)

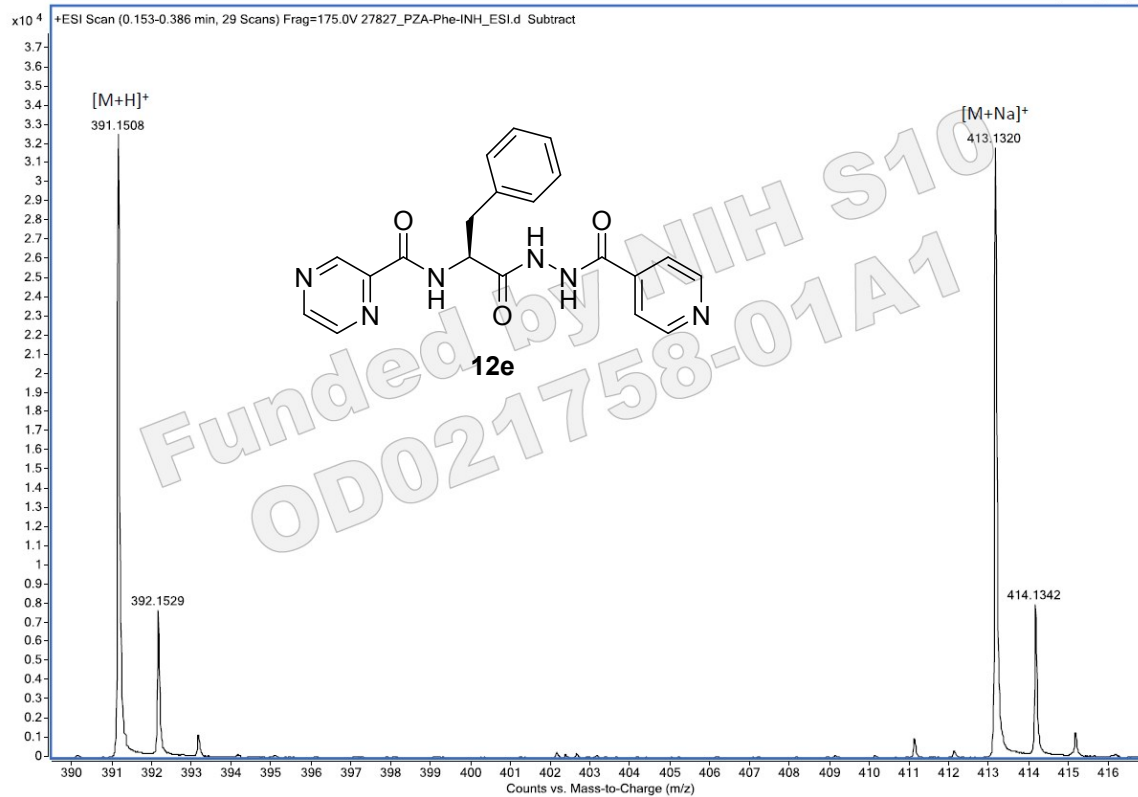
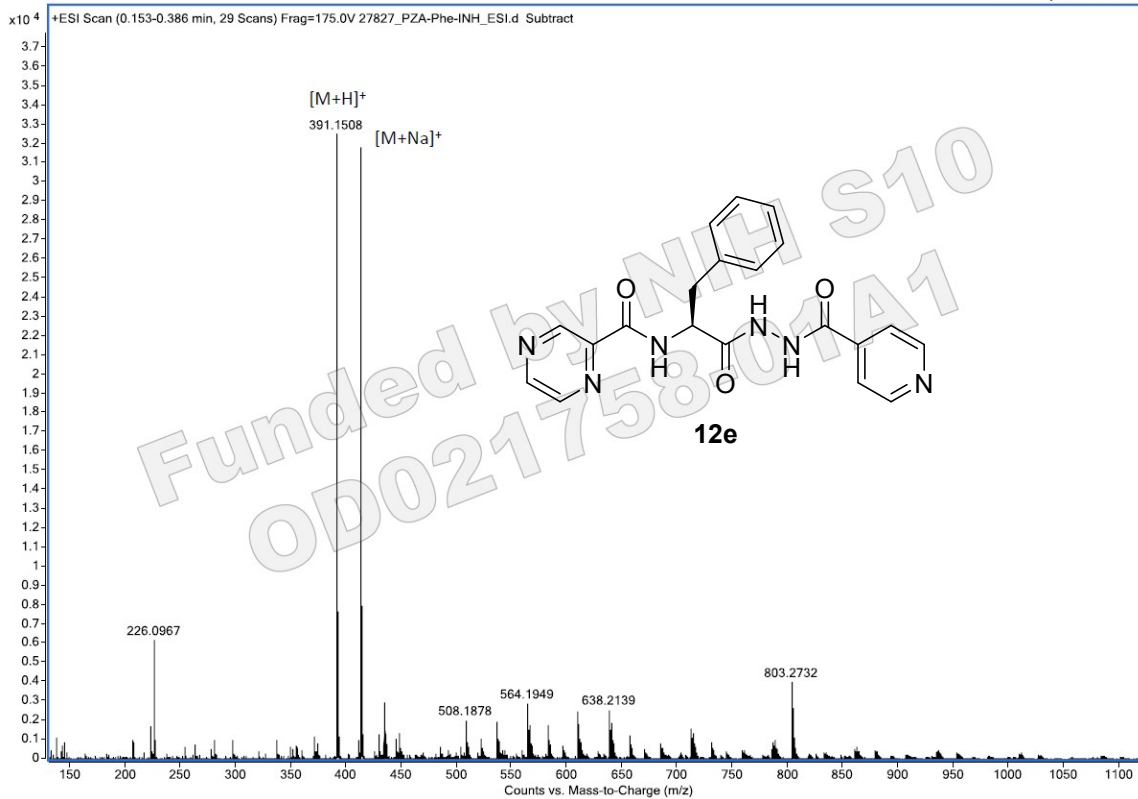


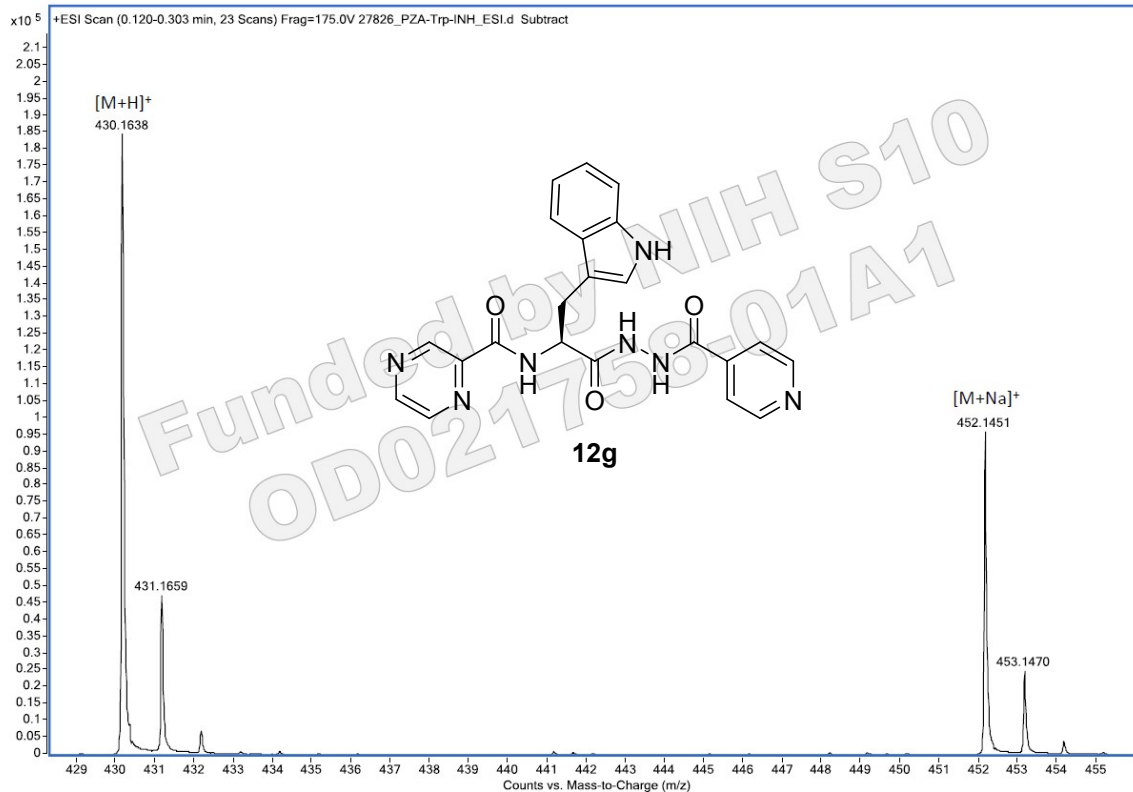
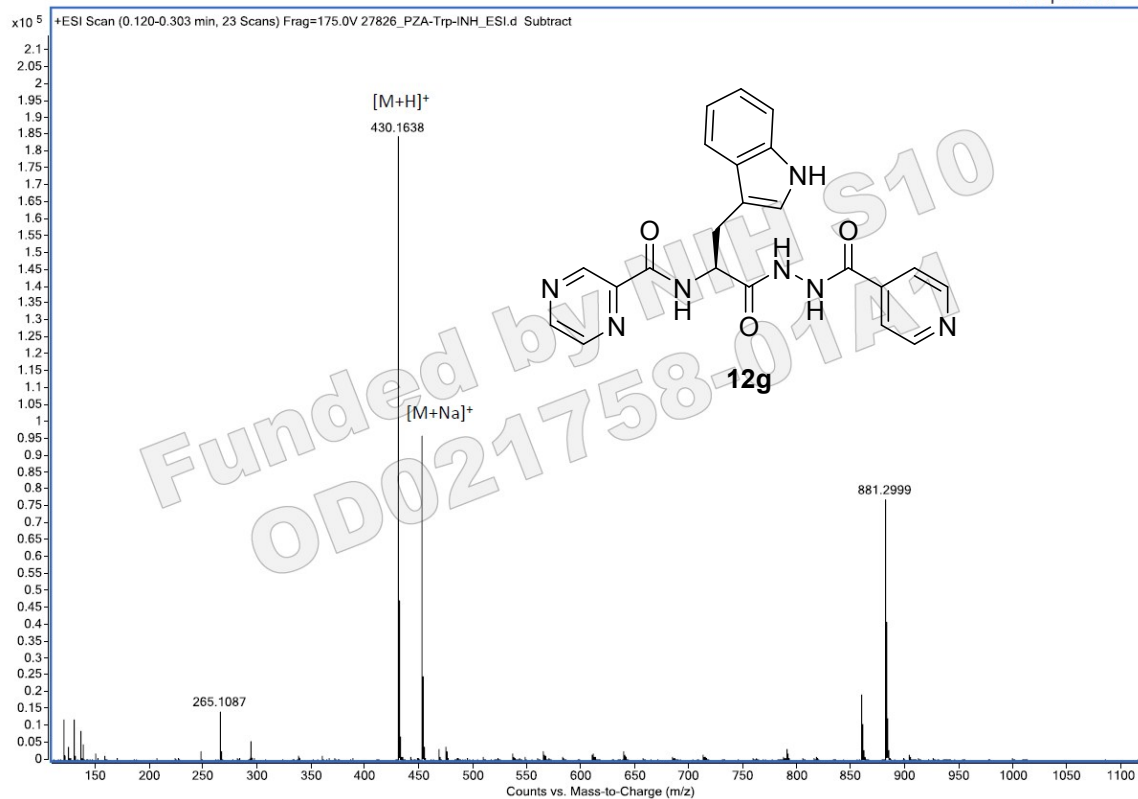


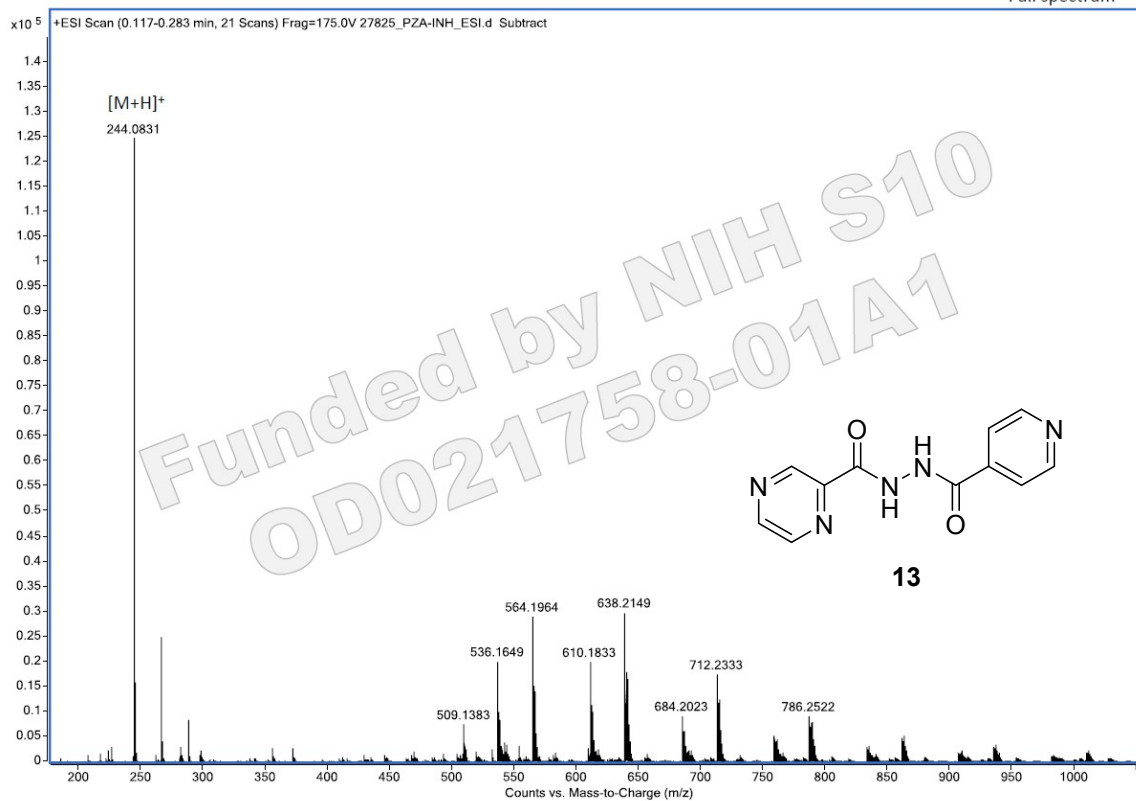
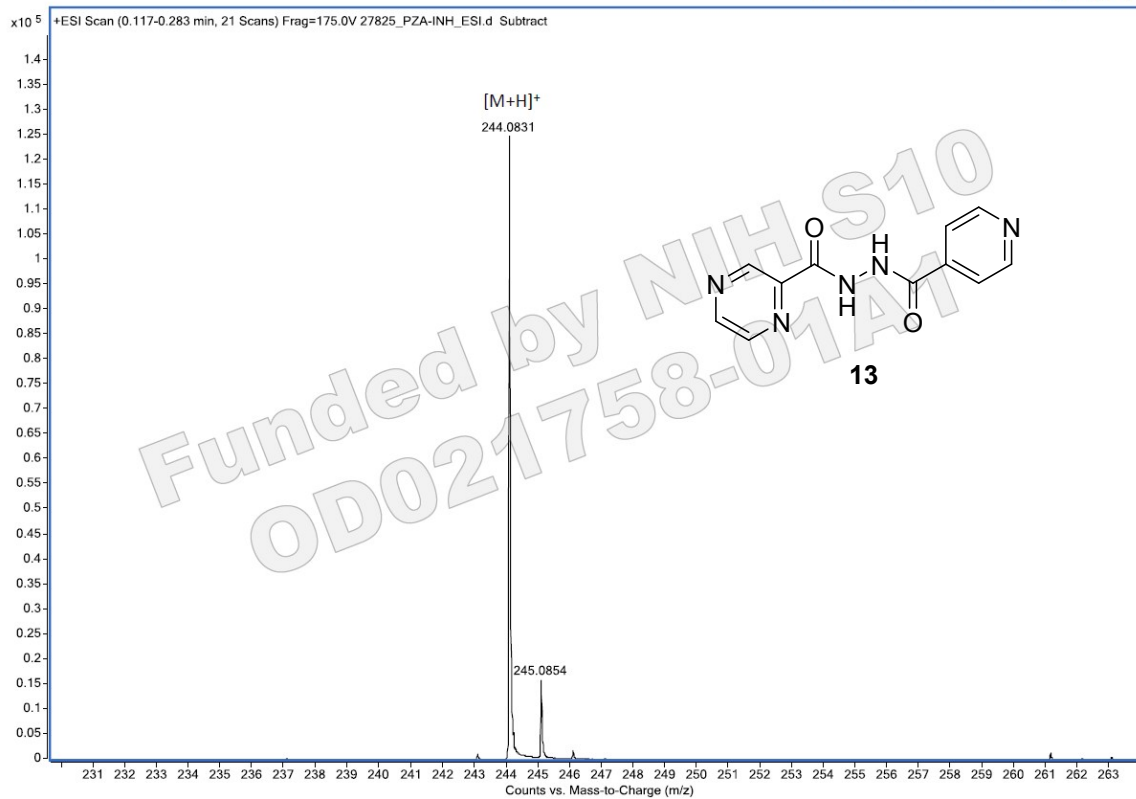
Theoretical [M+H]⁺ = 357.1670 (2.8 ppm)
Theoretical [M+Na]⁺ = 379.1489 (2.9 ppm)

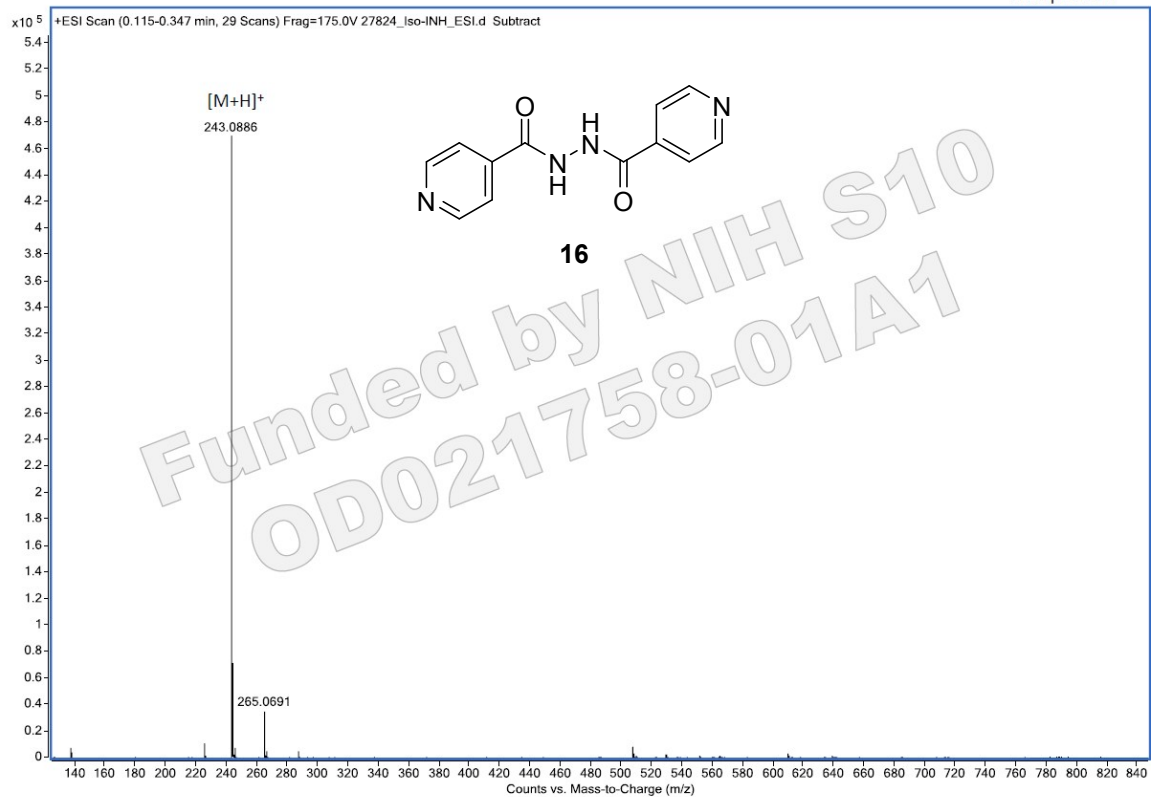
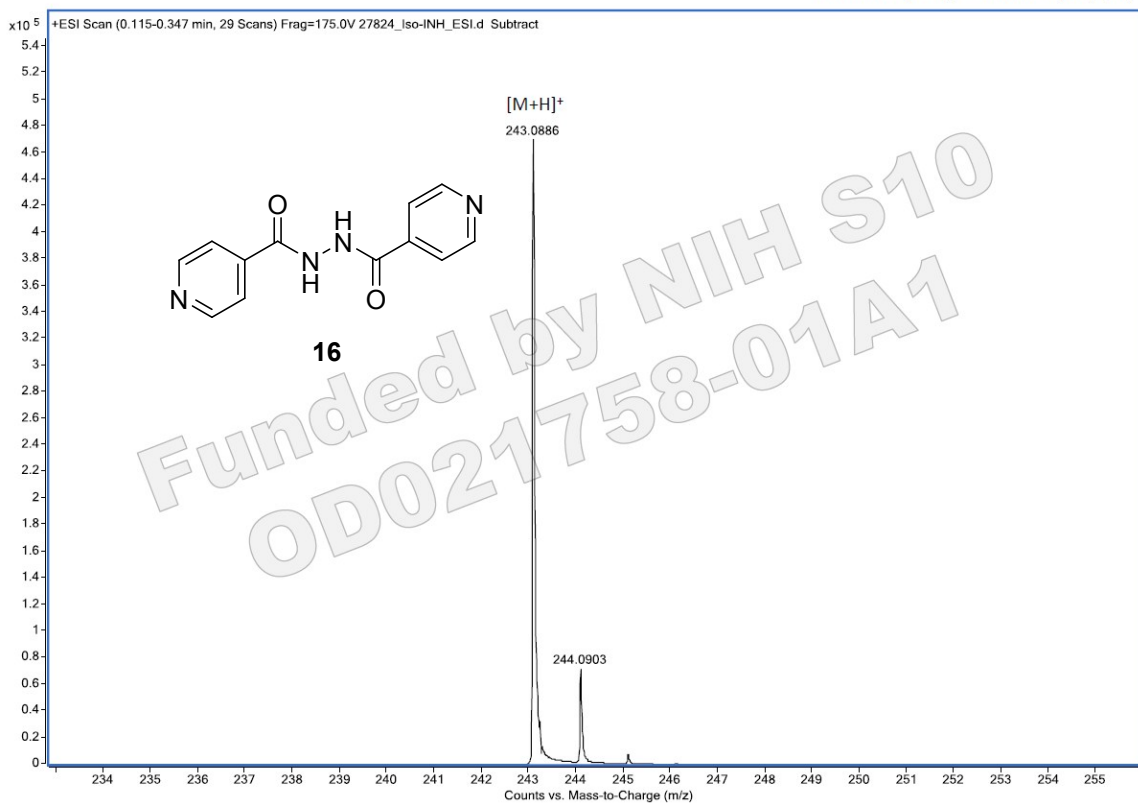








Theoretical [M+H]⁺ = 244.0829 (0.8 ppm)

Theoretical [M+H]⁺ = 243.0877 (3.7 ppm)

HPLC spectra of compounds 12e and 12f

Instrument: Agilent 6120

Column: Chirobiotic T

Detector: UV detector

Mobile phase: Methanol

Injection volume: 5 μ L

Flow rate: 0.5 mL/min

